Molecular mechanism of inducible crassulacean acid metabolism in *Talinum fruticosum*

Inaugural-Dissertation

zur Erlangung des Doktorgrades
der Mathematisch-Naturwissenschaftlichen Fakultät
der Heinrich-Heine-Universität Düsseldorf

vorgelegt von

Vanessa Reichel-Deland

aus Ratingen

Düsseldorf, August 2023

aus dem Institut für
Institut für Biochemie der Pflanzen
der Heinrich-Heine-Universität Düsseldorf

Gedruckt mit der Genehmigung der
Mathematisch-Naturwissenschaftlichen Fakultät der
Heinrich-Heine-Universität Düsseldorf

Referent: Prof. Dr. Andreas P. M. Weber

Korreferent: Prof. Dr. Matias D. Zurbriggen

Tag der mündlichen Prüfung: 17.11.2023

Eidesstattliche Erklärung

Ich versichere an Eides Statt, dass die Dissertation von mir selbständig und ohne unzulässige fremde Hilfe unter Beachtung der „Grundsätze zur Sicherung guter wissenschaftlicher Praxis an der Heinrich-Heine-Universität Düsseldorf“ erstellt worden ist.

Die Dissertation habe ich in der vorgelegten oder in ähnlicher Form noch bei keiner anderen Institution eingereicht.

Ich habe bisher keine erfolglosen Promotionsversuche unternommen.

Düsseldorf, den 08.08.2023

_____

Vanessa Reichel-Deland

"We keep moving forward, opening new doors, and doing new things, because we're curious and curiosity keeps leading us down new paths."

Walt Disney

Summary

With the rapidly changing climate conditions, the intricate ability of plants to adapt to their environment is crucial. Plants serve as the backbone of the natural ecosystem on earth, as they use carbon dioxide, sunlight and water to produce oxygen and carbohydrates, essential for sustaining life. Rising temperatures and droughts can challenge the resilience of plants (Manuscript I). Throughout evolution, plants have developed different strategies to overcome severe stresses. One strategy is the carbon concentrating crassulacean acid metabolism (CAM), with optimizes photosynthesis for growth in water-limited regions. CAM plants separate steps of its photosynthetic metabolism throughout a day/night rhythm, allowing CO_2 fixation during the cooler night and closing of the stomata during the day, when the temperatures are high. The facultative CAM plant *Talinum fruticosum* has adapted to recurring periods of drought by transitioning from C_3 to CAM photosynthesis under drought and reverting to C_3 upon water supply. This ability enables *T. fruticosum* to survive prolonged episodes of severe drought.

In this thesis we aimed to establish *T. fruticosum* as a model plant and to understand this reversible CAM switching to potentially utilizing these findings in reverse engineering crop drought tolerance in the future. We established protocols for molecular work with *T. fruticosum* (Manuscript II), which has the potential to unravel previously unexplored aspects of the CAM metabolic pathways, signaling cascades and gene regulatory networks. To understand the gene expression of *T. fruticosum* during environmental adaptation, we employed a synergy of transcriptome analysis, transcription factor binding prediction and verification through a synthetic biological test system in an orthogonal mammalian cell system (Manuscript III).

Our studies have laid the foundation for a promising platform with novel approaches to comprehend the complex regulatory network and adaptation mechanisms of the facultative CAM plant *T. fruticosum*, with the potential to investigate other species of interest, such as the facultative CAM plant *Coleus amboinicus* (Addendum). Our findings have deepened the understanding of a drought tolerance mechanism and pave the way for future investigations, which are indispensable in advancing crop engineering to meet the challenges of a changing climate.

Table of contents

Motivation and Aim 2

Introduction 3

- Photosynthesis 3
- CAM photosynthesis - a water-saving mechanism 5
- Diversity of CAM photosynthesis 7
- Phosphoenolpyruvate carboxylase – a key player in CAM photosynthesis 8
- The role of the circadian clock in CAM photosynthesis 9
- Model plants for CAM research 10
- Engineering CAM 12
- Omic studies – a new era of research 13
- Exploration of gene regulation 15
- Protein turnover 16
- References 18

Manuscript I 28

- Photorespiration is the solution, not the problem

Manuscript II 41

- A toolbox to study the facultative CAM plant *Talinum fruticosum*

Manuscript III 68

- Understanding molecular regulation
- of the facultative CAM plant *Talinum fruticosum*

Addendum 124

- *Coleus amboinicus* – a new model plant to understand CAM photosynthesis?

Journal version of published Manuscript I 140

- Photorespiration is the solution, not the problem

Acknowledgments 146

Motivation and aim

In 2021 the World Meteorological Organization measured a new temperature record in Europe, reaching 48.8 °C in Sicily, Italy. The heat, coupled with drought, has a profound impact on our environment and is a major challenge to ensure food security in the 21st century. One crucial aspect affected by high temperatures in plants performing C_3 photosynthesis is their photosynthetic efficiency, as photorespiration becomes more prevalent. In the first manuscript of the thesis, we aim to discuss if photorespiration is a wasteful process or a solution for plants.

Plants have evolved different carbon concentrating mechanisms to cope with environmental changes. Among these, crassulacean acid metabolism (CAM) photosynthesis performing plants are primarily found in semi-arid and arid regions. Certain species even use this water-use-efficient strategy in combination with C_3 photosynthesis to adapt to their environment. A representative example of this adaptability is the facultative CAM plant *Talinum fruticosum*, which can transition between C_3 and CAM photosynthesis. Previous research has already explored the genome and transcriptome of *T. fruticosum*. However, there is still a need for new protocols to gain deeper insights into the molecular mechanisms of CAM. Thus, the aim of the thesis is to establish new methodologies that will serve as the foundation for further research questions (Manuscript II). The primary objective is to unravel key mechanisms involved in the C_3 to CAM transition. This involves not only employing a transcriptomic approach, but also using new approaches to identify transcription factor binding sites and validating these findings through an orthogonal synthetic test system (Manuscript III). The aim is to apply these approaches and findings not only to *T. fruticosum*, but also to extent this knowledge to other plants, such as the facultative CAM plant *Coleus amboinicus* (Addendum).

Introduction

Photosynthesis

Photosynthesis, a fundamental biochemical process in nature from which most life on planet earth is dependent on. During photosynthesis plants and other photosynthetic organisms, including photosynthetic bacteria or algae, use sunlight, water and CO_2 to produce glucose as an energy storage and oxygen. Around 3.4 billion years ago, the first photosynthetic bacteria occurred. Eukaryotic photosynthesis emerged from endosymbiosis between cyanobacteria and a non-photosynthetic eukaryotic host, leading to the development of the chloroplast (Reyes-Prieto et al., 2007). The first land plants performed photosynthesis around 0.475 billion years ago (Raven and Edwards, 2014).

C_3 photosynthesis is the ancestral photosynthetic pathway found in terrestrial plants and is spread most throughout the plant kingdom (Ehleringer et al., 1991). The multi-step process fixes the carbon from CO_2 into organic products. The enzyme ribulose-1,5-bisphosphate carboxylase/oxygenase (Rubisco), probably the most abundant protein in the world (Ellis, 1979) and the key enzyme of the Calvin-Benson-Bassham cycle (CBB), performs the first step of CO_2 fixation. CO_2 is reduced stepwise to phosphoglycerate, which is further converted to sugar phosphates that are crucial for the plant metabolism. However, instead of CO_2, Rubisco also exhibits oxygenase activity, fixing O_2 by mistake, which leads to the formation of 3-phosphoglycolate (3-PGA) and 2-phosphoglycolate (2-PG). The molecule 2-PG inhibits metabolic regulators and is therefore metabolized by photorespiration (Flügel et al., 2017). Photorespiration, also known as the C_2 cycle, is a process that can reduce plant yield by about 30% (Walker et al., 2016). Rubisco evolved in a carbon-rich atmosphere, when the proportion of the oxygenation reaction was low. With the emergence of oxygen-producing autotrophic organisms, the partial pressure of O_2 in the atmosphere increased dramatically, leading to an increased ratio of the Rubisco oxygenation reaction (Ehlers et al., 2015; Sage, 2004). Organisms adjusted to the in turn higher levels of photorespiration by the evolution of carbon concentrating mechanisms (CCM), like C_4 and crassulacean acid metabolism (CAM) photosynthesis.

Figure 1 shows a simplified overview of the main differences between C_3, C_4 and CAM metabolism. While C_3 photosynthesis occurs in both mesophyll and bundle-sheath cells, plants performing C_4 photosynthesis separate the metabolic pathway spatially between the two cell

types. While in C_4 photosynthesis performing plants CO_2 is taken up into the mesophyll cells, Rubisco is located in the bundle-sheath cells. This allows higher carboxylase activity of Rubisco and makes C_4 favorable under low CO_2 concentration in the atmosphere and higher temperatures (Sage, 2004). C_4 photosynthesis is believed to have evolved stepwise from C_3 (Monson and Moore, 1989). The carbon concentration strategy of CAM plants shows water-use efficiency (WUE), which emerged as a response to a changing environment by separating the photosynthetic steps throughout different times of the day/night cycle. The evolution of CAM photosynthesis is less understood than C_3 and C_4 photosynthesis. Two different perspectives on CAM evolution are discussed in recent literature. Some views consider CAM evolution as a continuous pattern (Bräutigam et al., 2017; Schiller and Bräutigam, 2021). The authors propose that the CAM cycle framework is already present in C_3 plants as they can store acids in the night and use them during the day. Therefore, they argue that "it is not a question of rewiring metabolism but of selecting for increased flux" and that *de novo* fluxes are not needed for CAM photosynthesis. In contrast, Winter and Smith (2022) argue that CAM evolved as a discrete innovation, where the accumulation of organic acids in the vacuole takes place both for C_3 and CAM plants or those which can transition. They argue that malate accumulation in C_3 plants happens during the day and not, as proposed by Bräutigam et al. (2017) and Schiller and Bräutigam (2021) during the night. This argument would disprove that flux upregulation of C_3 metabolism explains a continuum for CAM evolution. However, to further underpin this hypothesis, experimental evidence is needed.

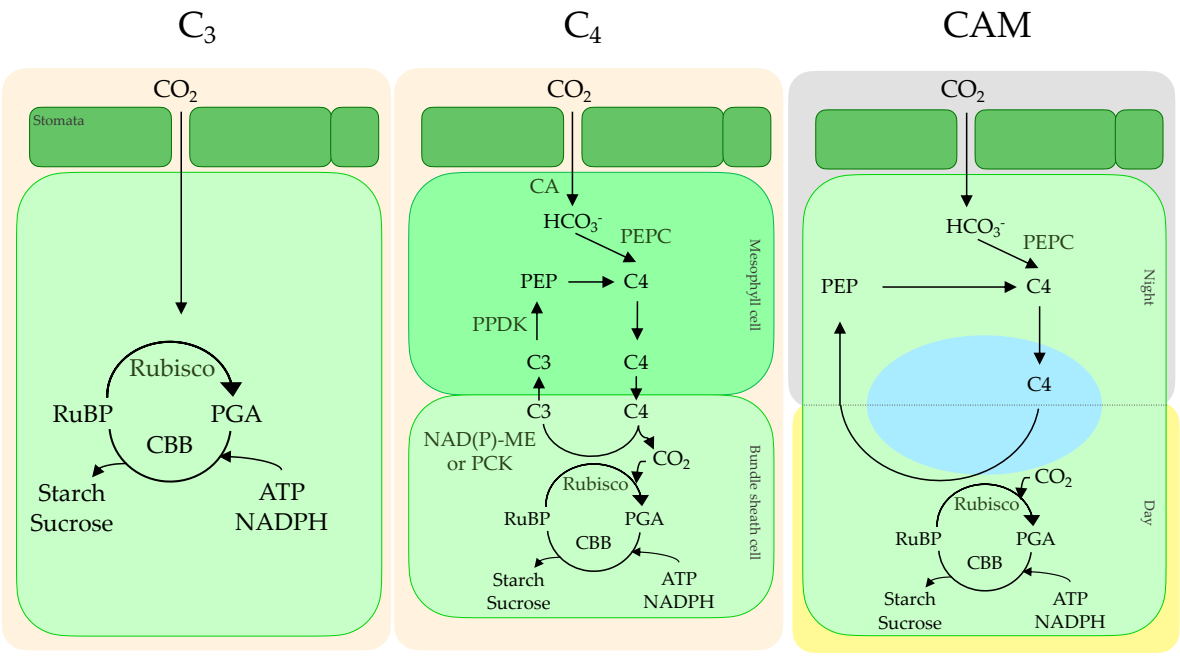

Figure 1: Schematic overview of the three main types of photosynthesis in land plants, C_3, C_4 and CAM. RuBP: Ribulose-1,5-bisphosphate, PGA: 3-Phosphoglyceric acid, CBB: Calvin-Benson-Bassham cycle, Rubisco: ribulose-1,5-bisphosphate carboxylase/oxygenase, PEP: Phosphoenolpyruvate, CA: carbonic anhydrase, PCK: Phosphoenolpyruvate carboxykinase, PPDK: Pyruvate phosphate dikinase, PEPC: Phosphoenol-pyruvatecarboxylase. Modified after da Rosa Ferraz Jardim et al. (2022).

CAM photosynthesis - a water-saving mechanism

Plants performing CAM photosynthesis are found across at least 400 genera and 40 families and in about 5% of vascular plants (Winter et al., 2015; Winter and Smith, 2022, 1996). CAM is mainly prevalent in plants growing in semi-arid habitats or regions with wet and dry seasons (West-eberhard et al., 2011). Its carbon concentrating mechanism relies on the storage of photosynthetic products during the night. CAM plants can therefore keep their stomata closed during the day to prevent water-loss. The CO_2 assimilation in plants with CAM activity can be divided into four phases, however all of them need to be considered together (Osmond, 1978). During the night, when the temperatures are rather low and the relative humidity is high, CAM plants open their stomata to allow CO_2 uptake. However, as there are exceptions, some CAM plants will not open their stomata but use internally respired CO_2 (Pierce et al., 2002). Nevertheless, CO_2 is not directly fed into the Calvin-Benson-Bassham cycle. The enzyme Phospho*enol*-pyruvatecarboxylase (PEPC) plays a key role in photosynthesis, where it catalyzes the carboxylation of CO_2. HCO_3^- is converted to CO_2 by the beta-carbonic anhydrase

(β-CA) In the presence of H_2O and CO_2 the enzyme PEPC catalyzes the carboxylation of phosphoenolpyruvate (PEP) to phosphate and oxaloacetate (OAA) (Boxall et al., 2020; Drennan and Nobel, 2000). Glycolytic breakdown of storage carbohydrates provides the PEP needed for the PEPC reaction. The used storage carbohydrate is dependent on the plant species. Usable carbohydrates include starch from the chloroplast or hexoses from the vacuole. Malate is synthesized from oxaloacetate and stored as malic acid in the vacuole and functions as an allosteric inhibitor for PEPC (Taybi et al., 2004). Transport into the central vacuole of the mesophyll cell is done by either one or both H^+ pumps, localized in the tonoplast. Accumulation of acids can be observed by titration, where one equivalent of malate is balanced by two equivalents of H^+ (Lüttge and Ball, 1980). During the first CAM photosynthesis phase, intracellular acidity can reach pH values of four or less by the end of the night (Winter and Smith, 2022). The early phase of dawn marks the beginning of phase II of CAM photosynthesis, where CO_2 is fixed. During the temperature increase in the beginning of the day, CAM plants close their stomata to prevent water loss due to evaporation. Malic acid is exported from the vacuole into the cytosol, where it is decarboxylated. The process of decarboxylation is dependent on the plant species and is either performed by PEP carboxykinase or NAD(P)-malic enzyme together with pyruvate P_i dikinase. The storage carbon pool is filled up by recycling the remaining PEP or pyruvate via gluconeogenesis. CO_2 is re-fixed by Rubisco and fed into the CBC (phase III). However, later in the day the stomata might need to be opened again if the malate is depleted and additional CO_2 needs to be fixed by Rubisco (phase IV) (Osmond, 1978). It is known that there is flexibility across the four phases, depending on different aspects including the species, developmental stage or environmental conditions (Burgos et al., 2022; Winter, 2019).

Besides the specialized biochemistry, CAM plants show an intricate set of anatomical specializations. Leaf succulence or leaf thickness is a phenotype not only found in CAM plants, but represents a typical functional trait in plants found in dry environments. Succulence occurs when cells are packed tight and contain large mesophyll cells and big vacuoles (Winter and Smith, 1996). In CAM plants the large vacuole is crucial for the storage of acids and water to maintain efficient photosynthesis. In addition to that, the reduced intracellular air space prevents the efflux of CO_2 (Nelson and Sage, 2008).

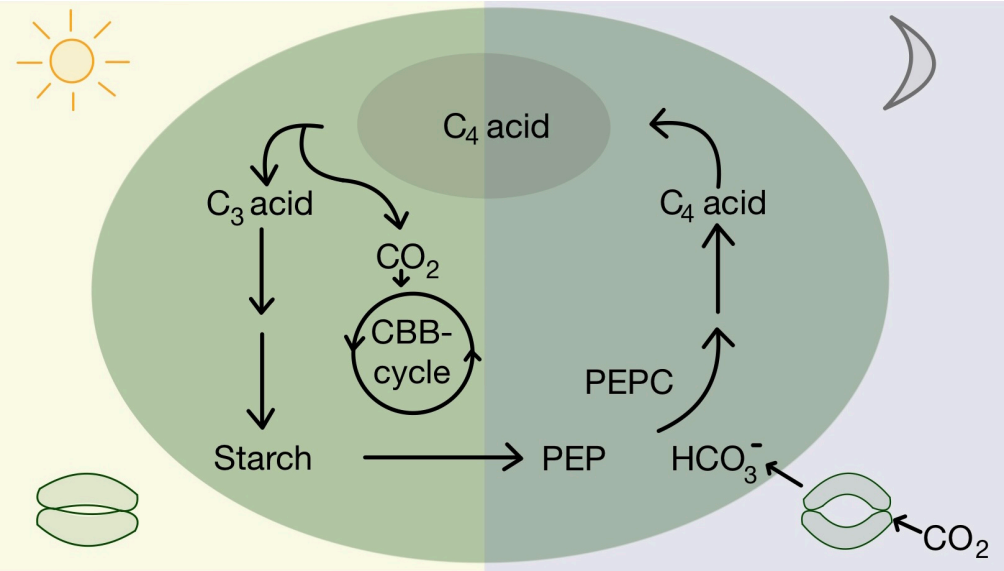

Figure 2: Schematic overview of CAM photosynthesis. It's a temporally separated pathway, where CO2 uptake it mainly done during the night, when stomata are open. C4 acids are stored in the vacuole and used for further conversion in the Calvin-Benson-Bassham cycle (CBB) during the day. PEP: Phosphoenolpyruvate, PEPC: Phosphoenol-pyruvatecarboxylase. Figure modified after Borland et al. (2014).

Diversity of CAM photosynthesis

The level of how CAM plants engage their specialized photosynthetic cycle is variable. The proportion of nocturnal CO_2 fixation relative to the total CO_2 uptake can range from <1% to 100% (Winter et al., 2015). A great variety and complexity are found in the biochemical variation of CAM, which suggests plasticity and (functional) diversity. Mature tissue can show CAM photosynthesis while C_3 photosynthesis is typically prevalent in early developmental stages (Bräutigam et al., 2017). Constitutive or obligate CAM is the most common form of CAM photosynthesis. However, other plants are able to transition between C_3 or C_4 photosynthesis and a switchable CAM cycle (Winter, 2019). Constitutive CAM plants are bound to a permanent CAM cycle in mature leaves. In contrast to that, the so-called facultative CAM plants can transition between C_3 (e.g., (Brilhaus et al., 2016; Dai et al., 1994; Maleckova et al., 2019) or C_4 (Ferrari et al., 2020) and CAM photosynthesis. This process is reversible and genetically encoded. Plants employing facultative CAM transition if environmental conditions are unfavorable (Gilman and Edwards, 2020; Winter, 2019), for example during drought or high salinity, which can cause low water availability. The first description of facultative CAM was done for *Mesembryanthemum crystallinum* in 1972, when a different CO_2 gas exchange reaction for plants treated with and without salt was observed (Von Wilbert and Kramer, 1972). Proof of facultative CAM in a species needs to be verified by the ability to transition

from C_3 or C_4 to CAM, but also always its reversibility back to the initial C_3 or C_4 state (Winter and Holtum, 2007). To date, facultative CAM is described in at least 54 species from 15 families, mostly found in Caryophyllales. It is predicted that further species will be identified, predominantly due to a great CAM survey, as described by Winter (2019).

Phospho*enol*pyruvate carboxylase – a key player in CAM photosynthesis

Phospho*enol*pyruvate carboxylase is a key enzyme in CAM and C_4 photosynthesis, where it plays a role in the primary CO_2 fixation (compare the chapter "CAM photosynthesis - a water-saving mechanism").

In C_3 plants however, PEPC has a non-photosynthetic function, including fruit ripening, seed formation and to restock intermediates of the tricarboxylic acid cycle (Aldous et al., 2014; Wang et al., 2016). It is known that PEPC plays a crucial role in C_4 and CAM photosynthesis. However, exploration of its role is not fully understood yet, since only a few *PEPC* mutant plants are reported. *PEPC* deficient mutants have been established for the C_4 plants *Setaria viridis* (Alonso-Cantabrana et al., 2018) and *Amaranthus edulis* (Dever et al., 1996) and the CAM plant *Kalanchoë laxiflora* (Boxall et al., 2020). The *PEPC* mutant C_4 plants could only grow or flower under high CO_2 conditions. The C_4 PEPC is important to achieve high concentrations of CO_2 around Rubisco and in this way suppresses photorespiration. *K. laxiflora* was the first CAM plant described, where *PEPC1* was silenced using RNA-interference experiments. Boxall et al. (2020) observed a change in stomatal conductance and arrythmia of CO_2 fixation, which led to the assumption that there is a connection between regulation of guard cells and stomatal movement in the *K. laxiflora PEPC1* mutant. Studies on PEPC in the context of plant development revealed the role of PEPC in diurnal changes (Ping et al., 2018) and transition between photosynthesis types (Theng et al., 2007). Wang et al. (2016) conducted a genome-wide analysis of *PEPC* homologs in soybean. The authors identified ten *PEPC* genes in *Glycine max* and found nineteen *cis*-regulatory elements that were related to stress responses or phytohormones in the upstream region of the *PEPC* genes. Three of the identified *PEPC* genes showed upregulation of gene expression as a response to abiotic stresses. This suggest that the *PEPC* genes of soybean do not only play a role in development, but also indicates their role in stress responses.

Analysis of bulk data sets and experimental confirmation for a variety of CAM and C_4 species might be needed to understand the underlying mechanism of PEPC and how its understanding can be used for future applications such as genetic engineering.

The role of the circadian clock in CAM photosynthesis

Measuring the time of the day and season is crucial for plants to survive and reproduce. A rhythm of approximately 24 hours is widespread throughout nature and it is regulated by the activity of an endogenous clock. An input signal, such as light or a temperature shift, a central oscillator and an output pathway, like gene expression or the movement of leaves, are the three basic components needed for circadian-dependent regulation. (McClung et al., 2002). This regulation is needed for almost all processes, such as adaptation of the metabolism or physiology to environmental stimuli (Kim et al., 2017).

The timing of photosynthetic steps in CAM plants is important and therefore optimized by the circadian clock (Bräutigam et al., 2014). Besides static circadian regulation, plants using facultative CAM also need to adapt to fluctuating environmental changes. In contrast to obligate CAM plants, where expression of the CAM machinery is pre-set in the plant's development, facultative CAM plants most often perform CAM photosynthesis optionally, as they are able to transition between photosynthetic types in a reversible manner (Winter and Holtum, 2014). It has been stated before that genes related to drought are regulated by the circadian clock (Covington et al., 2008).

For engineering purposes, the intricate interplay between the core CAM network and the circadian oscillator has to be considered. It is known that the circadian clock regulates CAM carboxylation, decarboxylation and timing (Hartwell, 2005). The central enzyme PEPC is temporally regulated by phosphorylation through the circadian clock-controlled phospho*enol*pyruvate carboxylase kinase (PPCK) in the dark (Hartwell et al., 1996; Taybi et al., 2017). Core CAM genes like *PPCK* and *Pyruvate phosphate dikinase* (*PPDK*) show diurnal transcript patterns and are conserved throughout different CAM species (Boxall et al., 2005). The CAM plant *K. fedtschenkoi* has been used to analyze the link how CAM physiology might be controlled by the circadian clock. By comparing *K. fedtschenkoi* to the C_3 plant *A. thaliana*, Moseley et al. (2018) could observe differential expression in core clock components as *EARLY FLOWERING 3*, *EARLY FLOWERING 4* and *LUX*. These genes, belonging to the evening complex, showed changes in the copy number and the timepoint of expression, suggesting

phase shifts between species of different photosynthetic types (Moseley et al., 2018). The facultative CAM plant *M. crystallinum* shows a 4-8 h phase shift in their pattern of circadian expression, which is suggested to be essential for photosynthetic transition from C_3 to CAM (Cushman et al., 2008). In *Sedum album*, research could identify a phase shift of the core circadian clock, which suggest rewiring of time of day needed to transition from C_3 to CAM photosynthesis. It has been shown that only 20% of the cycling genes are the same under C_3 and CAM. In addition to that, circadian *cis*-elements were identified to play a role in the *S. album* (Wai et al., 2019). Moreover, *Portulaca* species, which can transition between C_4 and CAM photosynthesis, also show adaptation through the circadian regulation. Most striking is the circadian control of *PPCK*, as it seems to be most susceptible to transcript level dampening. In the C_4-CAM species it is suggested that the intricate temporal gene expression is not only needed to promote expression of CAM genes, but also important to limit C_4-related gene expression (Ferrari et al., 2022a).

However, although multiple studies investigated the role of the circadian clock role in CAM regulation, still a lot of steps are unknown. This is especially true for facultative CAM plants, which not only need circadian regulation of the CAM pathway, but also for the transition from C_3 or C_4 photosynthesis to CAM and back.

Model plants for CAM research

In 1577 Johannes Thal described *Arabidopsis thaliana*, a plant that was collected in the Harz Mountains in Germany (Kück, 2005). In the era of molecular biology research, the interest in this plant was growing. *A. thaliana* features many advantages as a model plant, like fast and easy growth and seed production. In the 1980s genetic approaches were combined with molecular biology methods and offered new possibilities for research. The *A. thaliana* genome was published in the year 2000 (Kaul et al., 2000) and more researcher became interested in working with *A. thaliana*. Thus, establishment of protocols was needed for further investigation of molecular research questions. With the development of new tools, a greater variety of research questions could be addressed leading to new findings. The availability of different methods and their use of the community has led to great progress in understanding plant biology, with topics from cell biology, evolution, metabolisms, (epi)genetics to physiology. Recent research fields, as systems biology, are still quite new and will offer different ways of thinking to the community (Krämer, 2015).

In the field of CAM photosynthesis there is not yet any model plant like *A. thaliana*. There are species with promising properties and tools available, but this is still very limited compared to research in C_3 plants. However, with a rapidly changing climate and a steep increase in population, the generation of drought adapted crops should be promoted. CAM is present in about 6% of all plant species (Silvera et al., 2010) and therefore it is important to study a broad range of plant taxa to gain a deeper understanding of CAM evolution and its regulation.

Therefore, it will be beneficial to establish CAM model plants with an available genome, a broad variety of established methods and of high use for the research community (Chang et al., 2016). However, many of the known CAM plants might be rather difficult to investigate as they have a succulent tissue, a complex set of secondary metabolites and might need specific growth conditions (Yang et al., 2020). Some well-studied CAM plants belong to the genus *Kalanchoë*. *K. fedtschenkoi* and *K. laxiflora* are obligate CAM plants, whereas *K. gracilipes* is a facultative CAM plant. The close phylogenetic relationship between these species with different types of photosynthesis allows deep insights into the evolution and inner works of CAM photosynthesis. A detailed investigation of the *Kalanchoë* genome and generation of transgenic lines are has already been achieved (Boxall et al., 2020; Yang et al., 2017). However, most research has been done on species with an obligate CAM cycle and not yet on the facultative species. This leads to a lacking understanding of the transition from C_3 to CAM photosynthesis.

To date, *Mesembryanthemum crystallinum* is the most extensively studied plant with facultative CAM. CAM photosynthesis of *M. crystallinum* can be induced by drought or salinity stress or by the application of abscisic acid (ABA). Treatment using salt or ABA instead of drought stress, might make experiments easier to control and to reproduce (Chu et al., 1990; Taybi and Cushman, 2002). Besides the physiological and biochemical analysis of CAM induction, transcriptome data have the potential to identify genes that play a role in CAM induction and reveal genes that are being regulated by external stimuli or the circadian clock (Cushman et al., 2008). Facultative CAM plants can not only transition from and to C_3, but also from and to C_4 photosynthesis. One genus known is *Portulaca*, where research is mainly done on *P. afra* (Ting, 1981), *P. amilis* (Gilman et al., 2022) and *P. oleracea* (Ferrari et al., 2022b, 2020). Research was also done in additional CAM species including *Phalaenopsis* (Deng et al., 2016), *Agave* (Abraham et al., 2016), *Sedum album* (Wai et al., 2019), *Coleus amboinicus* (Winter et al., 2021) or *Talinum fruticosum* (Brilhaus et al., 2016; Maleckova et al., 2019). However, there are still a lot

of unsolved pathways of CAM photosynthesis, which could be addressed by establishing a CAM model plant, where a variety of methods and knowledge about its genome, transcriptome, metabolome and proteome are available. Two candidates of facultative CAM plants that have the potential to become a model plant of CAM research are introduced in this thesis. *Coleus amboinicus* belongs to the Lamaaceae (Winter et al., 2021) and combines weak constitutive and facultative CAM. *Talinum fruticosum* belongs to the Talinaceae (Brilhaus et al., 2016; Maleckova et al., 2019) and shows C_3 expression, but transitions to CAM under drought stress or as a short-term ABA response in a reversible manner.

Engineering CAM

As extreme weather conditions are becoming more frequent due to climate change, drought is an increasing problem especially for agriculture. CAM plants perform a water-use-efficient photosynthesis and understanding the genetic regulation is therefore valuable for improving crop resistance. Implementing important steps of the CAM pathway or shifting plants that use the C_3 pathway towards a CAM cycle could help to prevent stomatal water evaporation and improve plant performance and yield under drought (Yang et al., 2015). In comparison to C_4 photosynthesis, where plants are more resistant to higher temperatures due to their special anatomy (compare Figure 1) (Schlüter and Weber, 2019), an artificial CAM cycle might be easier to introduce into crop plants. This idea is due to the single-cell type of photosynthesis that is used by CAM plants, which has a less complex underlying genomic regulation. As facultative CAM plants are capable to transition between different types of photosynthesis, most often C_3 and CAM, one can assume that there are no metabolic incompatibilities between the C_3 and CAM biochemistry. Therefore, engineering CAM photosynthesis into C_3 crops can be considered a worthwhile undertaking (Borland et al., 2014; Liu et al., 2018; Yang et al., 2015). Shameer et al. (2018) surveyed the metabolic network of C_3 and CAM leaves. In a comparative analysis Shameer et al. (2018) showed that engineering CAM into C_3 plants could lead to an increase in the water-use efficiency without affecting the yield. First approaches to implement parts of the C_4 metabolism of CAM into *A. thaliana* were successful as described in the following. To optimize the expression of the CAM machinery into a C_3 plants (CAM Biodesign), Lim et al. (2019) created a carboxylation- and a decarboxylation-, as well as a core CAM module. The carboxylation module consists of β-CA, PEPC, PPCK, NAD-dependent malate dehydrogenase and NADP-dependent malate dehydrogenase. In addition to that, the

decarboxylation module includes the NAD(P)-dependent malic enzyme, PPDK, PPCK, which are needed for decarboxylation of the C_4 acid, regeneration of pyruvate, the release of CO_2 and regeneration of PEP. In this approach, the authors assembled multigene circuits, where the gene expression is driven by *A. thaliana* promoters. Lim et al. (2019) could show that overexpression of these components led to changes of stomatal conductance and measurements of titratable acidity. Their results lead to fundamental innovation in the CAM Biodesign. Moreover, other studies could show that a drought-responsive transcription factor (TF) of the family of myeloblastosis (MYB59) from *Kalanchoe fedtschenkoi* led to increased WUE when overexpressed in the model plant *A. thaliana* (Amin et al., 2019). These studies help to understand the basic mechanisms of CAM, but still lacking in its full understanding due to the fact that a C_3 plant is needed, which might react different than a CAM plant would. In combination with modeling approaches, such as considering temperature or humidity (Töpfer et al., 2020), engineering of CAM into C_3 crops could be made possible in the future.

Omic studies – a new era of research

Omic approaches can lead to the generation of big datasets with relatively low effort and at comparable low prices. To understand the complex pathways and networks in plants, data needs to be collected from all fields of omics, such as (epi-)genomics, transcriptomics, metabolomics and proteomics. Availability of a broad range of multimodal data, not only for one plant, but also across species, can lead to a deeper understanding of a plant's complex phenotypes. Introduction of Next Generation Sequencing (NGS) led to higher sequence capacity, sensitivity, easier handling and to a cheaper alternative than Sanger sequencing. Parallel sequencing is used to achieve high-throughput and therefore fast sequencing (Grada and Weinbrecht, 2013). The number of plants with whole genome assemblies has increase rapidly since then.

Additionally, enormous progress has also been made in transcriptome profiling. When sequencing became cheaper, RNA-sequencing has established as the preferred method for transcriptome analysis (Conesa et al., 2016). To further investigate synthetic (DePaoli et al., 2014) and systemic approaches (Yang et al., 2020) -omics studies of drought tolerant plants are needed. Transcriptomes of different CAM plants have been sequenced and analyzed towards different biological questions. Comparative analysis of time-course related gene expression in *Erycina* species showed differential expression of ABA and light-sensing related genes, when

comparing C_3 to CAM species. The authors therefore suggest that these transcriptional changes might be necessary for C_3 to CAM transition (Heyduk et al., 2019). RNA-seq studies in *T. fruticosum* have been performed to understand the transition of C_3 and CAM, under drought or ABA treatment (Brilhaus et al., 2016; Maleckova et al., 2019). The two studies showed changes of the transcriptome during CAM transition. Transcriptional increases in key players of the CAM cycle, including *PEPC* and *PPDK*, could be observed during the transition from C_3 to CAM, after plants have been drought stressed (Brilhaus et al., 2016) or treated with ABA exogenously (Maleckova et al., 2019). This expression was downregulated again, when plants reverted back to C_3 photosynthesis after water has been re-supplied to drought stressed plants. In addition to that, genes involved in light protection, like *EARLY LIGHT INDUCIBLE PROTEIN 1*, showed upregulation of transcripts after drought, suggesting a stress response to adapt to a changing environment. Besides genes that are known to play a role in the core CAM machinery, transcription factors were identified, which seem to be involved in the regulation of facultative CAM. The gene expression of the *NUCLEAR FACTOR Y SUBUNIT A9* (*NF-YA9*) was upregulated under drought and was identified as an ABA-responsive transcription factor (Brilhaus et al., 2016). When ABA was applied for a short period of time, upregulation of *NF-YA9* was also observed and therefore suggest a role in an ABA-dependent induction of CAM in *T. fruticosum* (Maleckova et al., 2019).

A number of RNA-seq experiments have been performed for a wide range of questions and revealed new important insights into CAM regulation. However, not all types of regulation necessary for a complex phenotype take place on the gene expression or transcription level. The complex suite of regulation might entail gene regulation by epigenetic mechanisms or RNA or protein modifications, which are not detectable using transcriptomic experiments. Therefore, it is necessary to combine available data with other approaches, such as proteomics or epigenomics. Integrating information about chromatin accessible genes using Assay for Transposase-Accessible Chromatin using sequencing (ATAC-seq) with RNA-seq can give not only insights about expression levels, but can also serve as an epigenetic mean of gene regulation. Using omic approaches to analyze CAM plants will lead to a deeper understanding of regulatory dynamics to environmental adaptations.

Exploration of gene regulation

All plant developmental and adaptative processes underly complex transcriptional regulation. The complex suite of regulatory DNA elements comprises, among others, of protein-coding, non-coding RNA genes and *cis*- regulatory elements (CRE) (Strader et al., 2022). There are different element types of CREs, including core promoters, enhancers and silencers (Schmitz et al., 2022). A core promoter has a length of usually 50-100 bp and is crucial for the initiation of the transcription. When a DNA sequence is bound by specific TFs and cofactors, if necessary, transcription rates can be altered. Enhancers increase these transcription rates, while silencers actively decrease it. Which TFs are being expressed and targeted to the CREs in specific cell types influences the CRE activity and function (Schmitz et al., 2022). CREs can mediate gene regulation and their differentiation might play an important role in CAM photosynthesis (Monson, 2012). Another promising aspect of exploring gene regulation is the analysis of promoters, which regulate differential expression in (facultative) CAM plants under drought-stress (Yang et al., 2015).

To identify the desiccation strategy in resurrection grasses, St. Aubin et al. (2022) used an approach based on the dynamic chromatin network and RNA levels. They found a strong association of the analyzed chromatin accessibility and transcriptional abundance. In their study they could identify several genes, which show a binding site for the TF *ABA INSENSITIVE 5 ABI5*, indicating an important role of transcriptional regulation when it comes to dry periods. However, complex signaling networks often involve various TFs. To get a deeper understanding about how this might be true for water stress in *A. thaliana*, (Song et al. (2016) studied DNA sequences that bind to 21 ABA-related TFs *in vivo*. They could observe that the binding to the TFs is mostly increased after ABA treatment, but some TFs showed a static or decreasing binding behavior, indicating the importance of locus-specific gene regulation. However, there are additional methods to identify *cis*-regulatory elements. The self-transcribing active regulatory region sequencing (STARR-seq) offers a high-throughput identification of potential enhancers (Jores et al., 2020). It is based on infiltration of *Nicotiana benthamiana* leaves with *Agrobacterium tumefaciens* containing a library of DNA sequences. This relative robust and fast method allows identification of *cis*-elements and can help to gain deeper understanding of the regulatory network of plants.

There is a variety of approaches, like the GUS (Jefferson, 1989) or the RUBY (He et al., 2020) reporter gene system, which target the understanding of gene regulation. However, studying

gene regulatory networks cannot only be done in the organism of interest, but also by using orthogonal systems, like mammalian cell lines or plant cells (Andres et al., 2019; Andres and Zurbriggen, 2022; Ochoa-Fernandez et al., 2020). Gene regulatory networks are highly complex, which can make their analysis *in planta* difficult. Taking advantage of the modular and combinatorial synthetic approaches can lead to a faster and easier understanding. As more methods become available, the regulation network can be explored in a more advanced way.

Protein turnover

Proteins can have structural functions, play a role in cell signaling or function as enzymes to catalyze reactions. Proteins can function as TFs and its amount is influenced by the regulation through protein turnover (Nelson and Millar, 2015). Updating the protein content is dependent on the number of proteins that are formed and degraded, a process which needs to be tightly regulated. Synthesis might be influenced by post-transcriptional modifications, while post-translational modifications can play a role in protein degradation (Nelson and Millar, 2015). Protein synthesis in plants takes place at the ribosome and is the single most costly process (Edwards et al., 2012). Degradation mostly takes place in the cytosol or nucleus by the ubiquitin proteasome system (UPS). E1, E2 and E3 ligases form the UPS and tag proteins, which need to be degraded. Multiple ubiquitin will be tagged, which gives the signal for the degradation through the proteasome. Protein stability is mainly influenced by the protein's location and its interaction with other proteins (Gibbs et al., 2014). To adapt to environmental or developmental changes, the balance between the rate of synthesis and degradation needs to be regulated (Edwards et al., 2012).

Availability of an increasing number of genomic and transcriptomic studies make it possible to connect protein turnover with photosynthetic metabolisms. In a recent study, Abraham et al. (2020) analyzed a large-scale proteomics dataset of epidermis and mesophyll cells from the obligate CAM plant *K. fedtschenkoi*. 5002 proteins with 2718 protein groups in epidermis cells and 3582 proteins and 1973 groups in mesophyll cell, with 60% overlap have been identified. Abraham et al. (2020) showed that there is tissue-specificity regarding malate, pyruvate and starch metabolism. In addition to that, Heinemann et al. (2021) observed that guard cells show a diel rescheduling of starch turnover, compared to findings from *A. thaliana*. Drought stressed *A. thaliana* plants show 40% loss of leaf protein mass, leading to a higher content of free amino

acids in the cell. This can be used from the plant to synthesize proline, needed as an alternative substrate for photosynthetic-derived carbohydrates.

As protein turnover interplays with the plant's metabolism, understanding this complex network will help to identify additional components of regulatory networks and can make plant engineering more fruitful.

References

Abraham, P.E., Hurtado Castano, N., Cowan-Turner, D., Barnes, J., Poudel, S., Hettich, R., Flütsch, S., Santelia, D., Borland, A.M., 2020. Peeling back the layers of crassulacean acid metabolism: functional differentiation between Kalanchoë fedtschenkoi epidermis and mesophyll proteomes. Plant Journal 103, 869–888. https://doi.org/10.1111/tpj.14757

Abraham, P.E., Yin, H., Borland, A.M., Weighill, D., Lim, S.D., De Paoli, H.C., Engle, N., Jones, P.C., Agh, R., Weston, D.J., Wullschleger, S.D., Tschaplinski, T., Jacobson, D., Cushman, J.C., Hettich, R.L., Tuskan, G.A., Yang, X., 2016. Transcript, protein and metabolite temporal dynamics in the CAM plant Agave. Nat Plants 2, 1–10. https://doi.org/10.1038/nplants.2016.178

Aldous, S.H., Weise, S.E., Sharkey, T.D., Waldera-Lupa, D.M., Stühler, K., Mallmann, J., Groth, G., Gowik, U., Westhoff, P., Arsova, B., 2014. Evolution of the phosphoenolpyruvate carboxylase protein kinase family in C3 and C4 flaveria spp. Plant Physiol 165, 1076–1091. https://doi.org/10.1104/pp.114.240283

Alonso-Cantabrana, H., Cousins, A.B., Danila, F., Ryan, T., Sharwood, R.E., Von Caemmerer, S., Furbank, R.T., 2018. Diffusion of CO2 across the mesophyll-bundle sheath cell interface in a C4 plant with genetically reduced PEP carboxylase activity. Plant Physiol 178, 72–81. https://doi.org/10.1104/pp.18.00618

Amin, A.B., Rathnayake, K.N., Yim, W.C., Garcia, T.M., Wone, B., Cushman, J.C., Wone, B.W.M., 2019. Crassulacean acid metabolism abiotic stress-responsive transcription factors: A potential genetic engineering approach for improving crop tolerance to abiotic stress. Front Plant Sci 10. https://doi.org/10.3389/fpls.2019.00129

Borland, A.M., Hartwell, J., Weston, D.J., Schlauch, K.A., Tschaplinski, T.J., Tuskan, G.A., Yang, X., Cushman, J.C., 2014. Engineering crassulacean acid metabolism to improve water-use efficiency. Trends Plant Sci. https://doi.org/10.1016/j.tplants.2014.01.006

Boxall, S.F., Foster, J.M., Bohnert, H.J., Cushman, J.C., Nimmo, H.G., Hartwell, J., 2005. Conservation and divergence of circadian clock operation in a stress-inducible Crassulacean acid metabolism species reveals clock compensation against stress. Plant Physiol 137, 969–982. https://doi.org/10.1104/pp.104.054577

Boxall, S.F., Kadu, N., Dever, L. V, Knerova, J., Waller, J.L., Gould, P.D., Hartwell, J., 2020. Kalanchoë PPC1 is Essential for Crassulacean Acid Metabolism and the Regulation of

Core Circadian Clock and Guard Cell Signaling Genes. Plant Cell. https://doi.org/10.1105/tpc.19.00481

Bräutigam, A., Schliesky, S., Külahoglu, C., Osborne, C.P., Weber, A.P.M., 2014. Towards an integrative model of C4 photosynthetic subtypes: Insights from comparative transcriptome analysis of NAD-ME, NADP-ME, and PEP-CK C4 species. J Exp Bot 65, 3579–3593. https://doi.org/10.1093/jxb/eru100

Bräutigam, A., Schlüter, U., Eisenhut, M., Gowik, U., 2017. On the evolutionary origin of CAM photosynthesis. Plant Physiol 174, 473–477. https://doi.org/10.1104/pp.17.00195

Brilhaus, D., Bräutigam, A., Mettler-Altmann, T., Winter, K., Weber, A.P.M., 2016. Reversible Burst of Transcriptional Changes during Induction of Crassulacean Acid Metabolism in Talinum triangulare . Plant Physiol 170, 102–122. https://doi.org/10.1104/pp.15.01076

Burgos, A., Miranda, E., Vilaprinyo, E., Meza-Canales, I.D., Alves, R., 2022. CAM Models: Lessons and Implications for CAM Evolution. Front Plant Sci 13. https://doi.org/10.3389/fpls.2022.893095

Chang, C., Bowman, J.L., Meyerowitz, E.M., 2016. Field Guide to Plant Model Systems. Cell 167, 325–339. https://doi.org/10.1016/j.cell.2016.08.031

Chen, L.Y., Xin, Y., Wai, C.M., Liu, J., Ming, R., 2020. The role of cis-elements in the evolution of crassulacean acid metabolism photosynthesis. Hortic Res 7. https://doi.org/10.1038/s41438-019-0229-0

Chu, C., Dai, Z., Ku, M.S.B., Edwards, G.E., 1990. Induction of crassulacean acid metabolism in the facultative halophyte Mesembryanthemum crystallinum by abscisic acid. Plant Physiol 93, 1253–1260. https://doi.org/10.1104/pp.93.3.1253

Conesa, A., Madrigal, P., Tarazona, S., Gomez-Cabrero, D., Cervera, A., McPherson, A., Szcześniak, M.W., Gaffney, D.J., Elo, L.L., Zhang, X., Mortazavi, A., 2016. A survey of best practices for RNA-seq data analysis. Genome Biol 17, 1–19. https://doi.org/10.1186/s13059-016-0881-8

Covington, M.F., Maloof, J.N., Straume, M., Kay, S.A., Harmer, S.L., 2008. Global transcriptome analysis reveals circadian regulation of key pathways in plant growth and development. Genome Biol 9. https://doi.org/10.1186/gb-2008-9-8-r130

Cushman, J.C., Tillett, R.L., Wood, J.A., Branco, J.M., Schlauch, K.A., 2008. Large-scale mRNA expression profiling in the common ice plant, Mesembryanthemum crystallinum,

performing C3 photosynthesis and Crassulacean acid metabolism (CAM), in: Journal of Experimental Botany. pp. 1875–1894. https://doi.org/10.1093/jxb/ern008

da Rosa Ferraz Jardim, A.M., de Morais, J.E.F., de Souza, L.S.B., da Silva, T.G.F., 2022. Understanding interactive processes: a review of CO2 flux, evapotranspiration, and energy partitioning under stressful conditions in dry forest and agricultural environments. Environ Monit Assess 194. https://doi.org/10.1007/s10661-022-10339-7

Dai, Z., Ku, M.S.B., Zhang, D., Edwards, G.E., 1994. Effects of growth regulators on the induction of Crassulacean acid metabolism in the facultative halophyte Mesembryanthemum crystallinum L. Planta 192, 287–294. https://doi.org/10.1007/BF00198562

Deng, H., Zhang, L.S., Zhang, G.Q., Zheng, B.Q., Liu, Z.J., Wang, Y., 2016. Evolutionary history of PEPC genes in green plants: Implications for the evolution of CAM in orchids. Mol Phylogenet Evol 94, 559–564. https://doi.org/10.1016/j.ympev.2015.10.007

DePaoli, H.C., Borland, A.M., Tuskan, G.A., Cushman, J.C., Yang, X., 2014. Synthetic biology as it relates to CAM photosynthesis: Challenges and opportunities. J Exp Bot 65, 3381–3393. https://doi.org/10.1093/jxb/eru038

Dever, L. V., Bailey, K.J., Lacuesta, M., Leegood, R.C., Lea, P.J., 1996. The isolation and characterization of mutants of the C4 plant Amaranthus edulis. Comptes Rendus de l'Academie des Sciences - Serie III 319, 951–959.

Drennan, P.M., Nobel, P.S., 2000. Responses of CAM species to increasing atmospheric CO2 concentrations. Plant Cell Environ 23, 767–781. https://doi.org/10.1046/j.1365-3040.2000.00588.x

Edwards, J.M., Roberts, T.H., Atwell, B.J., 2012. Quantifying ATP turnover in anoxic coleoptiles of rice (Oryza sativa) demonstrates preferential allocation of energy to protein synthesis. J Exp Bot 63, 4389–4402. https://doi.org/10.1093/JXB/ERS114

Ehleringer, J.R., Sage, R.F., Flanagan, L.B., Pearcy, R.W., 1991. Climate change and the evolution of C4 photosynthesis. Trends Ecol Evol 6, 95–99. https://doi.org/10.1016/0169-5347(91)90183-X

Ehlers, I., Augusti, A., Betson, T.R., Nilsson, M.B., Marshall, J.D., Schleucher, J., 2015. Detecting long-term metabolic shifts using isotopomers: CO2-driven suppression of photorespiration in C3 plants over the 20th century. Proc Natl Acad Sci U S A 112, 15585–15590. https://doi.org/10.1073/pnas.1504493112

Ellis, R.J., 1979. The most abundant protein in the world. Trends Biochem Sci 4, 241–244. https://doi.org/10.1016/0968-0004(79)90212-3

Ferrari, R.C., Cruz, B.C., Gastaldi, V.D., Storl, T., Ferrari, E.C., Boxall, S.F., Hartwell, J., Freschi, L., 2020. Exploring C4–CAM plasticity within the Portulaca oleracea complex. Sci Rep 10. https://doi.org/10.1038/s41598-020-71012-y

Ferrari, R.C., Kawabata, A.B., Ferreira, S.S., Hartwell, J., Freschi, L., 2022a. A matter of time: Regulatory events behind the synchronization of C4and crassulacean acid metabolism in Portulaca oleracea. J Exp Bot 73, 4867–4885. https://doi.org/10.1093/jxb/erac163

Ferrari, R.C., Kawabata, A.B., Ferreira, S.S., Hartwell, J., Freschi, L., 2022b. A matter of time: Regulatory events behind the synchronization of C4and crassulacean acid metabolism in Portulaca oleracea. J Exp Bot 73, 4867–4885. https://doi.org/10.1093/jxb/erac163

Flügel, F., Timm, S., Arrivault, S., Florian, A., Stitt, M., Fernie, A.R., Bauwe, H., 2017. The Photorespiratory Metabolite 2-Phosphoglycolate Regulates Photosynthesis and Starch Accumulation in Arabidopsis. Plant Cell 29, 2537. https://doi.org/10.1105/TPC.17.00256

Gibbs, D.J., Bacardit, J., Bachmair, A., Holdsworth, M.J., 2014. The eukaryotic N-end rule pathway: conserved mechanisms and diverse functions. Trends Cell Biol 24, 603–611. https://doi.org/10.1016/J.TCB.2014.05.001

Gilman, I.S., Edwards, E.J., 2020. Crassulacean acid metabolism. Current Biology 30, R57–R62. https://doi.org/10.1016/j.cub.2019.11.073

Gilman, I.S., Moreno-Villena, J.J., Lewis, Z.R., Goolsby, E.W., Edwards, E.J., 2022. Gene co-expression reveals the modularity and integration of C4 and CAM in Portulaca. Plant Physiol 189, 735–753. https://doi.org/10.1093/plphys/kiac116

Grada, A., Weinbrecht, K., 2013. Next-generation sequencing: Methodology and application. Journal of Investigative Dermatology 133, e11-4. https://doi.org/10.1038/jid.2013.248

Hartwell, J., 2005. The co-ordination of central plant metabolism by the circadian clock. Biochem Soc Trans 33, 945–948. https://doi.org/10.1042/BST20050945

Hartwell, J., Smith, L.H., Wilkins, M.B., Jenkins, G.I., Nimmo, H.G., 1996. Higher plant phosphoenolpyruvate carboxylase kinase is regulated at the level of translatable mRNA in response to light or a circadian rhythm. Plant Journal. https://doi.org/10.1046/j.1365-313X.1996.10061071.x

Heinemann, B., Künzler, P., Eubel, H., Braun, H.P., Hildebrandt, T.M., 2021. Estimating the number of protein molecules in a plant cell: protein and amino acid homeostasis during drought. Plant Physiol 185, 385–404. https://doi.org/10.1093/PLPHYS/KIAA050

Heyduk, K., Hwang, M., Albert, V., Silvera, K., Lan, T., Farr, K., Chang, T.-H., Chan, M.-T., Winter, K., Leebens-Mack, J., 2019. Altered Gene Regulatory Networks Are Associated With the Transition From C3 to Crassulacean Acid Metabolism in Erycina (Oncidiinae: Orchidaceae). Front Plant Sci 9, 1–15. https://doi.org/10.3389/fpls.2018.02000

Kaul, S., Koo, H.L., Jenkins, J., Rizzo, M., Rooney, T., Tallon, L.J., Feldblyum, T., Nierman, W., Benito, M.I., Lin, X., Town, C.D., Venter, J.C., Fraser, C.M., Tabata, S., Nakamura, Y., Kaneko, T., Sato, S., Asamizu, E., Kato, T., Kotani, H., Sasamoto, S., Ecker, J.R., Theologis, A., Federspiel, N.A., Palm, C.J., Osborne, B.I., Shinn, P., Dewar, K., Kim, C.J., Buehler, E., Dunn, P., Chao, Q., Chen, H., Theologis, A., Osborne, B.I., Vysotskaia, V.S., Lenz, C.A., Kim, C.J., Hansen, N.F., Liu, S.X., Buehler, E., Alta, H., Sakano, H., Dunn, P., Lam, B., Pham, P.K., Chao, Q., Nguyen, M., Yu, G., Chen, H., Southwick, A., Lee, J.M., Miranda, M., Toriumi, M.J., Davis, R.W., Federspiel, N.A., Palm, C.J., Conway, A.B., Conn, L., Hansen, N.F., Hootan, A., Lam, B., Wambutt, R., Murphy, G., Düsterhöft, A., Stiekema, W., Pohl, T., Entian, K.D., Terryn, N., Volckaert, G., Salanoubat, M., Choisne, N., Artiguenave, F., Weissenbach, J., Quetier, F., Rieger, M., Ansorge, W., Unseld, M., Fartmann, B., Valle, G., Wilson, R.K., Sekhon, M., Pepin, K., Murray, J., Johnson, D., Hillier, L., de la Bastide, M., Huang, E., Spiegel, L., Gnoj, L., Habermann, K., Dedhia, N., Parnell, L., Preston, R., Marra, M., McCombie, W.R., Chen, E., Martienssen, R., Mayer, K., Lemcke, K., Haas, B., Haase, D., Rudd, S., Schoof, H., Frishman, D., Morgenstern, B., Zaccaria, P., Mewes, H.W., White, O., Creasy, T.H., Bielke, C., Maiti, R., Peterson, J., Ermolaeva, M., Pertea, M., Quackenbush, J., Volfovsky, N., Wu, D., Salzberg, S.L., Bevan, M., Lowe, T.M., Rounsley, S., Bush, D., Subramaniam, S., Levin, I., Norris, S., Schmidt, R., Acarkan, A., Bancroft, I., Brennicke, A., Eisen, J.A., Bureau, T., Legault, B.A., Le, Q.H., Agrawal, N., Yu, Z., Copenhaver, G.P., Luo, S., Preuss, D., Pikaard, C.S., Paulsen, I.T., Sussman, M., Britt, A.B., Selinger, D.A., Pandey, R., Chandler, V.L., Jorgensen, R.A., Mount, D.W., Pikaard, C., Juergens, G., Meyerowitz, E.M., Dangl, J., Jones, J.D.G., Chen, M., Chory, J., Somerville, C., 2000. Analysis of the genome sequence of the flowering plant Arabidopsis thaliana. Nature 2000 408:6814 408, 796–815. https://doi.org/10.1038/35048692

Kim, J.A., Kim, H.S., Choi, S.H., Jang, J.Y., Jeong, M.J., Lee, S.I., 2017. The importance of the circadian clock in regulating plant metabolism. Int J Mol Sci 18. https://doi.org/10.3390/ijms18122680

Krämer, U., 2015. Planting molecular functions in an ecological context with Arabidopsis thaliana. Elife 4. https://doi.org/10.7554/eLife.06100

Kück, U. (Ed.), 2005. Praktikum der Molekulargenetik. Springer-Lehrbuch. https://doi.org/10.1007/B137618

Lim, S.D., Lee, S., Choi, W.G., Yim, W.C., Cushman, J.C., 2019. Laying the foundation for crassulacean acid metabolism (CAM) biodesign: Expression of the c 4 metabolism cycle genes of CAM in arabidopsis. Front Plant Sci 10, 1–20. https://doi.org/10.3389/fpls.2019.00101

Liu, D., Palla, K.J., Hu, R., Moseley, R.C., Mendoza, C., Chen, M., Abraham, P.E., Labbé, J.L., Kalluri, U.C., Tschaplinski, T.J., Cushman, J.C., Borland, A.M., Tuskan, G.A., Yang, X., 2018. Perspectives on the basic and applied aspects of crassulacean acid metabolism (CAM) research. Plant Science 274, 394–401. https://doi.org/10.1016/j.plantsci.2018.06.012

Lüttge, U., Ball, E., 1980. 2H+:1 malate2− stoichiometry during Crassulacean Acid Metabolism is unaffected by lipophilic cations. Plant Cell Environ 3, 195–200. https://doi.org/10.1111/1365-3040.ep11581541

Maleckova, E., Brilhaus, D., Wrobel, T.J., Weber, A.P.M., 2019. Transcript and Metabolite Changes during the Early Phase of ABA-mediated Induction of CAM in Talinum triangulare. J Exp Bot. https://doi.org/10.1093/jxb/erz189

McClung, C.R., Salomé, P.A., Michael, T.P., 2002. The Arabidopsis Circadian System. Arabidopsis Book 1, e0044. https://doi.org/10.1199/tab.0044

Monson, R.K., 2012. Gene Duplication , Neofunctionalization , and the Evolution of C4 Photosynthesis Author (s): Russell K . Monson Reviewed work (s): Source : International Journal of Plant Sciences , Vol . 164 , No . S3 , Evolution of Functional Traits in Plants (May 164.

Monson, R.K., Moore, B. d., 1989. On the significance of C3—C4 intermediate photosynthesis to the evolution of C4 photosynthesis. Plant Cell Environ 12, 689–699. https://doi.org/10.1111/J.1365-3040.1989.TB01629.X

Moseley, R.C., Mewalal, R., Motta, F., Tuskan, G.A., Haase, S., Yang, X., 2018. Conservation and diversification of circadian rhythmicity between a model crassulacean acid

metabolism plant kalanchoë fedtschenkoi and a model C3 photosynthesis plant arabidopsis thaliana. Front Plant Sci 871, 1–14. https://doi.org/10.3389/fpls.2018.01757

Nelson, C.J., Millar, A.H., 2015. Protein turnover in plant biology. Nature Plants 2015 1:3 1, 1–7. https://doi.org/10.1038/nplants.2015.17

Nelson, E.A., Sage, R.F., 2008. Functional constraints of CAM leaf anatomy: tight cell packing is associated with increased CAM function across a gradient of CAM expression. J Exp Bot 59, 1841–1850. https://doi.org/10.1093/JXB/ERM346

Osmond, C.B., 1978. Crassulacean Acid Metabolism: A Curiosity in Context. Annu Rev Plant Physiol 29, 379–414. https://doi.org/10.1146/annurev.pp.29.060178.002115

Pierce, S., Winter, K., Griffiths, H., 2002. Carbon isotope ratio and the extent of daily CAM use by Bromeliaceae. New Phytologist 156, 75–83. https://doi.org/10.1046/J.1469-8137.2002.00489.X

Ping, C.Y., Chen, F.C., Cheng, T.C., Lin, H.L., Lin, T.S., Yang, W.J., Lee, Y.I., 2018. Expression profiles of phosphoenolpyruvate carboxylase and phosphoenolpyruvate carboxylase kinase genes in phalaenopsis, implications for regulating the performance of crassulacean acid metabolism. Front Plant Sci 871, 1–10. https://doi.org/10.3389/fpls.2018.01587

Raven, J. a, Edwards, D., 2014. Photosynthesis in Bryophytes and Early Land Plants. Diversification in evolving enviroments 37, 29–58. https://doi.org/10.1007/978-94-007-6988-5

Reyes-Prieto, A., Weber, A.P.M., Bhattacharya, D., 2007. The Origin and Establishment of the Plastid in Algae and Plants. https://doi.org/10.1146/annurev.genet.41.110306.130134 41, 147–168. https://doi.org/10.1146/ANNUREV.GENET.41.110306.130134

Sage, R.F., 2004. The evolution of C4 photosynthesis. New Phytologist 161, 341–370. https://doi.org/10.1111/J.1469-8137.2004.00974.X

Schiller, K., Bräutigam, A., 2021. Engineering of Crassulacean Acid Metabolism. Annu Rev Plant Biol 72, 77–103. https://doi.org/10.1146/annurev-arplant-071720-104814

Schlüter, U., Weber, A.P., 2019. Synthetic evolution of C 4 photosynthesis. The FASEB Journal 33, 183–215. https://doi.org/10.1096/fasebj.2019.33.1_supplement.343.4

Schmitz, R.J., Grotewold, E., Stam, M., 2022. Cis-regulatory sequences in plants: Their importance, discovery, and future challenges. Plant Cell 34, 718. https://doi.org/10.1093/PLCELL/KOAB281

Shameer, S., Baghalian, K., Cheung, C.Y.M., Ratcliffe, R.G., Sweetlove, L.J., 2018. Computational analysis of the productivity potential of CAM. Nat Plants 4, 165–171. https://doi.org/10.1038/s41477-018-0112-2

Silvera, K., Santiago, L.S., Cushman, J.C., Winter, K., 2010. The incidence of crassulacean acid metabolism in Orchidaceae derived from carbon isotope ratios: A checklist of the flora of Panama and Costa Rica. Botanical Journal of the Linnean Society 163, 194–222. https://doi.org/10.1111/j.1095-8339.2010.01058.x

St. Aubin, B., Wai, C.M., Kenchanmane Raju, S.K., Niederhuth, C.E., VanBuren, R., 2022. Regulatory dynamics distinguishing desiccation tolerance strategies within resurrection grasses. Plant Direct 6, 1–14. https://doi.org/10.1002/pld3.457

Strader, L., Weijers, D., Wagner, D., 2022. Plant transcription factors — being in the right place with the right company. Curr Opin Plant Biol 65, 102136. https://doi.org/10.1016/j.pbi.2021.102136

Taybi, T., Cushman, J.C., 2002. Abscisic acid signaling and protein synthesis requirements for phosphoenolpyruvate carboxylase transcript induction in the common ice plant. J Plant Physiol 159, 1235–1243. https://doi.org/10.1078/0176-1617-00834

Taybi, T., Cushman, J.C., Borland, A.M., 2017. Leaf carbohydrates influence transcriptional and post-transcriptional regulation of nocturnal carboxylation and starch degradation in the facultative CAM plant, Mesembryanthemum crystallinum. J Plant Physiol 218, 144–154. https://doi.org/10.1016/j.jplph.2017.07.021

Taybi, T., Nimmo, H.G., Borland, A.M., 2004. Expression of phosphoenolpyruvate carboxylase and phosphoenolpyruvate carboxylase kinase genes. Implications for genotypic capacity and phenotypic plasticity in the expression of crassulacean acid metabolism. Plant Physiol 135, 587–598. https://doi.org/10.1104/pp.103.036962

Theng, V., Agarie, S., Nose, A., 2007. Regulatory properties of phosphoenolpyruvate carboxylase in crassulacean acid metabolism plants: Diurnal changes in phosphorylation state and regulation of gene expression. Plant Prod Sci 10, 171–181. https://doi.org/10.1626/pps.10.171

Ting, I.P., 1981. Effects of abscisic acid on CAM in Portulacaria afra. Photosynth Res 48, 39–48.

Töpfer, N., Braam, T., Shameer, S., Ratcliffe, R.G., Sweetlove, L.J., 2020. CAM emerges in a leaf metabolic model under water-saving constraints in different environments. bioRxiv. https://doi.org/10.1101/2020.01.20.912782

Villalobos, M.A., Bartels, D., Iturriaga, G., 2004. Stress tolerance and glucose insensitive phenotypes in Arabidopsis overexpressing the CpMYB10 transcription factor gene. Plant Physiol 135, 309–324. https://doi.org/10.1104/pp.103.034199

Von Wilbert, D.J., Kramer, D., 1972. Feinstruktur und Crassulaceen-Säurestoffwechsel in Blättern von Mesembryanthemum crystallinum während natürlicher und NaCl-induzierter Alterung, Source: Planta.

Wai, C.M., Weise, S.E., Ozersky, P., Mockler, T.C., Michael, T.P., Vanburen, R., 2019. Time of day and network reprogramming during drought induced CAM photosynthesis in Sedum album, PLoS Genetics. https://doi.org/10.1371/journal.pgen.1008209

Walker, B.J., Vanloocke, A., Bernacchi, C.J., Ort, D.R., 2016. The Costs of Photorespiration to Food Production Now and in the Future. Annu Rev Plant Biol 67, 107–129. https://doi.org/10.1146/annurev-arplant-043015-111709

Wang, N., Zhong, X., Cong, Y., Wang, T., Yang, S., Li, Y., Gai, J., 2016. Genome-wide Analysis of Phosphoenolpyruvate Carboxylase Gene Family and Their Response to Abiotic Stresses in Soybean. Sci Rep 6, 1–14. https://doi.org/10.1038/srep38448

West-eberhard, M.J., Smith, J.A.C., Winter, K., 2011. Photosynthesis, Reorganized 332.

Winter, K., 2019. Ecophysiology of constitutive and facultative CAM photosynthesis. J Exp Bot. https://doi.org/10.1093/jxb/erz002

Winter, K., Holtum, J.A.M., 2014. Facultative crassulacean acid metabolism (CAM) plants: powerful tools for unravelling the functional elements of CAM photosynthesis. J Exp Bot 65, 3425–3441. https://doi.org/10.1093/jxb/eru063

Winter, K., Holtum, J.A.M., 2007. Environment or development? Lifetime net CO2 exchange and control of the expression of Crassulacean acid metabolism in Mesembryanthemum crystallinum. Plant Physiol 143, 98–107. https://doi.org/10.1104/pp.106.088922

Winter, K., Holtum, J.A.M., Smith, J.A.C., 2015. Crassulacean acid metabolism: A continuous or discrete trait? New Phytologist. https://doi.org/10.1111/nph.13446

Winter, K., Smith, J.A.C., 2022. CAM photosynthesis: the acid test. New Phytologist. https://doi.org/10.1111/nph.17790

Winter, K., Smith, J.A.C., 1996. An Introduction to Crassulacean Acid Metabolism. Biochemical Principles and Ecological Diversity 1–13. https://doi.org/10.1007/978-3-642-79060-7_1

Winter, K., Virgo, A., Garcia, M., Aranda, J., Holtum, J.A.M., 2021. Constitutive and facultative crassulacean acid metabolism (CAM) in Cuban oregano, Coleus amboinicus (Lamiaceae). Functional Plant Biology 48, 647–654. https://doi.org/10.1071/FP20127

Yang, X., Cushman, J.C., Borland, A.M., Edwards, E.J., Wullschleger, S.D., Tuskan, G.A., Owen, N.A., Griffiths, H., Smith, J.A.C., De Paoli, H.C., Weston, D.J., Cottingham, R., Hartwell, J., Davis, S.C., Silvera, K., Ming, R., Schlauch, K., Abraham, P., Stewart, J.R., Guo, H.B., Albion, R., Ha, J., Lim, S.D., Wone, B.W.M., Yim, W.C., Garcia, T., Mayer, J.A., Petereit, J., Nair, S.S., Casey, E., Hettich, R.L., Ceusters, J., Ranjan, P., Palla, K.J., Yin, H., Reyes-García, C., Andrade, J.L., Freschi, L., Beltrán, J.D., Dever, L. V., Boxall, S.F., Waller, J., Davies, J., Bupphada, P., Kadu, N., Winter, K., Sage, R.F., Aguilar, C.N., Schmutz, J., Jenkins, J., Holtum, J.A.M., 2015. A roadmap for research on crassulacean acid metabolism (CAM) to enhance sustainable food and bioenergy production in a hotter, drier world. New Phytologist 207, 491–504. https://doi.org/10.1111/nph.13393

Yang, X., Cushman, J.C., Borland, A.M., Liu, Q., 2020. Editorial: Systems Biology and Synthetic Biology in Relation to Drought Tolerance or Avoidance in Plants. Front Plant Sci. https://doi.org/10.3389/fpls.2020.00394

Yang, X., Hu, R., Yin, H., Jenkins, J., Shu, S., Tang, H., Liu, D., Weighill, D.A., Cheol Yim, W., Ha, J., Heyduk, K., Goodstein, D.M., Guo, H.B., Moseley, R.C., Fitzek, E., Jawdy, S., Zhang, Z., Xie, M., Hartwell, J., Grimwood, J., Abraham, P.E., Mewalal, R., Beltrán, J.D., Boxall, S.F., Dever, L. V., Palla, K.J., Albion, R., Garcia, T., Mayer, J.A., Don Lim, S., Man Wai, C., Peluso, P., Van Buren, R., De Paoli, H.C., Borland, A.M., Guo, H., Chen, J.G., Muchero, W., Yin, Y., Jacobson, D.A., Tschaplinski, T.J., Hettich, R.L., Ming, R., Winter, K., Leebens-Mack, J.H., Smith, J.A.C., Cushman, J.C., Schmutz, J., Tuskan, G.A., 2017. The Kalanchoë genome provides insights into convergent evolution and building blocks of crassulacean acid metabolism. Nat Commun 8. https://doi.org/10.1038/s41467-017-01491-7

Manuscript I

Photorespiration is the solution, not the problem

Laia Segura Broncano[1], Krzysztof Robin Pukacz[1], Vanessa Reichel-Deland[1], Urte Schlüter[1], Sebastian Triesch[1], Andreas P.M. Weber[1]

[1]Institute of Plant Biochemistry, Cluster of Excellence on Plant Science (CEPLAS), Universitätsstraße 1, 40225 Düsseldorf, Germany

Authors contribution:

All authors equally contributed to this commentary and are listed in alphabetical order.

Abstract

The entry of carbon dioxide from the atmosphere into the biosphere is mediated by the enzyme Rubisco, which catalyzes the carboxylation of ribulose 1,5-bisphosphate (RuBP) as the entry reaction of the Calvin Benson Bassham cycle (CBBC), leading to the formation of 2 molecules of 3-phosphoglyceric acid (3PGA) per CO_2 fixed. 3PGA is reduced to triose phosphates at the expense of NADPH + H^+ and ATP that are provided by the photosynthetic light reactions. Triose phosphates are the principal products of the CBBC and the precursors for almost any compound in the biosphere.

Introduction

Every year, in the order of 150 Gt of carbon are transferred from the atmosphere to the biosphere by the Rubisco reaction (Jian et al., 2022). The current atmosphere contains approx. 900 Gt C (Friedlingstein et al., 2022), which means that every six to seven years, the entire atmospheric carbon pool is routed once through Rubisco in plants, algae, and cyanobacteria. However, the acronym Rubisco stands for RuBP carboxylase/oxygenase, specifying that Rubisco does not only carboxylate but also oxidize RuBP. The oxygenation reaction leads to the formation of 2-phosphoglycolic acid (2PG), which is an inhibitor of some CBBC enzymes and hence 2PG must be efficiently removed to avoid blockage of the CBBC by the oxygenation product of Rubisco. Further, 2PG must be transformed into molecules that are compatible with plant metabolism. This is achieved by a metabolic repair pathway called photorespiration.

Bauwe (2023) provides an authoritative account of photorespiration, with a particular emphasis on the involved enzymes, starting with the different forms of Rubisco and Rubisco-like proteins and their evolutionary history, and moving on to the "Magnificent Ten", the core set of enzymes in chloroplasts, peroxisomes, mitochondria and cytoplasm that jointly convert 2PG to 3PGA. Figure 4 in Bauwe (2023) shows the entire pathway, hence we refer to this figure for the details. A unique strength of this review is its focus on the enzyme components of the pathway, their structures (where available), and their catalytic mechanisms. Thereby Bauwe (2023) develops a detailed picture of how deeply photorespiration is embedded in plant metabolism, beyond its immediate role in enabling oxygenic photosynthesis.

Photorespiration is frequently portrayed as a wasteful pathway that reduces the efficiency of photosynthesis. Indeed, the removal of 2PG and its conversion to 3PGA requires energy and redox power and it leads to the release of previously fixed CO_2 and ammonia. Bauwe's review stands out by emphasizing that photorespiration is the solution to a problem (i.e., the oxygenation reaction of Rubisco), and not the problem itself. In fact, photosynthesis in an oxygen-containing environment would not be possible without photorespiration. Even cyanobacteria that utilize very efficient carbon concentrating mechanisms (CCMs) have multiple, partially redundant routes for detoxification of 2PG and their deletion is lethal. The same holds for C_4 plants – mutations in the photorespiratory pathway are lethal or lead to

severe growth retardation, indicating that carbon concentrating mechanisms are insufficient to fully suppress the oxygenation reaction (Levey et al., 2019; Zelitch et al., 2009).

Integration of photorespiration into leaf nitrogen network

Bauwe reminds us that photorespiration serves multiple functions beyond the detoxification of 2PG. In the C3 leaf, photorespiration considerably contributes to balancing of C, N and energy metabolism. The photorespiratory cycle does not just work as a closed system, but is interlinked with the metabolic network of the leaf and is dynamically redirecting C and N from the CBBC to a range of other pathways. Indeed, in C3 plants, photorespiration serves as the major source for Serine (Ser). Fu et al. (Fu et al., 2022) recently measured the rate of amino acid export from photorespiration and found that between 27 and 39% of Ser was exported from the pathway under ambient O_2 and CO_2 conditions (Figure 1). Although Ser can also be produced by the phosphorylated Ser biosynthesis pathway that is essential for plant growth and survival (Zimmermann et al., 2021), it seems to be advantageous for the C3 leaf to meet serine demands during the day mainly from photorespiration. Photorespiratory Ser serves also as dominant precursor for O-acetylserine and subsequent cysteine synthesis connecting photorespiration to Sulfur metabolism of the leaf (Samuilov et al., 2018). Ser derived compounds such as dehydrins, glutathione, glycine betaines or glucosinolates can also improve stress tolerance of the leaf (Busch, 2020).

Glycine (Gly), like Ser, can also directly feed into protein biosynthesis. Gly to Ser conversion in mitochondria during photorespiration is also deeply interlinked with C1 metabolism. Draining of glycine and C1 compounds from photorespiration alters the amount of CO_2 released from the oxygenase reaction of Rubisco (Busch, 2020). Fu et al. (2022) suggest that photorespiratory Gly serves as a dynamic, metabolically largely benign buffer that can store photorespiration-derived carbon and nitrogen until it can be further processed in the downstream pathways. Bauwe (2023) also highlights the substrate promiscuity of the peroxisomal serine:glyoxylate aminotransferase, which can use alanine (Ala) instead of Ser as an amino donor, thereby affording metabolic flexibility and balancing of leaf amino acid metabolism upon withdrawal of Ser or Gly from the pathway.

Photorespiration correlated positively to rates of N uptake and assimilation (Rachmilevitch et al., 2004). The mechanisms underpinning this phenomenon are not yet resolved, but

withdrawal of amino acids from photorespiration increases the demand for *de novo* N assimilation (Busch et al., 2018). Lower rates of photosynthesis during photorespiratory conditions could also improve availability of ferredoxin for N assimilation in the plastids (Huma et al., 2018; Rachmilevitch et al., 2004). Influence of photorespiration on whole plant performance is mainly discussed under the aspect of C and energy loss, but photorespiration can also have positive effects on plant composition and fitness (Rachmilevitch et al., 2004; Busch et al., 2018). Under elevated CO_2 concentrations, C3 species show a reduction in N content (Bloom et al., 2010). With the evolution of CO_2 concentrating mechanisms in land plants, such as C4, N metabolism apparently adjusted to the reduced rates of photorespiration in C4 leaves. Interestingly, C4 plants have lower rates of N assimilation compared to C3. This can be explained by lower demand for proteins in the assimilatory machinery of the leaf. Recent modelling studies, however, suggest that N metabolism and availability played an important role during evolution of C4 photosynthesis (Blätke and Bräutigam, 2019; Sundermann et al., 2021). In terms of resource allocation, phenotypic plasticity of C4 plants could be reduced (Sundermann et al., 2021).

Evolutionary origins of photorespiration

Being an integral part of the core heterotrophic metabolism, photorespiration was subject to rapid evolutionary turnovers. Bauwe (2023) reconstructs the ancient origins of photorespiration: while core enzymes were recruited from alpha-proteobacterial carbon metabolism, PGLP seems to originate from archaea and GLYK seems to be of cyanobacterial origin. PGLP, GS and SHMT can even be found in the minimal set of 102 gene families that are thought to be present in the last universal common ancestor (LUCA). The gene products might have played a role in the autotrophic methanogenic lifestyle of LUCA, e.g. in Gly and Ser biogenesis (Weiss et al., 2018, 2016). Bauwe (2023) goes even further back in time and reminds us that lower-molecular photorespiratory intermediates such as glycolate, glycine, sugars and even nucleobases can also be formed via ZnS-catalysis in abiotic environments (Omran et al., 2020).

Oxygenic photosynthesis arose with the emergence of heterodimeric PSII clusters with oxygen evolving complexes in cyanobacteria (Allen and Martin, 2007). Photorespiration in these organisms was likely built upon pre-existing metabolic modules. The peroxisome likely

evolved concomitantly with the installation of a mitochondrion as the result of an endosymbiosis event between an archaeal host and an alpha-proteobacterium. The installation of a chloroplast likely involved a eukaryotic cell with an endosymbiotic cyanobacterium. Glycolate excreted from the nascent plastid may have contributed to the carbon flux from endosymbiont to the host cell.

Apart from its evolution as a detoxification pathway for 2PG, photorespiration can also be seen as a keystone for further evolutionary progress: Bauwe (2023) points out that high levels of photorespiration reduce photosynthetic efficiency, which may have provided a selective force for the evolution of CCMs. In nature these mechanisms take the form of pyrenoids or carboxysomes in algae and cyanobacteria, respectively, or CAM and C4 photosynthesis in land plants. Bauwe (2023) highlights that in the evolution of C4 photosynthesis, photorespiration was initially split up between mesophyll and bundle-sheath cells, installing a photorespiratory glycine shuttle. Interestingly, this glycine shuttle created an N-imbalance between both cell types which required the installation of what today can be observed as a full C4 photosynthetic pathway (Mallmann et al., 2014).

The photorespiratory pathway in green algae differs from that of land plants

Recent work has also suggested an important role for photorespiration in algae. Most green algae have a reduced rate of photorespiration thanks to their CO_2 concentrating mechanism, which is based on the active transport of inorganic carbon into a phase-separated Rubisco condensate known as the pyrenoid. This increases the CO_2:O_2 ratio in proximity to Rubisco, preventing RuBP oxygenation. The photorespiration pathway in green algae is significantly different from that of plants, where the processing of glycolate occurs in the peroxisome (Figure 3 of Bauwe, 2023). In algae, glycolate oxidation occurs in the mitochondria, eliminating the peroxisome from the pathway. In addition, the photorespiration rate of *Chlamydomonas reinhardtii* increases significantly in response to decreasing CO_2 concentration, which is thought to protect the plants from increased 2-PG generation. For a more detailed review of the *C. reinhardtii* CCM and its relationship with photorespiration, see (Wang et al., 2015).

Photorespiration also plays a role in the regulation of the algal CCM itself. Previously thought to be induced by low CO_2 concentrations, recent studies (reviewed in (Adler et al., 2022)) suggest that photorespiratory intermediates play a role in regulating the CCM in *C. reinhardtii*.

Overall, it appears that photorespiration is still an essential part of the primary metabolism of green algae, protecting metabolism from toxins and acting as a regulator of photosynthesis.

Engineering of photorespiratory bypasses as a tool to better understand photorespiration

Photorespiration acts as a driving force for the transport of reducing equivalents between organelles during the day and as a pathway that enables the re-routing of carbon (and nitrogen). Bauwe (2023) reminds us that photorespiration is an open pathway that directly taps into core plant metabolism and enables, rather than limits plant photosynthesis and encourages a shift in photorespiration research towards a more positive view of the process. The study of photorespiration heavily relies on the availability of mutants that are defective in photorespiration-specific enzymes. However, mutations in photorespiration or photorespiration-associated genes are only viable under elevated CO_2 conditions. The strong alterations caused by the accumulation of intermediates in photorespiratory mutants, undeniably cause detrimental effects in several cellular processes (Timm and Bauwe, 2013). Overall, the physiology of photorespiratory mutants complicates the assessment of the impact of gene deletions compared to the impact of altered environmental conditions. While these studies have immensely contributed to a comprehensive understanding of the evolution of the photorespiratory pathway and its interplay with primary metabolism, Bauwe (2023) brings to our attention new research directions for further understanding this complicated process.

In attempts to increase plant yield, numerous approaches are being taken towards so-called CO_2-neutral and CO_2-positive photorespiratory bypasses (Trudeau et al., 2018). The consequences of the implementation of artificial bypasses in relationship to native metabolism and photorespiration itself are not fully understood yet. Taking the complex nature of photorespiration into account, it seems worth considering utilizing novel metabolic routes that bypass photorespiration to gain a more comprehensive view of the additional roles that photorespiration plays in plant metabolism. Photorespiratory bypasses present us with the opportunity to study the function of photorespiratory metabolites while still effectively detoxifying 2-PG, increasing the viability of mutants in ambient conditions.

Declaration of competing interest

The authors declare that they have no known competing financial interests or personal relationships that could have appeared to influence the work reported in this paper.

Data availability

No data was used for the research described in the article.

Acknowledgements

The authors appreciate funding by the ERA-CAPS project "C4BREED" under Project ID WE 2231/20–1, the Cluster of Excellence for Plant Sciences (CEPLAS) under Germany's Excellence Strategy EXC-2048/1 under project ID 390686111, the H2020 EU project "GAIN4CROPS", and the IRTG 2466 "NextPlant" grant by the German Research Foundation (DFG).

References

Adler, L., Díaz-Ramos, A., Mao, Y., Pukacz, K.R., Fei, C., McCormick, A.J., 2022. New horizons for building pyrenoid-based CO2-concentrating mechanisms in plants to improve yields. Plant Physiol 190, 1609–1627. https://doi.org/10.1093/plphys/kiac373

Allen, J.F., Martin, W., 2007. Out of thin air. Nature 445, 610–612. https://doi.org/10.1038/445610a

Blätke, M.-A., Bräutigam, A., 2019. Evolution of C4 photosynthesis predicted by constraint-based modelling. Elife 8, e49305. https://doi.org/10.7554/elife.49305

Bloom, A.J., Burger, M., Asensio, J.S.R., Cousins, A.B., 2010. Carbon Dioxide Enrichment Inhibits Nitrate Assimilation in Wheat and Arabidopsis. Science 328, 899–903. https://doi.org/10.1126/science.1186440

Busch, F.A., 2020. Photorespiration in the context of Rubisco biochemistry, CO2 diffusion and metabolism. Plant J. https://doi.org/10.1111/tpj.14674

Busch, F.A., Sage, R.F., Farquhar, G.D., 2018. Plants increase CO2 uptake by assimilating nitrogen via the photorespiratory pathway. Nat Plants 4, 46–54. https://doi.org/10.1038/s41477-017-0065-x

Friedlingstein, P., O'Sullivan, M., Jones, M.W., Andrew, R.M., Gregor, L., Hauck, J., Quéré, C.L., Luijkx, I.T., Olsen, A., Peters, G.P., Peters, W., Pongratz, J., Schwingshackl, C., Sitch, S., Canadell, J.G., Ciais, P., Jackson, R.B., Alin, S.R., Alkama, R., Arneth, A., Arora, V.K., Bates, N.R., Becker, M., Bellouin, N., Bittig, H.C., Bopp, L., Chevallier, F., Chini, L.P., Cronin, M., Evans, W., Falk, S., Feely, R.A., Gasser, T., Gehlen, M., Gkritzalis, T., Gloege, L., Grassi, G., Gruber, N., Gürses, Ö., Harris, I., Hefner, M., Houghton, R.A., Hurtt, G.C., Iida, Y., Ilyina, T., Jain, A.K., Jersild, A., Kadono, K., Kato, E., Kennedy, D., Goldewijk, K.K., Knauer, J., Korsbakken, J.I., Landschützer, P., Lefèvre, N., Lindsay, K., Liu, J., Liu, Z., Marland, G., Mayot, N., McGrath, M.J., Metzl, N., Monacci, N.M., Munro, D.R., Nakaoka, S.-I., Niwa, Y., O'Brien, K., Ono, T., Palmer, P.I., Pan, N., Pierrot, D., Pocock, K., Poulter, B., Resplandy, L., Robertson, E., Rödenbeck, C., Rodriguez, C., Rosan, T.M., Schwinger, J., Séférian, R., Shutler, J.D., Skjelvan, I., Steinhoff, T., Sun, Q., Sutton, A.J., Sweeney, C., Takao, S., Tanhua, T., Tans, P.P., Tian, X., Tian, H., Tilbrook, B., Tsujino, H., Tubiello, F., Werf, G.R. van der, Walker, A.P., Wanninkhof, R., Whitehead, C., Wranne, A.W., Wright, R., Yuan, W., Yue, C., Yue, X., Zaehle,

S., Zeng, J., Zheng, B., 2022. Global Carbon Budget 2022. Earth Syst Sci Data 14, 4811–4900. https://doi.org/10.5194/essd-14-4811-2022

Fu, X., Gregory, L.M., Weise, S.E., Walker, B.J., 2022. Integrated flux and pool size analysis in plant central metabolism reveals unique roles of glycine and serine during photorespiration. Nat Plants 1–10. https://doi.org/10.1038/s41477-022-01294-9

Huma, B., Kundu, S., Poolman, M.G., Kruger, N.J., Fell, D.A., 2018. Stoichiometric analysis of the energetics and metabolic impact of photorespiration in C3 plants. Plant J 96, 1228–1241. https://doi.org/10.1111/tpj.14105

Jian, J., Bailey, V., Dorheim, K., Konings, A.G., Hao, D., Shiklomanov, A.N., Snyder, A., Steele, M., Teramoto, M., Vargas, R., Bond-Lamberty, B., 2022. Historically inconsistent productivity and respiration fluxes in the global terrestrial carbon cycle. Nat Commun 13, 1733. https://doi.org/10.1038/s41467-022-29391-5

Levey, M., Timm, S., Mettler-Altmann, T., Borghi, G.L., Koczor, M., Arrivault, S., Weber, A.P., Bauwe, H., Gowik, U., Westhoff, P., 2019. Efficient 2-phosphoglycolate degradation is required to maintain carbon assimilation and allocation in the C4 plant Flaveria bidentis. J Exp Bot 70, 575–587. https://doi.org/10.1093/jxb/ery370

Mallmann, J., Heckmann, D., Bräutigam, A., Lercher, M.J., Weber, A.P.M., Westhoff, P., Gowik, U., 2014. The role of photorespiration during the evolution of C4 photosynthesis in the genus Flaveria. Elife 3, e02478–e02478. https://doi.org/10.7554/elife.02478

Omran, A., Menor-Salvan, C., Springsteen, G., Pasek, M., 2020. The Messy Alkaline Formose Reaction and Its Link to Metabolism. Life 10, 125. https://doi.org/10.3390/life10080125

Rachmilevitch, S., Cousins, A.B., Bloom, A.J., 2004. Nitrate assimilation in plant shoots depends on photorespiration. Proc Natl Acad Sci USA 101, 11506–10. https://doi.org/10.1073/pnas.0404388101

Samuilov, S., Brilhaus, D., Rademacher, N., Flachbart, S., Arab, L., Alfarraj, S., Kuhnert, F., Kopriva, S., Weber, A.P.M., Mettler-Altmann, T., Rennenberg, H., 2018. The Photorespiratory BOU Gene Mutation Alters Sulfur Assimilation and Its Crosstalk With Carbon and Nitrogen Metabolism in Arabidopsis thaliana. Front Plant Sci 9, 1709. https://doi.org/10.3389/fpls.2018.01709

Sundermann, E.M., Lercher, M.J., Heckmann, D., 2021. Modeling photosynthetic resource allocation connects physiology with evolutionary environments. Sci Rep 11, 15979. https://doi.org/10.1038/s41598-021-94903-0

Timm, S., Bauwe, H., 2013. The variety of photorespiratory phenotypes - employing the current status for future research directions on photorespiration. Plant Biol 15, 737–747. https://doi.org/10.1111/j.1438-8677.2012.00691.x

Trudeau, D.L., Edlich-Muth, C., Zarzycki, J., Scheffen, M., Goldsmith, M., Khersonsky, O., Avizemer, Z., Fleishman, S.J., Cotton, C.A.R., Erb, T.J., Tawfik, D.S., Bar-Even, A., 2018. Design and in vitro realization of carbon-conserving photorespiration. Proc Natl Acad Sci USA 115, E11455–E11464. https://doi.org/10.1073/pnas.1812605115

Wang, Y., Stessman, D.J., Spalding, M.H., 2015. The CO2 concentrating mechanism and photosynthetic carbon assimilation in limiting CO2: how Chlamydomonas works against the gradient. Plant J 82, 429–448. https://doi.org/10.1111/tpj.12829

Weiss, M.C., Preiner, M., Xavier, J.C., Zimorski, V., Martin, W.F., 2018. The last universal common ancestor between ancient Earth chemistry and the onset of genetics. PLoS Genet 14, e1007518. https://doi.org/10.1371/journal.pgen.1007518

Weiss, M.C., Sousa, F.L., Mrnjavac, N., Neukirchen, S., Roettger, M., Nelson-Sathi, S., Martin, W.F., 2016. The physiology and habitat of the last universal common ancestor. Nat Microbiol 1, 16116. https://doi.org/10.1038/nmicrobiol.2016.116

Zelitch, I., Schultes, N.P., Peterson, R.B., Brown, P., Brutnell, T.P., 2009. High glycolate oxidase activity is required for survival of maize in normal air. Plant Physiol 149, 195–204. https://doi.org/10.1104/pp.108.128439

Zimmermann, S.E., Benstein, R.M., Flores-Tornero, M., Blau, S., Anoman, A.D., Rosa-Téllez, S., Gerlich, S.C., Salem, M.A., Alseekh, S., Kopriva, S., Wewer, V., Flügge, U.-I., Jacoby, R.P., Fernie, A.R., Giavalisco, P., Ros, R., Krueger, S., 2021. The phosphorylated pathway of serine biosynthesis links plant growth with nitrogen metabolism. Plant Physiol 186, 1487–1506. https://doi.org/10.1093/plphys/kiab167

Figures

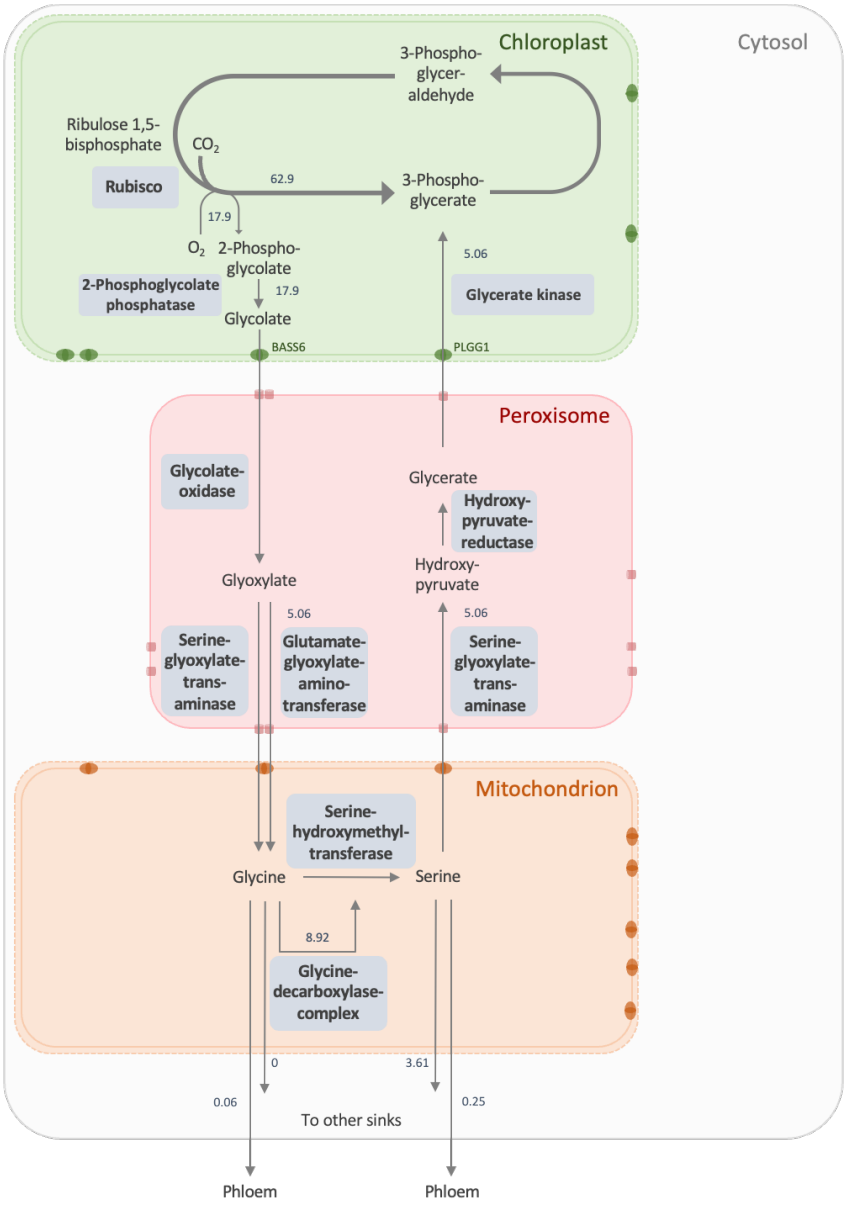

Figure 1: (A) Simplified scheme of the ten key enzymatic steps ("Magnificent Ten") and central metabolites of photorespiration in a single plant cell. Photorespiration in plants is distributed between the chloroplast, the peroxisome and the mitochondrion. The relative fluxes are taken from modelling approaches described in Fu (2022) assuming an atmospheric O_2 concentration of 21 %. Glycine and serine leave the mitochondria either via passive diffusion or transporters and to a substantial degree enter amino acid metabolism.

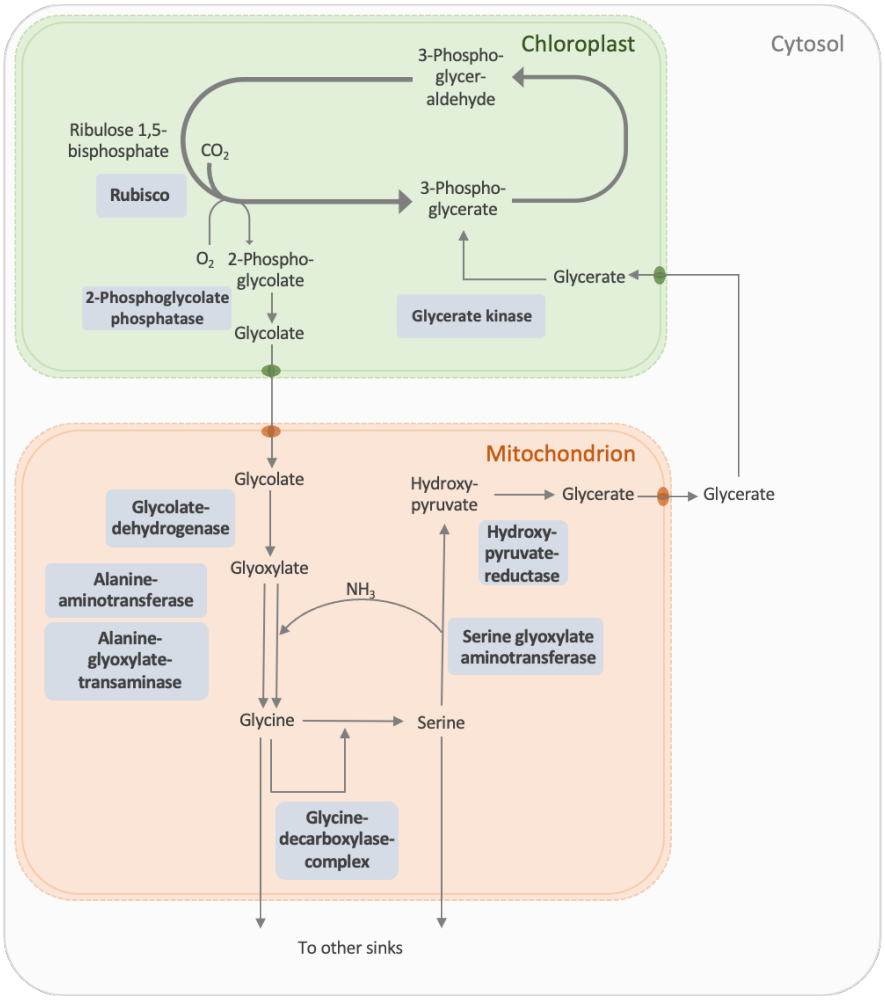

Continued Figure 1: (B) Simplified scheme of the nine key enzymatic steps and central metabolites of photorespiration in a single *Chlamydomonas reinhardtii* cell. In contrast to land plants, where glycolate processing takes place in the peroxisome, photorespiration in *C. reinhardtii* is limited to the chloroplast and mitochondrion. As a result, parts of the pathway are catalysed by different enzymes. Glycine and serine are transported to the cytosol and are fed into amino acid metabolism as well as other pathways.

Manuscript II

A toolbox to study the facultative CAM plant *Talinum fruticosum*

Vanessa Reichel-Deland[1], Marcel Derendorf[1], Jonas Schön[2], Astrid Daniela Aguierre Boyd[1], Matias D. Zurbriggen[2,3], Andreas P. M. Weber[1,3]

[1]Institute of Plant Biochemistry, Heinrich Heine University, Universitaetsstrasse 1, 40225 Duesseldorf, Germany

[2]Institute of Synthetic Biology, Heinrich Heine University, Universitaetsstrasse 1, 40225 Duesseldorf, Germany

[3]Cluster of Excellence on Plant Science (CEPLAS), Heinrich Heine University, Universitaetsstrasse 1, 40225 Duesseldorf, Germany

Author contribution:

V.R.-D., designed and performed the experiments and established the protocols for *T. fruticosum* protoplast isolation, *T. fruticosum* protoplast transformation and *T. fruticosum* nuclei isolation, supervised M.D. and A.D.A. and wrote the manuscript, M.D. performed the experiments for *T. fruticosum* seed sterilization, growth conditions and protein isolation, J.S. and A.D.A. assisted in performing the experiments, A.P.M.W. and M.D.Z. supervised the experiments. M.D., J.S., A.D.A. M.D.Z. and A.P.M.W. contributed to the writing of the manuscript.

Abstract

The earth´s environment is constantly changing, so plants need to adapt in order to survive. These major challenges are encountered by a variety of strategies evolved in the plant kingdom. The facultative crassulacean acid metabolism (CAM) plant *Talinum fruticosum* can overcome environmental stresses, such as drought, by reversibly transition from C_3 photosynthesis to the water-saving CAM photosynthesis. This strategy is not yet fully understood and knowledge of key players in metabolic pathways is lacking. *T. fruticosum* offers the opportunity to study two types of photosynthesis within one organism. Here we introduce new molecular methods that are crucial to gain a deeper understanding about signaling pathways and gene regulatory networks.

Introduction

In the year 2000 the Arabidopsis Genome Initiative published the genome sequence of the C_3 model plant *Arabidopsis thaliana* (Kaul et al., 2000). Availability of this genome sequence enabled the mechanistic understanding of many important functions in C_3 plants and it facilitated the formation of a big scientific community focusing on the model organism *A. thaliana*. Investigation of the establishment of a broad method spectrum has been fulfilled and in combination with an available genome made *A. thaliana* an easy C_3 model organism to work with.

The carbon concentrating strategy crassulacean acid metabolism (CAM) is present in 6% of all plant species (Silvera et al., 2010). Constitutive CAM plants are bound to its photosynthetic type and represent the most common form of CAM photosynthesis. In contrast to that, facultative CAM plants can adapt to its environment, by transitioning between C_3 or C_4 photosynthesis and CAM (Winter, 2019). Understanding the plants mechanism is from great interest in a rapidly changing environment, to make engineering of CAM photosynthesis into C_3 crops possible. CAM research has been well established in *Kalanchoë* species, most prominent in *Kalanchoë fedtschenkoi* or *Kalanchoë laxiflora* (Boxall et al., 2020; Yang et al., 2017). Both species perform a constitutive form of CAM photosynthesis and addressing research questions focusing on the transition from C_3 to CAM activity will therefore not be possible. The halophyte *Mesembryanthemum crystallinum* is a well-studied facultative CAM plant (Adams et al., 1998). However, the mechanism underlying this transition is not fully understood yet and therefore a greater variety of model plants is needed in order to solve questions regarding molecular mechanisms of CAM. To establish a model plant, it is necessary to develop a broad range of methods and make these available to the community. In this toolbox paper we introduce new approaches for working with the facultative CAM plant *Talinum fruticosum* (prev. *Talinum triangulare*). It is a perennial herbaceous dicot, native to semiarid or tropical regions, with dry and wet seasons (West-eberhard et al., 2011). *T. fruticosum* can transition between C_3 and CAM in a reversible manner, which makes it a suitable system to study and understand physiological and genetic underlying mechanisms of two types of photosynthesis in one plant. The genome (Brilhaus et al., 2023) and transcriptome data (Reichel-Deland, PhD thesis, Brilhaus et al., 2016; Maleckova et al., 2019) are available for *T. fruticosum*, which lays a great foundation for future work. However, deeper insights into

the underlying mechanisms of C_3 to CAM transition is missing, due to the lack of molecular approaches available.

Here we show a protocol for sterile propagation of seeds, necessary for *in planta* studies where a sterile environment is crucial. It will be needed for a number of approaches, such as screening of mutants as well as hormone or signal cascade studies. Moreover, we established protocols for protoplast isolation from mature *T. fruticosum* leaves and seedlings and its successful transformation. This important tool is crucial for understanding metabolic pathways and also allows a broad range of downstream applications. To further understand the gene regulatory networks, approaches such as the Assay for Transposase-Accessible Chromatin using sequencing (ATAC-seq) might be applied in the future. Thus, we established a protocol for nuclei isolation and sorting. In addition to that, a protocol for protein isolation is introduced, which might be needed for future proteomic approaches.

T. fruticosum offers great potential to serve as a model plant in CAM research. This toolbox manuscript lays the foundation to unravel new aspects that can lead to successful engineering of the CAM pathway into C_3 crops.

Material and Methods

Plant material and growth conditions

Talinum fruticosum can be sown directly into the soil or first germinated on half strength Murashige and Skoog (MS) plates before transferring to the soil. The pots are filled with potting soil (2/3 D400 with fertilizer and 1/3 Floraton) mixed with Vermiculite. The plants are grown in a controlled environment growth chamber in 12 h light at 25 °C and 65% humidity and 12 h dark at 22 °C and 70% humidity.

Sterilization of seeds and axenic growth

For the sterilization, about 100 seeds are soaked in 2 ml tap water and/or 5% (w/v) thiourea. After 48 h, the water is removed and the seeds are surface sterilized with 2 ml sterilization solution (2% sodium hypochlorite, 0.01% Triton X-100) for 15 min with gentle agitation from time to time. The sterilization solution is removed and three washing steps with sterile H_2O are performed. After the last washing step, the water is removed and it is suggested to move the seeds to the site of the tube to allow easier drying, preferably under a laminar-flow sterile hood. When the seeds are air dried, they can be sown on plates containing half strength Murashige and Skoog (MS). The plates should be sealed using Micropore tape to reduce evaporation and entry of contaminants. Depending on the downstream applications, the plates can either be placed vertically or flat in a controlled environmental growth-chamber with a 14 h light/10 h dark cycle with temperatures of 23 °C and 20 °C, respectively.

Protoplast isolation of *T. fruticosum* leaves

Two different approaches for protoplast isolation are suggested to allow work with *T. fruticosum* under sterile and non-sterile conditions, as well as for mature plants or seedlings.

Protoplast isolation of mature leaves

The protoplasts can be isolated from mature leaves of soil-grown plants. The protocol is modified from the TAPE-method (Wu et al., 2009). A leaf is gently adhered to a petri dish or, for younger leaves, to a 6-well-plate. The upper epidermis is attached to the plate by double-sided tape (Tesa, universal tape). Then, a single-sided tape (Tesa, transparent, 50 mm) is

applied to the lower epidermis and the lower epidermis is pulled of together with the tape. 4 ml or 10 ml, for smaller or bigger leaves respectively, of the enzyme solution (400 mM Mannitol, 20 mM MES-KOH, 20 mM KCl, 10 mM $CaCl_2$, 0.1% (w/v) Bovine serum albumin, 1.2% (w/v) Cellulase R-10, 0.4% w/v) Macroenzyme R-10 and 0.1% (w/v) Pectolyase Y-23 (enzymes: Duchefa Biochemie, The Netherlands) is added to a 6 well-plate or a petri-dish, respectively. The plate is sealed with parafilm and covered with aluminum foil. The incubation is done for 4 to 5 h in a growth chamber at 28 °C. To release the protoplasts, after incubation, the plate is slightly agitated. Protoplasts should be carefully resuspended using wide open tips (1 ml, sterile with filter, alpha laboratories). The filtering can be performed by usage of either four layers of miracloth or a 100 µm filter (Greiner). After a filtering step, protoplasts will sediment and supernatant can be removed. A washing step using 2-5 ml W5 buffer (154 mM NaCl, 125 mM $CaCl_2$, 5 mM KCl, 2 mM MES pH5.7) should be performed. The protoplasts will sediment by gravity and the supernatant can be removed again. Finally, the protoplasts are resuspended in an appropriate volume of W5 buffer for further application of the protoplasts.

Sterile protoplast isolation of seedlings

T. fruticosum seedlings are sterilized (as described above) and grown for 2-3 weeks on half strength MS plates without sucrose. The protocol is modified from Ochoa-Fernandez et al. (2020). 10 ml of MMC solution (400 mM Mannitol, 20 mM MES-KOH, 20 mM KCl, 10 mM $CaCl_2$, 0.1% (w/v) Bovine serum albumin) are added into a petri dish. Seedlings from four petri dishes (100 x 25 mm, about 50-75 seeds per plate), are chopped off. A sharp and sterile scalpel should be used to cut off the leaves and attention needs to be given to not transfer roots or media to the buffer. The leaves are chopped for three minutes in the buffer, until they are cut in very thin pieces. The chopped leaves are transferred to a new petri dish, containing 10 ml chopping buffer with enzymes (1.2% (w/v) Cellulase R-10, 0.4% w/v) Macroenzyme R-10 and 0.1% (w/v) Pectolyase Y-23 (enzymes: Duchefa Biochemie, The Netherlands). The plate should be sealed using parafilm. An incubation step is done at 28 °C for 4 h in the dark. After 4 h, the protoplasts are resuspended by using a 25 ml pipette. It is important to perform slow pipetting using a pipetting device. The resuspension is filtered through a 100 µm filter (Greiner) into a 50 ml falcon tube. Centrifugation is performed for 10 min at 100 g with low breaks in a swing bucket rotor. The supernatant can be removed and the protoplasts are resuspended in 3 ml W5 solution (154 mM NaCl, 125 mM $CaCl_2$, 5 mM KCl, 2 mM MES pH5.7) using a wide-bored tip

(1 ml, sterile with filter, alpha laboratories). Directly prior to downstream approaches, attention has to be paid that the protoplasts are fully suspended.

Preparation of a Percoll cushion for a clear protoplast solution

An isotonic Percoll stock is prepared by adding nine parts of Percoll (Sigma-Aldrich, USA, CAS: 65455-52-9) and one part 1.5 M NaCl (v/v). A dilution to a lower percentage can be achieved by using 0.15 M NaCl. 1.5 ml of a 20% Percoll solution is added to a 2 ml tube. 500 µl protoplast solution is carefully pipetted on top, using a wide-bored tip (1 ml, sterile with filter, alpha laboratories). After 20 min at room temperature, the protoplast solution is separated in the Percoll dilution. The protoplasts can be collected from the dark green layer underneath the surface (compare Figure 1 and Figure 4A).

PEG-mediated protoplast transformation

Transformation of *T. fruticosum* protoplasts was adapted from the protoplast transformation protocol of *A. thaliana*, published in Ochoa-Fernandez et al. (2020). 100 µl protoplast solution is taken after separation through a Percoll cushion. In a 6-well plate, 15 µg of plasmid DNA is mixed with the protoplast solution by gently mixing using a wide-bored tip. After 5 min of incubation at RT, the mixture is gently dispersed throughout the rim of the plate. 120 µl polyethylene glycol (PEG) solution (4 g PEG_{4000}, 3 ml H_2O, 2.5 ml 800 mM Mannitol, 1 ml 1M $CaCl_2$) is added dropwise to the entire surface. The plate should not be agitated from this point on. After an 8 min incubation step, two times 720 µl W5 (154 mM NaCl, 125 mM CaCl2, 5 mM KCl, 2 mM MES pH5.7) solution is added.

The plasmid used in this study, pROF144, carries a *UBQ10* promoter, the fluorescence reporter *Venus* and a *Nos* terminator (BsaI restricction-ligation reaction, GoldenBraid (Sarrion-Perdigones et al., 2013), with pPAtUbq10 (GB0223) + Venus (GB0053) + Tnos (GB0037) in 1alpha1 as destiny vector, compare Supplemental Figure S 1). The plasmid has been prepared using the NucleoBond Xtra Midi kit (Macherey-Nagel).

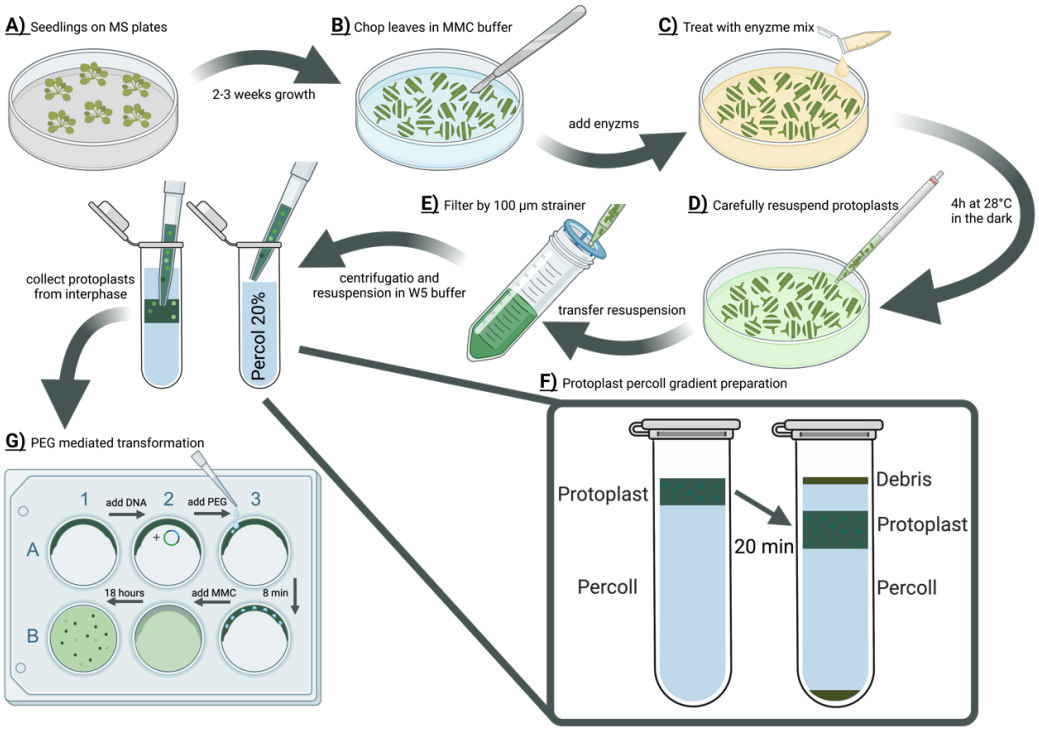

Figure 1: Overview of protoplast isolation from 2-3 weeks old sterile grown *T. fruticosum* seedlings. Leaves of the seedlings are separated from the roots and chopped in MMC solution (B). The thin leaf pieces are treated with an enzyme mixture to digest the cell wall (C). An incubation step is done in the dark at 28 °C for 4 h. The protoplasts are carefully resuspended (D) and the solution is filtered through a 100 µm filter (E). After centrifugation the supernatant containing digestive enzymes is removed and 500 µl protoplast solution is carefully added on top of 1.5 ml 20% Percoll solution (F). After 20 min the isolated protoplast layer can be recovered and used for subsequent PEG-mediated transformation (G).

Nuclei isolation of *T. fruticosum* leaves

Nuclei extraction is performed as published by Lu et al. (2017), with modifications. 0.5 g tissue is ground to coarse powder and filled in a 50 ml falcon tube. 30 mg Pectolyase Y-23 (Duchefa Biochemie), dissolved in 3 ml 15 mM acetate buffer (pH 5.5), is added to the tube. To allow enzymatic activity, a 10 min incubation step is performed at RT. Then, 37 ml isolation buffer (15 mM Tris pH 7.5, 2 mM EDTA, 80 mM KCl, 20 mM NaCl, 15 mM 2-Mercaptoethanol, 0.15% Triton-X 100 and 0.5 mM spermine) is added. During a 15 min incubation step on ice, the tube should be agitated gently every three minutes. After the incubation, the suspension is filtered using one layer of miracloth, followed by a second filtration through four layers of miracloth and subsequently a filtration through a 20 µM membrane (pluriSelect). The filtrate is then pipetted on top of an equal volume of a density gradient centrifugation buffer (1.7 M sucrose, 10 mM Tris pH 8, 2 mM $MgCl_2$, 5 mM 2-Mercaptoethanol, 1 mM EDTA and 0.15% Triton-X 100). After centrifugation (1800 g, 4 °C, 50 min), the pellet is carefully resuspended in 600 µl

Phosphate Buffered Saline (137 mM NaCl, 2.7 mM KCl, 10 mM Na_2HPO_4, and 1.8 mM KH_2PO_4) using wide-bored tips (1 ml, sterile with filter, alpha laboratories). For visualization, the nuclei are stained with 4,6-diamidino-2-phenylindole (DAPI). To separate the nuclei from debris, sorting can be done by using Fluorescence Activated Nuclei Sorting (FANS). Here, we sorted them at the Core Flow Cytometry Facility at the Düsseldorf University hospital. We used a MoFlo XDP sorter from Beckmann Coulter. A blue laser with 488 nm and a near UV laser with 375 nm wavelength is applied. A 100 µm nozzle, with 26 PSI and a maximal sorting speed of 10,000 events/sec is used for sorting.

Total protein isolation of *T. fruticosum* leaves

TCA/acetone extraction is modified from (Damerval et al., 1986). The steps are performed on ice and the solutions are pre-cooled at -20 °C. 1 ml ice cold 90% acetone/10% trichloroacetic acid (TCA) (v/w) with 0.07% (v/v) 2-Mercaptoethanol is added to 30 mg of powdered leaf tissue and vigorously mixed. The samples are frozen at -20°C for at least one hour followed by centrifugation at 16,000 g for 1 min at 4 °C. The pellet is washed with 500 µl acetone containing 0.07% 2-Mercaptoethanol, three times. After the third centrifugation step, the pellet is briefly dried at 37 °C and finally dissolved in resuspension buffer.

TCA/phenol extraction is adapted from (Wang et al., 2006). The steps are performed on ice and the solutions are pre-cooled at -20 °C. 200 mg of powdered leaf material is transferred to a 2 ml tube. The tube is filled up with 10% (w/v) TCA/phenol, followed by vigorous mixing. The mixture is kept on ice for 10 min and centrifuged at 16,000 g for 3 min at 4 °C. The supernatant is removed and the pellet is washed. 2 ml 80% (v/v) methanol containing 0.1 M ammonium acetate is added and vigorous mixing to remove TCA residuals. The centrifugation is done as before and the supernatant is decanted. To remove methanol residuals, the pellet is washed with 2 ml 80% (v/v) acetone by vigorous mixing. The sample is placed on ice for 5 min and centrifuged 16,000 g for 5 min at 4 °C. The supernatant is air-dried for 10 min and resuspension buffer can be added to the pellet.

The resuspension buffers tested include 0.1 M NaOH (with or without 5% SDS), Laemmli buffer (62.6 mM Tris base pH 6.8, 2% (w/v) SDS, 10% (v/v) glycerol, 5% 2-Mercaptoethanol) and 2% SDS in Tris-HCl pH 8.0. The pellet is resuspended by pipetting and/or shaking at 75 rpm at 10 °C when using Laemmli buffer.

The bicinchoninic acid assay (BCA) using the Pierce BCA Protein Assay Kit (Thermo Fisher Scientific Inc., USA, Cat. No. 23225) is performed following manufacturer's instruction for microplate procedure. A Bovine serum albumin (BSA) standard curve is generated and used for calculations. The protein samples are diluted 1:30 and assayed in triplicates. The proteins are detected in a Synergy H1 microplate reader (BioTek Instruments, USA) at 562 nm.

Results

As a yet non-model plant, where only a few methods are established, working with *T. fruticosum* is limited. However, as studies of this plant could lead to groundbreaking findings in adaptation to drought and its implication for crop engineering, we introduce new approaches to extend the possibilities of molecular research in *T. fruticosum*.

Sterilization of seeds and axenic growth

The sterile growth of seedlings is essential when it comes to molecular studies. In addition to the presence of a sterile environment, a high germination rate is needed to efficiently work with plants. *T. fruticosum* is native to tropics, but also faces semiarid and seasonally dry regions with periods of drought followed by rainfalls (Herrera, 2009; Herrera et al., 2015; Taisma and Herrera, 1998; Winter and Holtum, 2014). We experienced that sowing the seeds on soil without pre-treatment leads to a relatively low germination rate. Considering the origin of *T. fruticosum* we mimicked the wet season by pre-treatment with water to increase the germination rate. In order to find the best treatment possible, we included a second pre-treatment solution containing Thiourea. Thiourea is known for its seed dormancy breaking properties (Denny, 1930). It has already been applied to a variety of plant species to improve the germination (Patel et al., 2017). However, we did not only want to increase the germination rate, but also allow germination and growth in sterile conditions. This will allow to use sterile downstream approaches. *T. fruticosum* seeds are either soaked in water, water and 5% (w/v) thiourea or thiourea only, prior seed sterilization. The seeds are sterilized using bleach treatment, washed with sterile water and are air-dried before sowing on half-strength MS plates. Sterilization using ethanol treatment, does not lead to germination. For evaluation of the germination rate, it is monitored over 35 days after sowing. The influence of the different pre-treatments to the germination rate are compared. Figure 1 shows the germination rate in percentage from day 0 to day 35. We can show that seeds, which are soaked in water only, show the highest germination rate. In contrast to that 5% thiourea does not seem to increase the germination of *T. fruticosum*. Using the method described we can increase the germination rate of *T. fruticosum* seeds from almost 40% without pre-treatment to over 90% when soaked in water, after 35 days. Given the chance of sterile *T. fruticosum* seedlings we could design further studies using methods not yet established for this species.

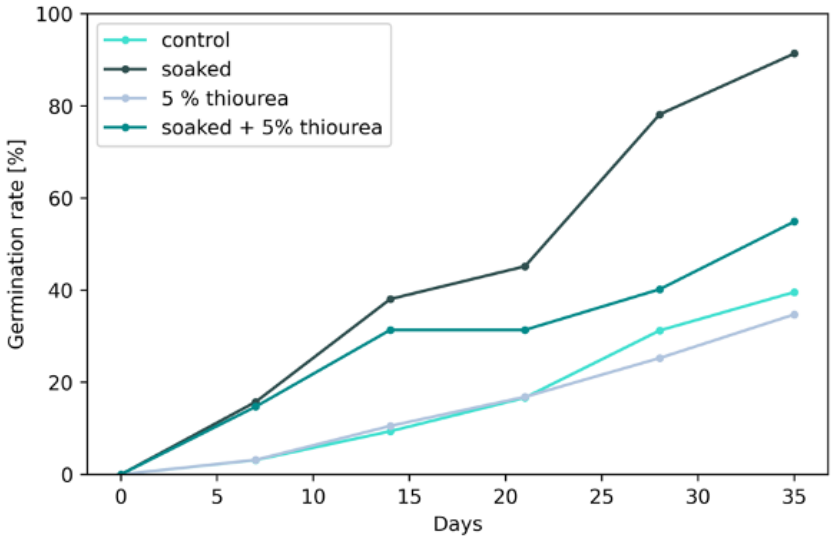

Figure 2: Germination rate of sterile *T. fruticosum* seeds.
Germination rate (%) is shown over 35 days. Treatments with water (soaked), 5% thiourea and water + 5% thiourea are compared and indicated by different colors, n=90-110.

T. fruticosum protoplasts as a new tool for CAM research

Protoplasts, cells with removed cell walls, can be used for a broad variety in plant research. Successful isolation and transformation of intact protoplasts can be used to gain a deeper understanding of metabolic pathways and gene regulatory networks on a single cell level. Moreover, approaches could include the cultivation of transformed protoplasts to regenerate new plants or hormone treatment to study signaling cascades. To make use of the benefits of the special photosynthetic plant *T. fruticosum*, we established methods to isolate protoplasts from its leaves. Two different protocols are introduced for isolating intact protoplasts. They can either be isolated from mature leaves or from sterile-grown seedlings, which will be needed for studies under sterile conditions. Using mature leaves instead of seedlings is cheaper and can therefore also be used from groups where possibilities for sterile work is limited.

Protoplast isolation of mature *T. fruticosum* leaves

T. fruticosum plants are grown in soil and the mature leaves are cut off for protoplast isolation. The protocol described is adapted from the TAPE-method established for *A. thaliana* (Wu et al., 2009). Using double-sided tape, the leaf is attached to a petri-dish (Figure 2A) and the upper epidermis is removed (Figure 2B). The addition of enzyme solution, containing

Pectolyase Y-23, will lead to protoplast release after an incubation of 4-5 h at 28 °C in the dark (Figure 2C). We experienced that the addition of Pectolyase Y-23 is necessary for receiving intact protoplasts from *T. fruticosum* leaves. Moreover, the pipetting should be done very carefully, always using wide-bored tips, to not damage the protoplasts. A washing step with W5 solution (Figure 2D) is performed to remove the debris. The intact protoplasts can be observed under the microscope (Figure 2E). The established protocol makes it possible to isolate protoplasts from mature *T. fruticosum* leaves, which can be used for further studies. However, it should be kept in mind that plants are not grown in sterile conditions.

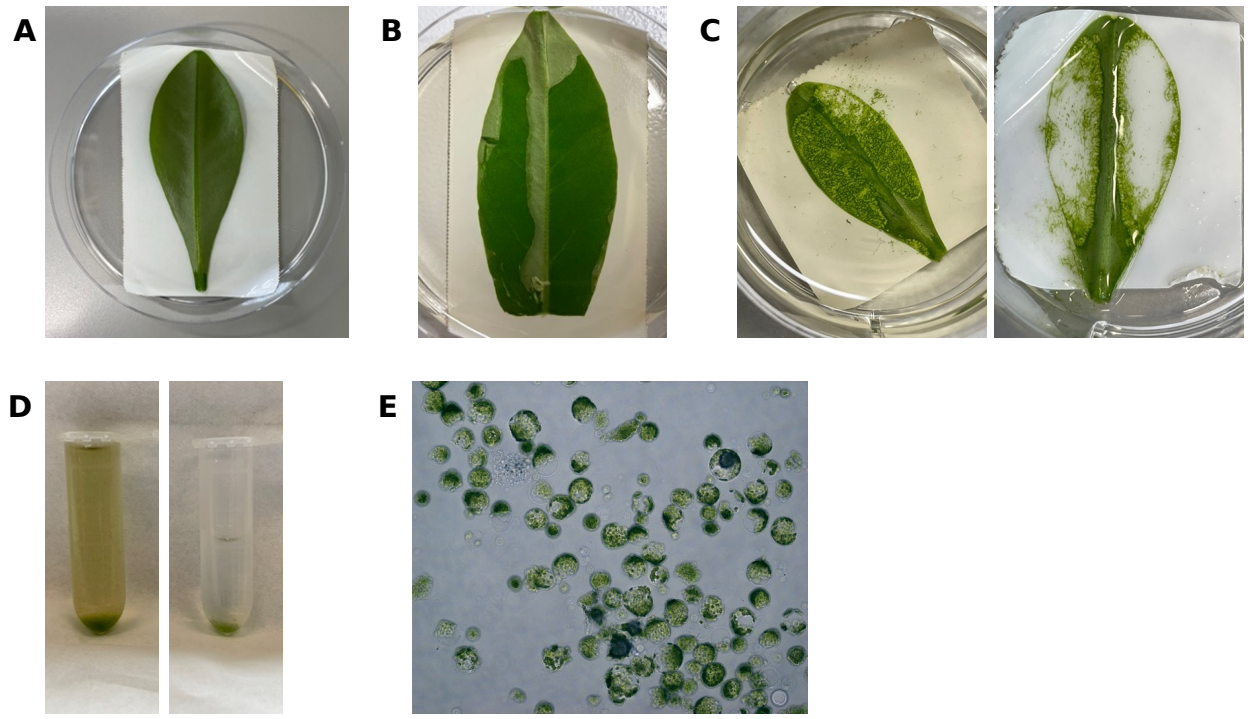

Figure 3: Overview of protoplast isolation from mature leaves of *T. fruticosum*.
A: A *T. fruticosum* leaf is sticked to double-sided tape with adaxial side facing the tape. B: The epidermis is removed using single-sided tape. C: Treatment with enzymes leads to release of the protoplasts into the solution after careful pipetting. D: The protoplasts are washed with W5 solution and can be observed under the microscope (Transmitted-light microscope, 20x) (E).

Protoplast isolation and transformation from sterile-grown *T. fruticosum* seedlings

To allow a broader range of molecular follow-up approaches, we established a protocol to isolate protoplasts from seedlings grown in sterile conditions. A schematic overview of the method can be seen in Figure 1. The leaves of the seedlings are chopped in isolation buffer, containing Pectolyase Y-23. The addition of enzymes and careful pipetting will lead to protoplast release after 4 h 28 °C incubation in the dark. Careful pipetting should be performed to homogenize the solution, followed by a filtering step. While filtering, the falcon tube should

be in an inclined angle, so that the protoplast can carefully slide through the side of the tube. Holding the falcon tube in a vertical position will lead to burst of a high number of the protoplasts. After the filtering step is done, the protoplasts are centrifuged. W5 solution is applied to the pellet and the protoplasts are released by careful pipetting. The isolated protoplasts can be observed under the microscope (Figure 4B).

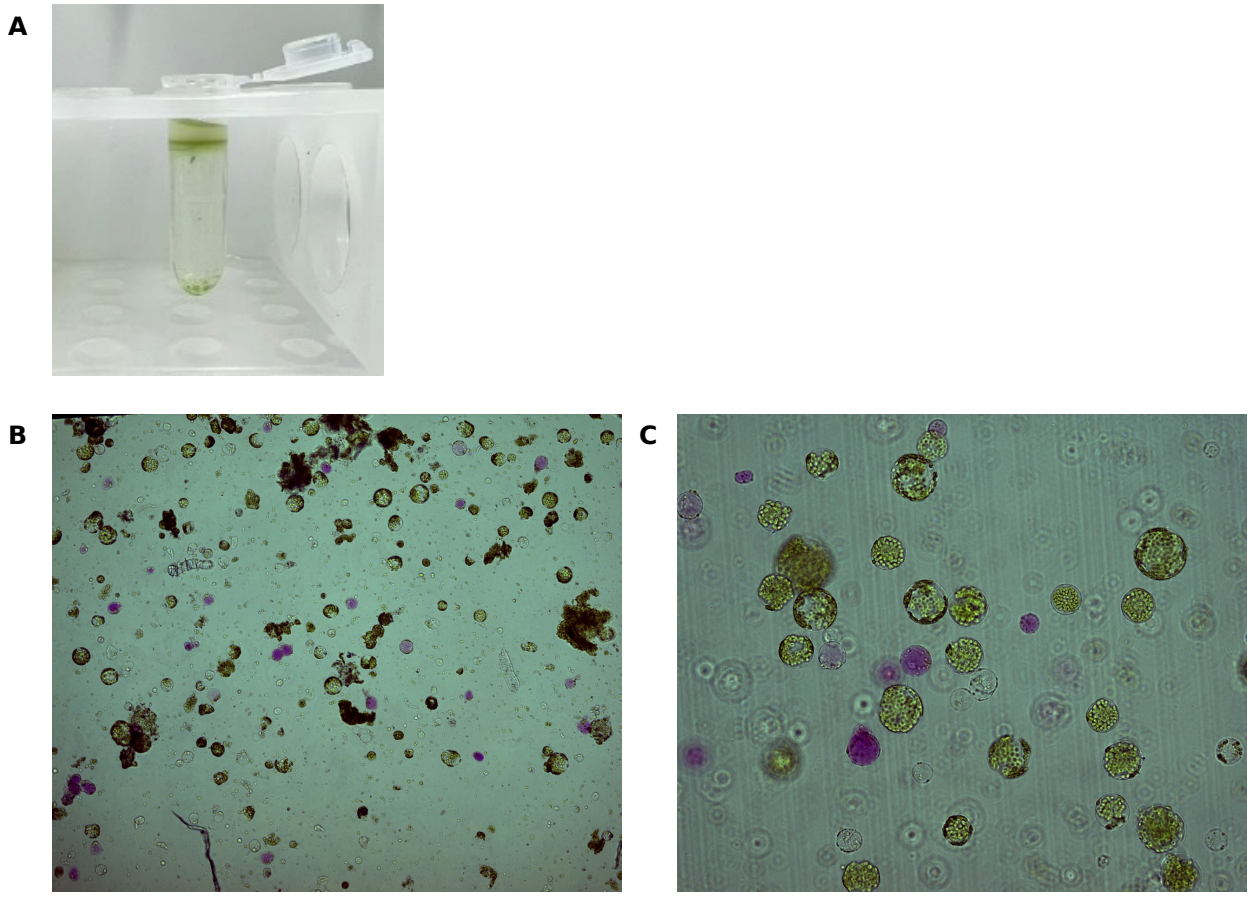

Figure 4: Protoplast isolation of T. fruticosum seedlings.
Microscopy images of the protoplast solution before (B, 10x) and after (C, 20x) clearance through a 20% Percoll-NaCl solution Percoll layer. The protoplasts are collected in one layer underneath the surface after 20 min incubation on a Percoll cushion (A).

However, the isolated protoplasts are intact, the solution still contains a lot of debris, which can make follow-up approaches, such as transformation and precise quantitative assays, difficult. Therefore, we suggest transferring the protoplast solution to a Percoll cushion. Here, a 20% Percoll-NaCl solution is prepared and overlaid with the protoplast solution. After 20 min at room temperature, the protoplasts are collected in the dark green layer underneath the surface (Figure 4A). Between the protoplast layer and the surface, damaged protoplasts and chlorophyll are found. Additional debris might also sink to the bottom of the tube. Using a

Percoll cushion for separation of protoplasts from debris and chlorophyll, leads to a clear solution of intact protoplasts (Figure 4C), which can be used for downstream applications.

Transformation of *T. fruticosum* protoplasts

Intact protoplasts, which are separated through a Percoll cushion can be used for downstream approaches. To study signaling pathways and gene regulatory networks, transformation of protoplasts might be essential. Therefore, we established a PEG-mediated protoplast transformation protocol. As a proof of principle, we used a construct expressing *Venus* under the control of a *UBQ10* promoter (compare Supplemental Figure S 1 for a detailed plasmid map). Venus is a fluorescent-based YFP reporter variant with an excitation peak at 515 nm and an emission peak at 528 nm (Nagai et al., 2002). 100 µl of the intact protoplast solution is transformed with 15 µg plasmid DNA. The transformed protoplasts are kept in the dark overnight. Then, the transformed protoplasts can be detected easily using a confocal or fluorescent microscope. Here, we performed confocal microscopy 18 h after transformation. Figure 5 shows two protoplasts by autofluorescence (B), where only one shows signal when excited at the specific wavelength for Venus expression (A). Both protoplasts show a round shape, indicating that the protoplasts are still intact after 18 h of incubation.

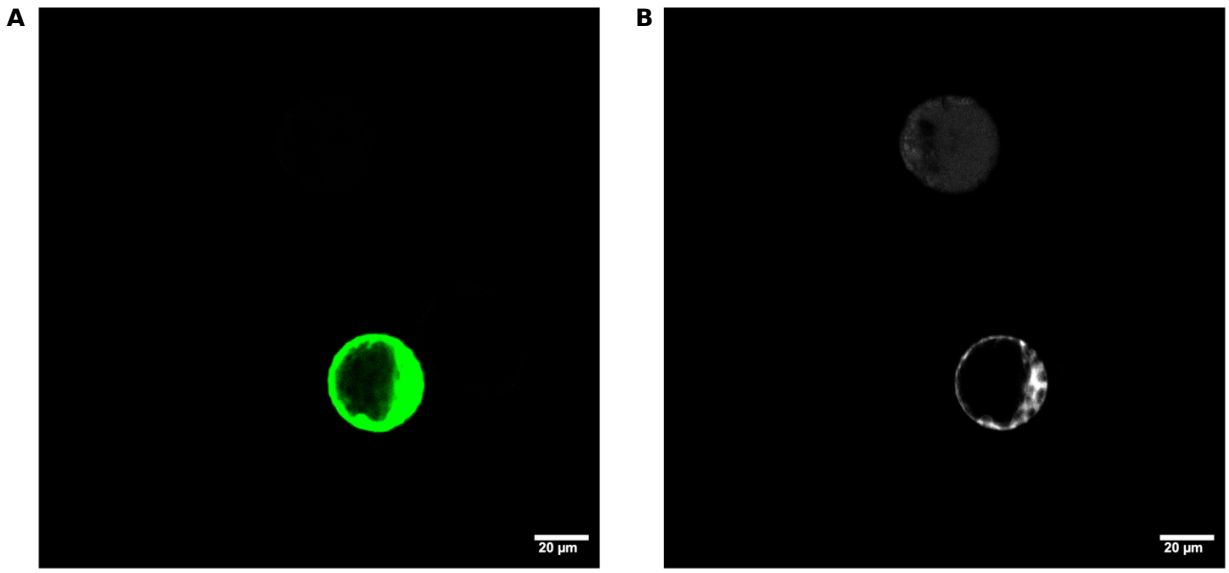

Figure 5: Protoplast transformed with a construct carrying *UBQ10:Venus:NosT*.
A: Image taken in GFP-channel, wo detect *Venus* expression, B: Image is taken without any filters to capture all autofluorescence. Both 20x.

Two protocols have been established to isolate intact protoplasts from *T. fruticosum* leaves. The protoplast isolation is possible from mature leaves or sterile-grown seedlings and the protoplasts can be used for downstream approaches such as transformation. Here, we could show successful transformation of *T. fruticosum* leaf protoplasts, proofed by detection of a Venus signal using confocal microscopy.

Nuclei isolation of *T. fruticosum* leaves

To understand the complexity of genetic regulation, assays about chromatin accessibility might be a promising approach. Therefore, we developed a protocol to isolate a high number of intact nuclei from *T. fruticosum* leaves. The nuclei are isolated from flash-frozen leaves, which are ground to coarse powder. Prior to addition of the lysis buffer, we add a 10 min incubation step with Pectolyase Y-23 to achieve a less viscous solution to continue with. We experienced that excluding the enzymatic step does lead to a very viscous solution, from which nuclei cannot be isolated successfully. The lysis is done for 15 min on ice, followed by filtration steps to remove the debris. The nuclei are separated by centrifugation over a sucrose gradient. Then, the pellet is resuspended in PBS buffer. Careful resuspension of the nuclei pellet is important. Therefore, it is suggested to use wide-bored tips. The nuclei can be visualized by staining with DAPI and observation can be done using a confocal or fluorescence microscope. Here, we observed different sizes of nuclei. However, the nuclei are shaped round and can be found separated from one another (Figure 6A and B). As a follow-up approach, we elucidated possible left-over debris using Fluorescence Activated Nuclei Sorting (FANS). This method is also used to receive a specific number of nuclei in an appropriate volume. As a proof of principle, we sorted the DAPI stained nuclei using a FANS with a 100 µm nozzle and a 375 nm and 488 nm laser. Figure 6C and D show the nuclei distribution for unstained and stained samples. The nuclei are distributed by their scattered light parameter. On the left side, respectively, the forward scatter is shown against the DAPI signal. When the nuclei are stained, the population changes it position to an increasing log height (D). The right diagram, of C and D respectively, shows the populations found in the forward and the side scatter. A population can only be found for the stained nuclei sample (D).

This protocol can be used for nuclei extraction of *T. fruticosum* leaves and might be adapted easily for other plant species.

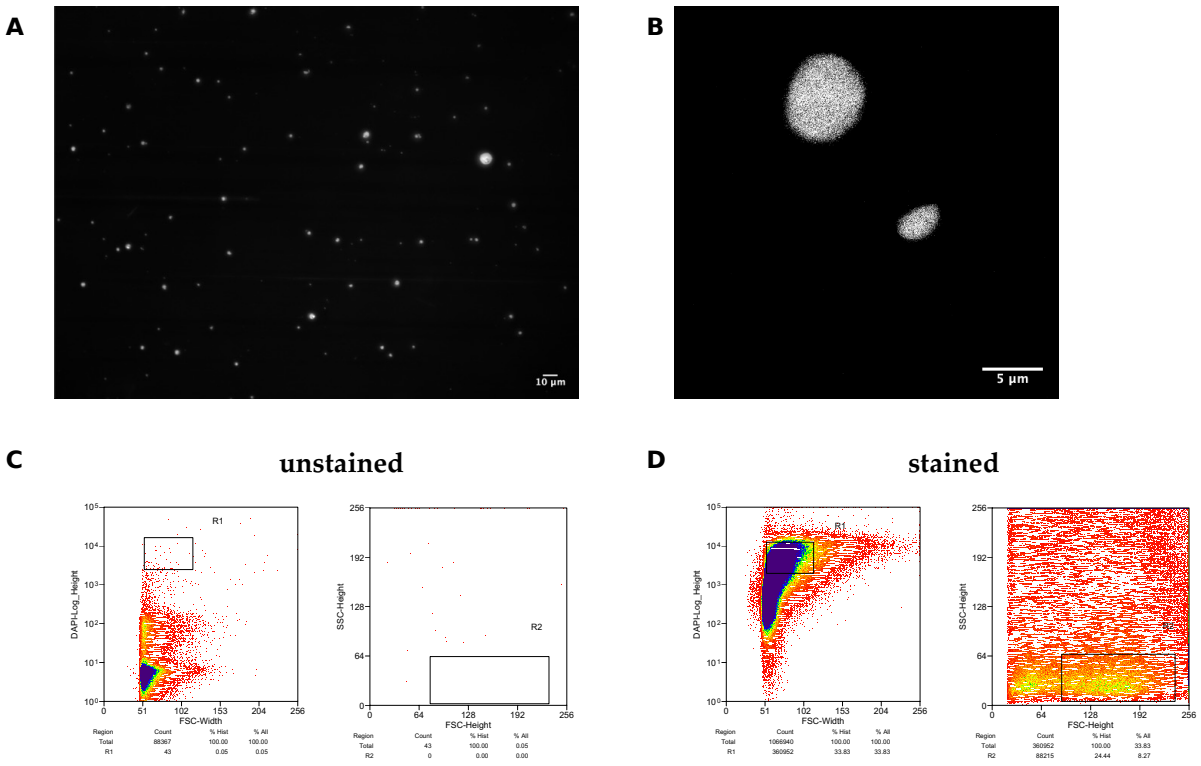

Figure 6: Isolated and sorted nuclei of *T. fruticosum*.
A: Fluorescence microscope image of DAPI-stained nuclei with a 10 µm scale bar (20x); B: Confocal microscope image of DAPI-stained nuclei with a 5 µm scale bar (96x); C and D: FANS Diagram of unstained and DAPI-stained nuclei, respectively. A forward scatter against DAPI signal plot is shown on the left, a forward against side scatter plot is shown on the right.

Protein isolation of *T. fruticosum* leaves

Until today, only little is known about proteins in facultative CAM plants. Analysis of thousands of proteins and characterization of their role in C_3 to CAM transition could be investigated by proteomic approaches. However, the protein preparation is challenging. As proteins are structurally and physicochemical complex, its extraction, solubilization and handling can be difficult. In addition to that, *T. fruticosum* is a waxy plant and contains secondary metabolites, which makes isolation even more complex. Here we compare different methods for the total protein isolation from *T. fruticosum* leaves, which could be used for downstream approaches, such as proteomics.

Two different buffers are tested for protein extraction. The pellets are resuspended using NaOH supplied with 5% SDS. The soluble protein concentration is measured using the bicinchoninic acid assay (BCA). Extraction using TCA/acetone as an isolation buffer, leads to 19 µg/mg FW protein measurable. The extraction of proteins using TCA/phenol results in 42 µg/mg FW protein that can be measured (Figure 7A). To isolate the highest number of proteins possible, we continued with the TCA/phenol method. To determine the most suitable

resuspension buffer for the TCA/phenol extraction, we tested four different buffers (Figure 7B). It was shown that solubility of proteins is lower in acidic pH than in alkaline (Ma et al., 2022). Therefore, the pellet is resuspended in 0.1 M NaOH (with or without SDS), Laemmli buffer or 2% SDS in Tris-HCl (pH 8.0). Resuspending the pellet in NaOH without SDS shows the lowest amount of protein measurable. Application of Laemmli buffer leads to higher protein amounts than NaOH with or without SDS. However, resuspending the pellet with 2% SDS dissolved in Tris-HCl shows the highest measurable protein concentration after TCA/Phenol extraction. Protein isolation from *T. fruticosum* leaves could therefore be isolated best when using TCA/phenol extraction buffer with resuspending the pellet in 2% SDS Tris-HCl (pH 8.0).

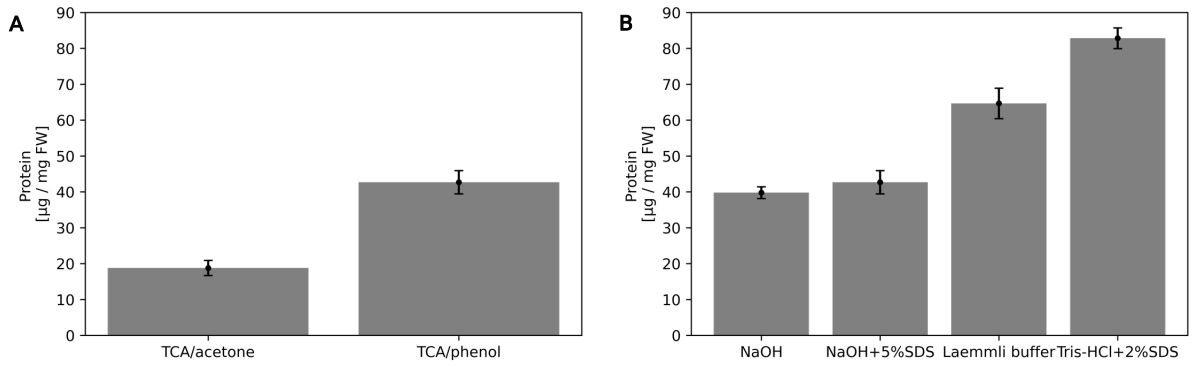

Figure 7: The amount of total protein that can be isolated is dependent of extraction methods and resuspension buffers.
The protein amount measured with BCA is shown in µg per mg fresh weight. A: Proteins are extracted TCA/acetone or TCA/phenol and resuspended in NaOH supplied with 5% SDS. (Biological replicates=6) B: Samples are extracted using TCA/phenol and resuspended in NaOH, NaOH supplied with 5% SDS, Laemmli buffer or Tris-HCl supplied with 3% SDS (Biological replicates=3).

Discussion

Here, we introduce new protocols for molecular work with *T. fruticosum*. Establishment of additional methods will make further analysis and characterizations of C_3 and CAM metabolism possible. We showed that germination of *T. fruticosum* seeds can be done in a sterile environment, which is crucial to perform downstream processes, where sterile conditions are needed. In addition to that, application of chemicals on plates or in liquid media enables more controlled conditions and a higher reproducibility rate than it could be achieved in soil. Moreover, we could increase the germination rate by soaking the seeds in water prior to sowing. This will allow working with a high number of plants, which is needed for a variety of approaches. These involves screening for specific phenotypes, protoplast isolation of seedlings and treatments with amino acids or hormones. The phytohormone abscisic acid (ABA) is known to play a role in stress responses to drought and CAM photosynthesis (Taybi, 1995; Taybi and Cushman, 2002; Ting, 1981). One follow-up approach might be ABA treatment on seedlings. This has already been done for *A. thaliana* seedlings and let to the identification of a network of transcription factors, which control stress responses due to water limitation (Song et al., 2016). Understanding the interplay of ABA and the transition from C_3 to CAM photosynthesis in *T. fruticosum* will help to unravel key players in the signaling cascade.

For deeper understanding of metabolic pathways and gene regulatory networks, protoplasts represent a promising tool to work with. Here we show a protocol to isolate protoplasts from *T. fruticosum* seedlings and its successful transformation using a *UBQ10* driven *Venus* construct. The protoplasts of *T. fruticosum* leaves might be used to study phytohormone signaling cascades (Andres and Zurbriggen, 2022; Hwang and Sheen, 2001; Lehmann et al., 2020) or circadian rhythms (Hansen and van Ooijen, 2016; Nakamura and Oyama, 2018). The circadian clock regulates a variety of metabolic processes of the plant and is needed for adaptation to environmental stimuli. Regulation of CAM photosynthesis is highly dependent on the circadian clock, since its pathway is separated throughout a day/night rhythm. Research has already investigated key questions in the interplay of CAM and the circadian clock (Cushman et al., 2008; Hartwell, 2005; Wai et al., 2019), but knowledge of the full pathway is lacking.

Another target that might be investigated is the subcellular localization of proteins or protein-protein interaction analysis (Komarova et al., 2012). Proteomic approaches are large-scale

studies, which form an important part of functional genomics. Here we established a method for total protein isolation of *T. fruticosum* leaves. We suggest using TCA/phenol to isolate the proteins and to resuspend the pellet in Tris-HCl supplied with 2% SDS. This protocol can be applied for proteomic analysis as a next step towards understanding CAM photosynthesis. However, to identify the subcellular localization of a specific protein, proteomics might not be sufficient and therefore, transformation of protoplasts is a needed. Analysis of the subcellular localization of a protein will help to determine the protein´s environment and unravel its function and potential interaction partners (Dönnes and Höglund, 2004) to solve open questions in the field of CAM research. Moreover, we suggest to use protoplast transformation to regenerate a transformed plant (Reed and Bargmann, 2021; Swarna and Ravindhran, 2012). As protoplasts might allow fast and efficient manipulation of genes and pathways, regeneration to a fully developed plant could lead to new findings and understanding of how plants can cope with drought. In addition to protoplast isolation from sterile-grown seedlings, we introduced a method for protoplast isolation of plants grown in soil. This approach can be performed when sterile conditions cannot be provided or are not needed for the specific downstream method. However, the plants could still be semi-sterilized using ethanol to reduce contamination of the leaves. The two methods of protoplast isolation of *T. fruticosum* leaves shown here, can be used for a variety of downstream approaches. Analysis and manipulation of *T. fruticosum* protoplasts offers not only a great tool to investigate signaling cascades and gene regulatory networks, but also gives the chance to study two types of photosynthesis in one organism.

In addition to protoplast isolation, we established a method for the isolation of intact nuclei. These nuclei can also be sorted successfully using FANS. Intact and sorted nuclei can be used for downstream approaches such as ATAC-seq, diploidy measurements or gDNA isolation. ATAC-seq (Buenrostro et al., 2013) could be performed to unravel the chromatin landscape of *T. fruticosum* and how it changes when the plant transitions from C_3 to CAM photosynthesis. ATAC-seq was already used to study accessible genome regions in other plant species. In the desiccation plant *Craterostigma plantagineum* this approach was used to understand the plants gene regulatory network. Analysis of temporal and spatial gene expression unraveled genes responsive for desiccation (VanBuren et al., 2023). The establishment of a protocol for intact nuclei isolation and sorting lays the foundation for further downstream approaches, which can lead to new understanding in the photosynthetic adaptation of *T. fruticosum*.

Here we show new methods for molecular work with the facultative CAM plant *Talinum fruticosum*. This work will support future studies to solve key questions in the field of CAM research. Unraveling key players of the transition from C_3 to CAM photosynthesis is crucial to engineer CAM traits into C_3 plants to gain more drought resistant crops.

Acknowledgment:

We would like to thank Rocio Ochoa-Fernandez from the institute of Synthetic Biology, HHU, for providing the plasmid pROF144, Vanessa Valencia from the institute of Plant Biochemistry, for taking the nuclei image at the center for advanced imaging, HHU and Katharina Raba from the FACS facility at university hospital for nuclei sorting.

References

Adams, P., Nelson, D.E., Yamada, S., Chmara, W., Jensen, R.G., Bohnert, H.J., Griffiths, H., 1998. Growth and development of Mesembryanthemum crystallinum (Aizoaceae). New Phytol 138, 171–190. https://doi.org/10.1046/J.1469-8137.1998.00111.X

Andres, J., Zurbriggen, M.D., 2022. Genetically Encoded Biosensors for the Quantitative Analysis of Auxin Dynamics in Plant Cells. Methods in Molecular Biology 2379, 183–195. https://doi.org/10.1007/978-1-0716-1791-5_11/COVER

Boxall, S.F., Kadu, N., Dever, L. V., Knerová, J., Waller, J.L., Gould, P.J.D., Hartwell, J., 2020. Kalanchoë PPC1 is essential for crassulacean acid metabolism and the regulation of core circadian clock and guard cell signaling genes[CC-BY]. Plant Cell 32, 1136–1160. https://doi.org/10.1105/TPC.19.00481

Brilhaus, D., Bräutigam, A., Mettler-Altmann, T., Winter, K., Weber, A.P.M., 2016. Reversible Burst of Transcriptional Changes during Induction of Crassulacean Acid Metabolism in Talinum triangulare . Plant Physiol 170, 102–122. https://doi.org/10.1104/pp.15.01076

Brilhaus, D., Denton, A.K., Maleckova, E., Reichel-Deland, V., Weber, A.P.M., 2023. The genome of Talinum fruticosum. BioRxiv. https://doi.org/10.1101/2023.04.20.537669

Buenrostro, J.D., Giresi, P.G., Zaba, L.C., Chang, H.Y., Greenleaf, W.J., 2013. Transposition of native chromatin for fast and sensitive epigenomic profiling of open chromatin, DNA-binding proteins and nucleosome position. Nat Methods 10, 1213–1218. https://doi.org/10.1038/nmeth.2688

Cushman, J.C., Tillett, R.L., Wood, J.A., Branco, J.M., Schlauch, K.A., 2008. Large-scale mRNA expression profiling in the common ice plant, Mesembryanthemum crystallinum, performing C3 photosynthesis and Crassulacean acid metabolism (CAM), in: Journal of Experimental Botany. pp. 1875–1894. https://doi.org/10.1093/jxb/ern008

Damerval, C., De Vienne, D., Zivy, M., Thiellement, H., 1986. Technical improvements in two-dimensional electrophoresis increase the level of genetic variation detected in wheat-seedling proteins. Electrophoresis 7, 52–54. https://doi.org/10.1002/ELPS.1150070108

Denny, F.E., 1930. Shortening the Rest Period of Gladiolus by Treatment with Chemicals. Am J Bot 17, 602. https://doi.org/10.2307/2435703

Dönnes, P., Höglund, A., 2004. Predicting Protein Subcellular Localization: Past, Present, and Future. Genomics Proteomics Bioinformatics 2, 209. https://doi.org/10.1016/S1672-0229(04)02027-3

Hansen, L.L., van Ooijen, G., 2016. Rapid Analysis of Circadian Phenotypes in Arabidopsis Protoplasts Transfected with a Luminescent Clock Reporter. J Vis Exp 2016, 54586. https://doi.org/10.3791/54586

Hartwell, J., 2005. The co-ordination of central plant metabolism by the circadian clock. Biochem Soc Trans 33, 945–948. https://doi.org/10.1042/BST20050945

Herrera, A., 2009. Crassulacean acid metabolism and fitness under water deficit stress: If not for carbon gain, what is facultative CAM good for? Ann Bot 103, 645–653. https://doi.org/10.1093/aob/mcn145

Herrera, A., Ballestrini, C., Montes, E., 2015. What is the potential for dark CO2 fixation in the facultative crassulacean acid metabolism species Talinum triangulare? J Plant Physiol 174, 55–61. https://doi.org/10.1016/j.jplph.2014.10.006

Hwang, I., Sheen, J., 2001. Two-component circuitry in Arabidopsis cytokinin signal transduction. Nature 2001 413:6854 413, 383–389. https://doi.org/10.1038/35096500

Kaul, S., Koo, H.L., Jenkins, J., Rizzo, M., Rooney, T., Tallon, L.J., Feldblyum, T., Nierman, W., Benito, M.I., Lin, X., Town, C.D., Venter, J.C., Fraser, C.M., Tabata, S., Nakamura, Y., Kaneko, T., Sato, S., Asamizu, E., Kato, T., Kotani, H., Sasamoto, S., Ecker, J.R., Theologis, A., Federspiel, N.A., Palm, C.J., Osborne, B.I., Shinn, P., Dewar, K., Kim, C.J., Buehler, E., Dunn, P., Chao, Q., Chen, H., Theologis, A., Osborne, B.I., Vysotskaia, V.S., Lenz, C.A., Kim, C.J., Hansen, N.F., Liu, S.X., Buehler, E., Alta, H., Sakano, H., Dunn, P., Lam, B., Pham, P.K., Chao, Q., Nguyen, M., Yu, G., Chen, H., Southwick, A., Lee, J.M., Miranda, M., Toriumi, M.J., Davis, R.W., Federspiel, N.A., Palm, C.J., Conway, A.B., Conn, L., Hansen, N.F., Hootan, A., Lam, B., Wambutt, R., Murphy, G., Düsterhöft, A., Stiekema, W., Pohl, T., Entian, K.D., Terryn, N., Volckaert, G., Salanoubat, M., Choisne, N., Artiguenave, F., Weissenbach, J., Quetier, F., Rieger, M., Ansorge, W., Unseld, M., Fartmann, B., Valle, G., Wilson, R.K., Sekhon, M., Pepin, K., Murray, J., Johnson, D., Hillier, L., de la Bastide, M., Huang, E., Spiegel, L., Gnoj, L., Habermann, K., Dedhia, N., Parnell, L., Preston, R., Marra, M., McCombie, W.R., Chen, E., Martienssen, R., Mayer, K., Lemcke, K., Haas, B., Haase, D., Rudd, S., Schoof, H., Frishman, D., Morgenstern, B., Zaccaria, P., Mewes, H.W., White, O., Creasy, T.H., Bielke, C., Maiti, R., Peterson, J., Ermolaeva, M., Pertea, M., Quackenbush, J., Volfovsky, N., Wu, D., Salzberg, S.L., Bevan, M., Lowe, T.M., Rounsley, S., Bush, D., Subramaniam, S., Levin, I., Norris, S., Schmidt, R., Acarkan, A., Bancroft, I., Brennicke, A., Eisen, J.A., Bureau, T., Legault, B.A., Le, Q.H.,

Agrawal, N., Yu, Z., Copenhaver, G.P., Luo, S., Preuss, D., Pikaard, C.S., Paulsen, I.T., Sussman, M., Britt, A.B., Selinger, D.A., Pandey, R., Chandler, V.L., Jorgensen, R.A., Mount, D.W., Pikaard, C., Juergens, G., Meyerowitz, E.M., Dangl, J., Jones, J.D.G., Chen, M., Chory, J., Somerville, C., 2000. Analysis of the genome sequence of the flowering plant Arabidopsis thaliana. Nature 2000 408:6814 408, 796–815. https://doi.org/10.1038/35048692

Komarova, N.Y., Meier, S., Meier, A., Grotemeyer, M.S., Rentsch, D., 2012. Determinants for Arabidopsis peptide transporter targeting to the tonoplast or plasma membrane. Traffic 13, 1090–1105. https://doi.org/10.1111/J.1600-0854.2012.01370.X

Lehmann, S., Dominguez-Ferreras, A., Huang, W.J., Denby, K., Ntoukakis, V., Schäfer, P., 2020. Novel markers for high-throughput protoplast-based analyses of phytohormone signaling. PLoS One 15, e0234154. https://doi.org/10.1371/JOURNAL.PONE.0234154

Lu, Z., Hofmeister, B.T., Vollmers, C., DuBois, R.M., Schmitz, R.J., 2017. Combining ATAC-seq with nuclei sorting for discovery of cis-regulatory regions in plant genomes. Nucleic Acids Res 45, 1–13. https://doi.org/10.1093/nar/gkw1179

Ma, K.K.;, Greis, M ;, Lu, J ;, Nolden, A.A.;, Mcclements, D.J.;, Kinchla, A J, Ma, K.K., Greis, Maija, Lu, Jiakai, Nolden, A.A., Mcclements, D.J., Kinchla, Amanda J, 2022. Functional Performance of Plant Proteins. Foods 2022, Vol. 11, Page 594 11, 594. https://doi.org/10.3390/FOODS11040594

Maleckova, E., Brilhaus, D., Wrobel, T.J., Weber, A.P.M., 2019. Transcript and Metabolite Changes during the Early Phase of ABA-mediated Induction of CAM in Talinum triangulare. J Exp Bot. https://doi.org/10.1093/jxb/erz189

Nagai, T., Ibata, K., Park, E.S., Kubota, M., Mikoshiba, K., Miyawaki, A., 2002. A variant of yellow fluorescent protein with fast and efficient maturation for cell-biological applications. Nature Biotechnology 2002 20:1 20, 87–90. https://doi.org/10.1038/nbt0102-87

Nakamura, S., Oyama, T., 2018. Long-term monitoring of bioluminescence circadian rhythms of cells in a transgenic Arabidopsis mesophyll protoplast culture. Plant Biotechnology 35, 291. https://doi.org/10.5511/PLANTBIOTECHNOLOGY.18.0515A

Ochoa-Fernandez, R., Abel, N.B., Wieland, F.G., Schlegel, J., Koch, L.A., Miller, J.B., Engesser, R., Giuriani, G., Brandl, S.M., Timmer, J., Weber, W., Ott, T., Simon, R., Zurbriggen, M.D.,

2020. Optogenetic control of gene expression in plants in the presence of ambient white light. Nat Methods 17, 717–725. https://doi.org/10.1038/s41592-020-0868-y

Patel, R.J., Ahlawat, T.R., Patel, A.I., Amarcholi, J.J., Patel, B.B., Sharma, K., 2017. Growth of mango (Mangifera indica L.) rootstocks as influenced by pre-sowing treatments. Journal of Applied and Natural Science 9, 582–586. https://doi.org/10.31018/JANS.V9I1.1234

Reed, K.M., Bargmann, B.O.R., 2021. Protoplast Regeneration and Its Use in New Plant Breeding Technologies. Front Genome Ed 3, 734951. https://doi.org/10.3389/FGEED.2021.734951/BIBTEX

Sarrion-Perdigones, A., Vazquez-Vilar, M., Palací, J., Castelijns, B., Forment, J., Ziarsolo, P., Blanca, J., Granell, A., Orzaez, D., 2013. Goldenbraid 2.0: A comprehensive DNA assembly framework for plant synthetic biology. Plant Physiol 162, 1618–1631. https://doi.org/10.1104/pp.113.217661

Silvera, K., Santiago, L.S., Cushman, J.C., Winter, K., 2010. The incidence of crassulacean acid metabolism in Orchidaceae derived from carbon isotope ratios: A checklist of the flora of Panama and Costa Rica. Botanical Journal of the Linnean Society 163, 194–222. https://doi.org/10.1111/j.1095-8339.2010.01058.x

Song, L., Huang, S.S.C., Wise, A., Castanoz, R., Nery, J.R., Chen, H., Watanabe, M., Thomas, J., Bar-Joseph, Z., Ecker, J.R., 2016. A transcription factor hierarchy defines an environmental stress response network. Science (1979) 354. https://doi.org/10.1126/science.aag1550

Swarna, J., Ravindhran, R., 2012. In vitro propagation and assessment of genetic integrity of Talinum triangulare (Jacq.) Willd: A valuable medicinal herb. Acta Physiol Plant 34, 1987–1996. https://doi.org/10.1007/S11738-012-0999-6

Taisma, M.A., Herrera, A., 1998. A relationship between fecundity, survival, and the operation of crassulacean acid metabolism in Talinum triangulare.

Taybi, T., 1995. Differential Effects of Abscisic Acid on 108, 240–246.

Taybi, T., Cushman, J.C., 2002. Abscisic acid signaling and protein synthesis requirements for phosphoenolpyruvate carboxylase transcript induction in the common ice plant. J Plant Physiol 159, 1235–1243. https://doi.org/10.1078/0176-1617-00834

Ting, I.P., 1981. Effects of abscisic acid on CAM in Portulacaria afra. Photosynth Res 48, 39–48.

VanBuren, R., Wai, C.M., Giarola, V., Župunski, M., Pardo, J., Kalinowski, M., Grossmann, G., Bartels, D., 2023. Core cellular and tissue-specific mechanisms enable desiccation

tolerance in Craterostigma. The Plant Journal 114, 231–245. https://doi.org/10.1111/TPJ.16165

Wai, C.M., Weise, S.E., Ozersky, P., Mockler, T.C., Michael, T.P., Vanburen, R., 2019. Time of day and network reprogramming during drought induced CAM photosynthesis in Sedum album. PLoS Genet 15. https://doi.org/10.1371/journal.pgen.1008209

Wang, W., Vignani, R., Scali, M., Cresti, M., 2006. A universal and rapid protocol for protein extraction from recalcitrant plant tissues for proteomic analysis. Electrophoresis 27, 2782–2786. https://doi.org/10.1002/elps.200500722

West-eberhard, M.J., Smith, J.A.C., Winter, K., 2011. Photosynthesis, Reorganized 332.

Winter, K., 2019. Ecophysiology of constitutive and facultative CAM photosynthesis. J Exp Bot. https://doi.org/10.1093/jxb/erz002

Winter, K., Holtum, J.A.M., 2014. Facultative crassulacean acid metabolism (CAM) plants: powerful tools for unravelling the functional elements of CAM photosynthesis. J Exp Bot 65, 3425–3441. https://doi.org/10.1093/jxb/eru063

Wu, F.H., Shen, S.C., Lee, L.Y., Lee, S.H., Chan, M.T., Lin, C.S., 2009. Tape-arabidopsis sandwich - A simpler arabidopsis protoplast isolation method. Plant Methods 5, 1–10. https://doi.org/10.1186/1746-4811-5-16/FIGURES/9

Yang, X., Hu, R., Yin, H., Jenkins, J., Shu, S., Tang, H., Liu, D., Weighill, D.A., Cheol Yim, W., Ha, J., Heyduk, K., Goodstein, D.M., Guo, H.B., Moseley, R.C., Fitzek, E., Jawdy, S., Zhang, Z., Xie, M., Hartwell, J., Grimwood, J., Abraham, P.E., Mewalal, R., Beltrán, J.D., Boxall, S.F., Dever, L. V., Palla, K.J., Albion, R., Garcia, T., Mayer, J.A., Don Lim, S., Man Wai, C., Peluso, P., Van Buren, R., De Paoli, H.C., Borland, A.M., Guo, H., Chen, J.G., Muchero, W., Yin, Y., Jacobson, D.A., Tschaplinski, T.J., Hettich, R.L., Ming, R., Winter, K., Leebens-Mack, J.H., Smith, J.A.C., Cushman, J.C., Schmutz, J., Tuskan, G.A., 2017. The Kalanchoë genome provides insights into convergent evolution and building blocks of crassulacean acid metabolism. Nat Commun 8. https://doi.org/10.1038/s41467-017-01491-7

Supplemental information

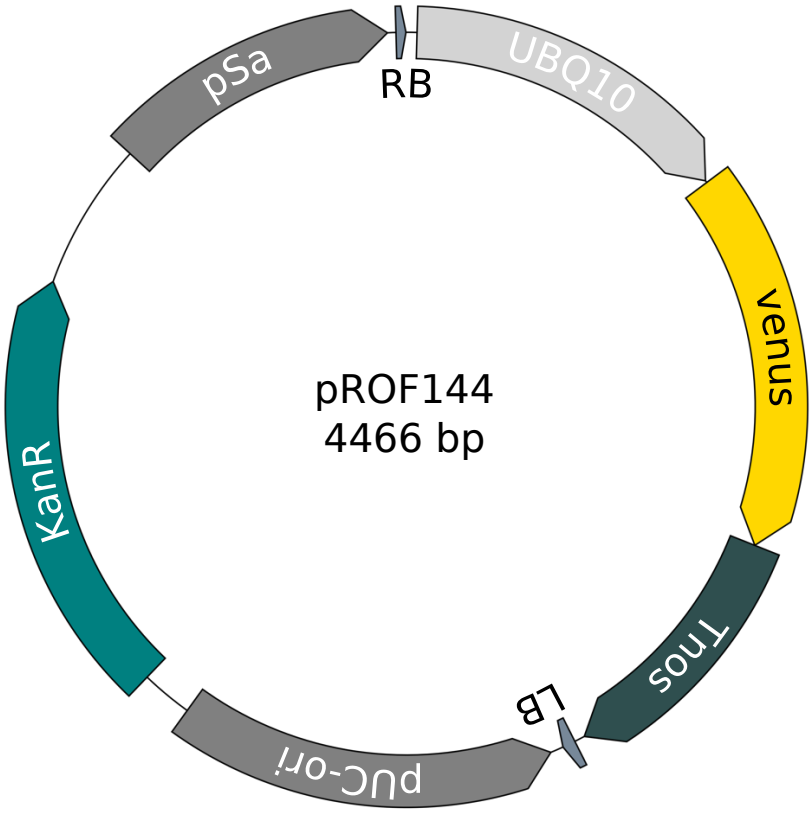

Supplemental Figure S 1: Plasmid map pROF144
Venus expression is driven by a *UBQ10* promoter. A Kanamycin (Kan) cassette is implemented for selection in *Escherichia coli*. RB: right boarder, LB: left boarder.

Manuscript III

Understanding molecular regulation of the facultative CAM plant *Talinum fruticosum*

Vanessa Reichel-Deland[1], Sebastian Triesch[1,4], Uriel Urquiza-Garcia[2,4], Franziska Fichtner[1,4], Jennifer Andres[2], Philipp Westhoff[1,4], Felicitas Kindel[1], Alisandra K. Denton[1,4], Robert VanBuren[3], Matias D. Zurbriggen[2,4], Andreas P.M. Weber[1,4]

[1]Institute of Plant Biochemistry, Heinrich Heine University, Universitaetsstrasse 1, 40225 Duesseldorf, Germany

[2]Institute of Synthetic Biology, Heinrich Heine University, Universitaetsstrasse 1, 40225 Duesseldorf, Germany

[3]Department of Horticulture, Plant Resilience Institute, Michigan State University, 1066 Bogue St, East Lansing, MI, USA

[4]Cluster of Excellence on Plant Science (CEPLAS), Heinrich Heine University, Universitaetsstrasse 1, 40225 Duesseldorf, Germany

Authors contribution:

V.R.-D. designed and planned and performed the experiments, sampled and processed the plants for biochemical analysis, cloned the constructs, ran experiments in mammalian tissue culture, analyzed the data and wrote the manuscript; S.T. analyzed RNA-seq data; U.U.-G. suggested the positive controls for mammalian cell assays and helped constructing plasmids; F.F. extracted and analyzed the metabolites; J.A. assisted with the mammalian cell assays; P.W. performed the metabolic analysis; F.K. performed ChIP and ATAC-seq predictions, A.K.D. assisted in the bioinformatical analysis; R.V. designed the RNA-seq experiment and assisted in bioinformatical analysis; M.D.Z. designed the experiments and supervised mammalian cell assays; A.P.M.W. designed and supervised the experiments; S.T., U.U.-G., F.F., J.A., P.W., F.K., A.K.D., R.V., M.D.Z. and A.P.M.W. edited and revised the manuscript.

Abstract

Developmental plasticity is a key factor for plants to adapt to environmental changes. Drought is a major challenge for the sessile organisms and climate change favors longer and more severe dry periods throughout the year. Different strategies evolved in the plant kingdom to overcome these challenges, one of them is the water-saving photosynthesis crassulacean acid metabolism (CAM). The facultative CAM plant *Talinum fruticosum* can transition between C_3 and CAM photosynthesis to adapt to changes in its natural ecosystem. Here we studied the physiological and transcriptional adaptations of *T. fruticosum* during this process and corroborated our findings using a synthetic biology approach. Besides identification of distinct up- and downregulated transcript clusters, we found transcription factors that we predict to be involved in drought stress responses in *T. fruticosum*. To further investigate their characteristics, we established a synthetic test system in an orthogonal mammalian cell system. Using a synergy of RNA-seq analysis, transcription factor binding prediction and its verification, our study established a promising platform to understand the complex regulatory network of the facultative CAM plant *T. fruticosum* and pinpoints at pivotal key regulatory mechanisms during the C_3-CAM transition.

Introduction

Whereas animals can react to environmental changes via behavior, plants need to adjust via developmental plasticity. Understanding the plant´s mechanism to cope with dry periods can help to improve crops in a changing environment.

Three main metabolic pathways of photosynthesis can be found in the plant kingdom, C_3, C_4 and crassulacean acid metabolism (CAM). C_3 photosynthesis is the most widespread and oldest form of photosynthesis (Ehleringer et al., 1991). In the C_3 metabolic pathway, CO_2 is initially fixed by the enzyme ribulose-1,5-bisphosphate carboxylase/oxygenase (Rubisco), the key enzyme of the Calvin-Benson-Bassham (CBB) cycle. This is followed by a stepwise reduction to phosphoglycerate and conversion to sugar phosphates, which are needed for metabolic functions. Because of its properties as a dual-function enzyme, instead of fixing CO_2, Rubisco can also fix O_2, leading to the formation of 2-phosphoglycolate (2-PG) and 3-phosphoglycolate (3-PGA). 2-PG inhibits important metabolic regulators and is therefore metabolized by photorespiration (Flügel et al., 2017). The unspecific fixation by Rubisco can lower plant yield by about 30% (Walker et al., 2016). To reduce the energetic burden and nitrogen loss due to photorespiration, plants have evolved different strategies to overcome this.

In plants that perform the water-saving photosynthesis CAM, the CO_2 assimilation can be separated in four phases throughout the day (Osmond, 1978). During the night, when the temperatures are lower and the humidity is higher, most CAM plants open their stomata and CO_2 is taken up. The key enzyme Phosphoenol-pyruvatecarboxylase (PEPC) combines CO_2 in form of bicarbonate with phosphoenolpyruvate (PEP), as a result of which oxaloacetate is formed (Boxall et al., 2020; Drennan and Nobel, 2000). PEPC can be found in most photosynthetic organisms and also have other metabolic functions besides its role in photosynthesis. PEPCs from plants can be grouped into plant (PPC-1) and bacterial-type PEPC (PPC-2) (Deng et al., 2016). Evolution of PEPC seems to be connected to mutations in the *PEPC* gene, which might lead to amino acid changes (Christin et al., 2014). Oxaloacetate is further converted to malate, which can be stored as malic acid in the vacuole. Accumulation of acids in the vacuole can be identified with titration and gives indication about the presence of CAM activity (Lüttge and Ball, 1980). In the plant leaf, at the beginning of dawn, stomata might be

closed and malic acid is re-mobilized and decarboxylated. CO_2 is re-fixed by Rubisco and used in the CBB-cycle (Osmond, 1978).

At least 5% of all known vascular plants to date, spanning 40 families and 400 genera, are known to perform CAM photosynthesis (Winter et al., 2015; Winter and Smith, 2022, 1996). It is likely that more species will be identified in the future as genome sequencing is getting cheaper and an attempt for identification is made by a CAM survey (Winter, 2019). Species performing CAM are typically found in semi-arid or dry/wet season regions (West-eberhard et al., 2011). There is a variety of plant species known that perform different levels of CAM photosynthesis. Besides other form of CAM photosynthesis, it can be distinguished between constitutive CAM plants, where components of CAM photosynthesis irreversibly expressed and facultative CAM plants, that can switch between to CAM photosynthesis from the basal C_3 or C_4 photosynthesis and back as a response to environmental cues. To understand evolution and molecular mechanisms of CAM, studies from a large variety of plant species is needed.

Talinum fruticosum (former *Talinum triangulare*), a tropical and herbaceous dicot from the family Talinaceae, is a facultative CAM plant, which can transition from C_3 to CAM photosynthesis and back (Herrera, 2009; Herrera et al., 2015; Taisma and Herrera, 1998; Winter and Holtum, 2014). This strategy makes it a potential organism to study the transition between the two types of photosynthesis in one organism. Understanding the mechanisms behind this C_3-CAM transition in detail will be crucial to engineer CAM traits into a C_3 chassis to create more drought-resilient plants. It has been shown that CAM can be induced in a reversible manner by drought (Brilhaus et al., 2016) or by external application of abscisic acid (ABA) (Maleckova et al., 2019) in *T. fruticosum*. Drought is known to induce a stress response, where upregulation of transcription factors binding to drought responsive elements could be observed (Brilhaus et al., 2016; Zhu, 2002). ABA-mediated signaling response genes were upregulated after the initial stress response, but also switched off after water was re-supplied, indicating an interplay with a carbon starvation signal (Brilhaus et al., 2016).

In addition to the transcriptome and metabolic studies, a scaffolded genome of *T. fruticosum* has been published recently (Brilhaus et al., 2023), which promotes genomic and transcriptomic studies. In the genome, there are six *PEPC* genes found, from which four could be identified to be in close proximity to each other on the same scaffold. One of them contains an amino acid change from alanine to serine, which has also been found in C_4, but is not typical

for C_3 plants. The genes also show differences in their transcript expression pattern, suggesting that only some of the *PEPC* genes might be function as a CAM-specific isoform (Brilhaus et al., 2023).

In this study we investigated the physiological and transcriptomic characteristics of *T. fruticosum* during drought stress. Besides identification of distinct transcript clusters, we analyzed transcription factor binding sites (TFBS) in a presumably strictly regulated genomic region containing four *PEPC* genes. To this end, we used prediction data from predmoter, a deep learning ATAC-seq and ChIP-seq prediction tool which is currently being developed and combined this data with predicted TFBS motifs. However, experimental corroboration of these findings is still crucial for deeper understanding of regulatory networks. Studying pathways and gene regulation in the plant itself can be difficult, especially since CAM plants might need specific growth conditions and can show succulent tissue and a high number of secondary metabolites (Yang et al., 2020). To overcome to these challenges, we established a synthetic reconstruction approach in mammalian cells to confirm interaction pairs identified by our *in silico* approaches.

Here we show that combination of computational analysis and experimental verification creates a basis for unraveling molecular mechanisms in the facultative CAM plant *Talinum fruticosum*.

Material and methods

Plant growth conditions

Talinum fruticosum plants were grown in pots, containing potting soil with fertilizer and Vermiculite, in a controlled environment growth chamber. Plants were grown in 12 h light at 25 °C and 65% humidity and 12 h dark at 22 °C and 70% humidity. Growth conditions have been documented using a HOBO data logger (ONSET) (Supplemental Figure S 1). All experiments have been performed with 44 days old plants, counting after sowing. Leaves were harvested and flash-frozen in liquid nitrogen on day 0, as well as four and nine days after water withhold (drought, D) and two days after re-watering. Control plants were watered on a regularly basis. Timepoints of harvesting were chosen for two hours after dawn (end of night, EN) and after dusk (end of day, ED). One replicate represents six to eight leaves starting from the third recent leaf of the same plant. Two to three (five for metabolomic measurements) replicates were analyzed. Pooled leaves were ground into powder and aliquots were used for further analysis. To determine fresh and dry weight, leaves of three individual plants were cut off and dried at 60 °C for 24 h, until no further weight loss was observable.

Titratable acidity

To determine leaf acidity, 0.5 g of leaf tissue were sequentially boiled in 20 ml 50% MeOH (v/v in H2O). After half of the solution was evaporated, a second extraction step was performed. The extract was filled up with dH_2O prior to titration. Titration with 2.5 mM NaOH was performed to determine the volume needed to neutralize the extract to pH 6.5. For determining the titratable acidity per mg dry weight, the dry weight was calculated using the measured fresh weight to dry weight ratio as shown in Figure 2A.

Metabolomics

Three mature leaves from five individual plants were pooled and flash frozen. The leaves were ground to fine powder and 100 mg FW was freeze dried over night to normalize relative values per gram dry weight. Metabolite extractions was done as described in Lunn et al. (2006). In brief, 350 µl ice-cold Chloroform/Methanol (3:7) solution were added to the dried material. Samples were vigorously shaken and incubated at -20 °C for 2 h. 350 µl ice-cold water was added, samples were vigorously shaken and centrifuged at 4 °C for 15 min. The 350 µL of the

upper aqueous phase were collected and the sample was extracted a second time with 300 µl ice-cold water. The samples were spiked during extractions with 2-Desoxy-D-glucose-6-phosphate to correct for differences in extraction efficiencies. The combined aqueous extract was evaporated to dryness at room temperature using a vacuum concentrator and dissolved in 400 µl H2O. Samples were filtered through MultiScreen PCR 96 plates for removal of molecular weight contaminants (200 µl at 2200 g for 30 min). Filtered samples were diluted with an equal amount of a α-D-[UL-13C6] glucopyranosyl 1-phosphate solution to correct for matrix effects. Measurements were performed on an anion exchange chromatography system (Dionex ICS-6000 HPIC) coupled to a high field quadrupole-Orbitrap mass spectrometer (Thermo Scientific Q Exactive Plus) based on Curien et al. (2021). For the untargeted approach the mass spectrometer operated in a combination of full mass scan and a data-dependent Top5 MS2 (ddMS2) experiment. The full scan (60-800 m/z) was conducted with a resolution of 70.000 and an automatic gain control (AGC) target of 1e6 ions with a maximum injection time (IT) of 500 ms. The Top5 ddMS2 experiment was carried out with a resolution of 17.500 and an AGC target of 1e5 and a maximum IT of 50 ms. The stepped collision energy was used with the steps (15,25,35) to create an average of NCE 25. The Skyline software was used for targeted data analysis of organic acids (Adams et al., 2020).

Library construction for RNA-seq

RNA was isolated using Macherey-Nagel NucleoSpin RNA Plant and Fungi, Mini kit for RNA from plant and fungi (REF: 740120.50). DNase treatment was done as on-column DNA digestion using Macherey-Nagel rDNase Set (REF: 740963). Methods were performed according to manufacturer´s protocol.

RNA-seq library was prepared using VAHTS Universal V6 RNA-seq library prep Kit for Illumina from Vazyme, according to manufacturer´s protocol. Paired-end sequencing was done with NextSeq2000 aiming for 10 million reads per sample.

Read mapping and analysis

Read trimming was performed using *trimmomatic* v0.39 (Bolger et al., 2014). *Kallisto* v0.46.1 was used for pseudoalignment (Bray et al., 2016). A reference gene model annotation for *Kallisto* and for further downstream annotation was obtained using the *ab-initio* gene caller

Helixer (Brilhaus et al., 2023; Holst et al., 2023). *Sleuth* v0.30.1 was used for transcript level estimation and normalization(Bray et al., 2016). GO terms were obtained from syntenic homologs to the *Arabidopsis thaliana* TAIR10 genome release (Berardini et al., 2015). To this end, syntenic gene sets between *A. thaliana* and *T. fruticosum* were obtained using *CoGE SynMap* (Haug-Baltzell et al., 2017). *REVIGO* (Supek et al., 2011) was used for multidimensional scaling of enriched GO terms. Besides GO Terms, MapMan bins obtained using *Mercator* (Schwacke et al., 2019), were used for analysis of enriched gene clusters. Clustering of co-expressed transcripts was performed using *Clust* v1.18.1 (Abu-Jamous and Kelly, 2018). Base-wise read mapping was performed using *STAR* v2.7.10b (Dobin et al., 2013). *FIMO* and the *fasta-get-markov* program from the *MEME* Suite were used for sequence scanning to identify individual matches of transcription factor binding motifs using the *A. thaliana JASPAR* transcription factor database (Bailey et al., 2015). *Predmoter*, a deep learning algorithm, was used to predict Assay for Transposase Accessible Chromatin using sequencing (ATAC-seq) and chromatin immunoprecipitation DNA-sequencing (ChIP-seq) read coverage using the DNA sequence of *T. fructicosum* as an input. The neural network was trained on publicly available, experimental plant ATAC- and histone ChIP-seq, histone H3 tri-methylated at lysine 4 (K4) (H3K4me3), data.

Downstream analyses were performed in R v4.1.3 and Python v3.8.8.

All raw and processed data as well as all complied software, scripts and script outputs were uploaded in an Annotated Research Format (ARC) at the *dataplant* repository under: https://git.nfdi4plants.org/hhu-plant-biochemistry/talinum_fruticosum_drought_synbio_2023

Plasmid generation

Plasmids were constructed using Gibson assembly cloning (Gibson et al., 2009) or the Goldenbraid assembly strategy (Sarrion-Perdigones et al., 2013). Design and virtual construction of polycistronic tRNA+sgRNA (PTG) were done using the PolyGEN software (Urquiza-Garcia, unpublished). A list of plasmid constructs and used oligonucleotides can be found in Supplemental Table S 2 and Supplemental Table S 3, respectively. Q5 or Phusion High-Fidelity DNA Polymerase (New England Biolabs) was used for PCR amplifications. For insert and/or plasmid verification Sanger sequencing was performed (Microsynth AG). Plasmids were purified using NucleoBond Xtra Midi kit (Macherey-Nagel) prior mammalian cell transfection.

Isolation and transformation of *Arabidopsis thaliana* protoplasts

Protoplasts were isolated and transformed as described in (Ochoa-Fernandez et al., 2020). In short, 14-day old *A. thaliana* seedlings have been used to cut off the leaves, which were sliced and incubated in enzyme solution in the dark overnight. Released protoplasts have been washed and counted prior transformation using a PEG-mediated approach in a 6-well-plate. Plate-reader measurements of Firefly and Renilla have been performed after 18-20 h of incubation.

Cell culture and transfection

Chinese ovary hamster-K1 (CHO) cells were grown in Ham´s F12 medium (PAN Biotech). 24 h prior to transfection, 50,000 CHO cells per well were seeded in 500 µl medium in a 24 well plate (Corning). 50 µl OptiMEM (Invitrogen, Thermo Fisher Scientific) were used to dilute 0.75 µg DNA/well. This was mixed with PEI/OptiMEM (2.5 µl PEI (1 mg/ml, Polysciences Europe GmbH) in 50 µl OptiMEM) (compare (Baaske et al., 2018). Incubation time was 15 min at RT, followed by addition of 100 µl mix to each well dropwise. Medium exchange was done 4 h after transfection.

SEAP reporter assay

24 h after transfection, 200 µl supernatant were taken for heat-inactivation for 1 h at 65 °C. 80 µl inactivated sample was transferred to a transparent, flat-bottomed 96 well plate. 100 µl SEAP buffer (20 mM L-homoarginine, 1 mM MgCl2 21 % (v/v) diethanolamine) and 20 µl of 120 nM para-Nitrophenylphosphate (pNPP, Sigma-Aldrich) were added prior to measurement at 405 nM for 1 h in Berthold technologies Tristar2S LB942 Multimode Plate Reader. Analysis of SEAP activity was calculated from the slope together with Lambert-Beers-law. Calculation and analysis were performed using Excel and Python v3.8.8.

Equation 1: Calculation of SEAP activity
With E = optical density/pNPP increase per minute, ε = 18,600 M^{-1} cm^{-1}, d = light path length [cm] and the supernatant and its dilution factor.

$$\frac{U}{L} = \frac{E}{\varepsilon \times d} \times 10^6 x \frac{200}{80}$$

Results

Water withhold leads to alterations in *T. fruticosum* metabolism

T. fruticosum plants were grown under well-watered conditions for 44 days. We performed a time-course analysis with samples takes on a time course during eleven days. Samples were taken at the end of the day (ED) and at the end of the night (EN) on day zero (ED0/EN0), day four (ED4/EN4), day nine (ED9/EN9) and two days after re-watering (EDre/ENre), compare Figure 1. To induce a drought-response the water was withheld for nine days, followed by two days of re-watering. Fresh and dry weight were determined for pooled mature leaves of three individually potted plants. We observed a decrease in the fresh-to-dry-weight ratio by about 23% after four days compared to day zero. After nine days of drought the plants showed a 52% decrease (Figure 2A). At day nine of water withhold, leaves showed leaf rolling and a change in the leaf angle, where the leaf rosette was rather closed (compare Figure 1). After nine days of drought stress, the plants were watered again. The fresh-to-dry-weight ratio increased again to about 7% compared to day nine (Figure 2A).

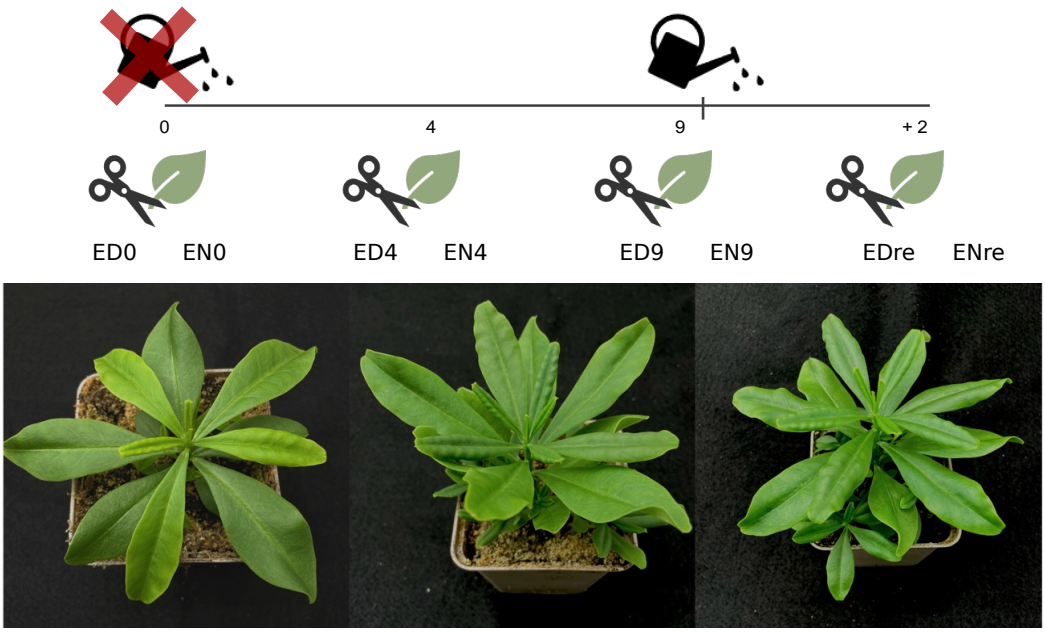

Figure 1: Experimental overview and phenotype of *T. fruticosum* during a 11-day time-course.
44 days old plants were on water-withhold for nine days, followed by two days of re-watering or watered on a regular basis as a control. Pictures are taken on day zero, day nine and after two days of re-watering. Samples are taken either at the end of the day (ED) or at the end of the night (EN) on day 0, 4, 9 or two days after re-watering (re).

Titratable acidity was determined as an indicator for CAM activity in the leaves. Therefore, flash-frozen leaves were pooled, extracted and titration was performed. Titratable acidity has been determined for leaf dry weight. Well-watered plants showed a slight difference between samples taken at the end of the day and the end of the night. Samples from the end of the night showed slightly higher titratable acidity levels compared to end of the day samples. This pattern did not change during the time course, but the overall titratable acidity levels increased over time. The plants that were drought-stressed showed a greater difference between titratable acidity at end of day and end of night. This was true for plants that have been on water-withhold for four and nine days. Titratable acidity levels of two days rewatered plants showed a similar pattern of plants from day zero. Changes in titratable acidity levels during the time-course could been shown for drought-stressed *T. fruticosum* plants, but not for plants that were well-watered.

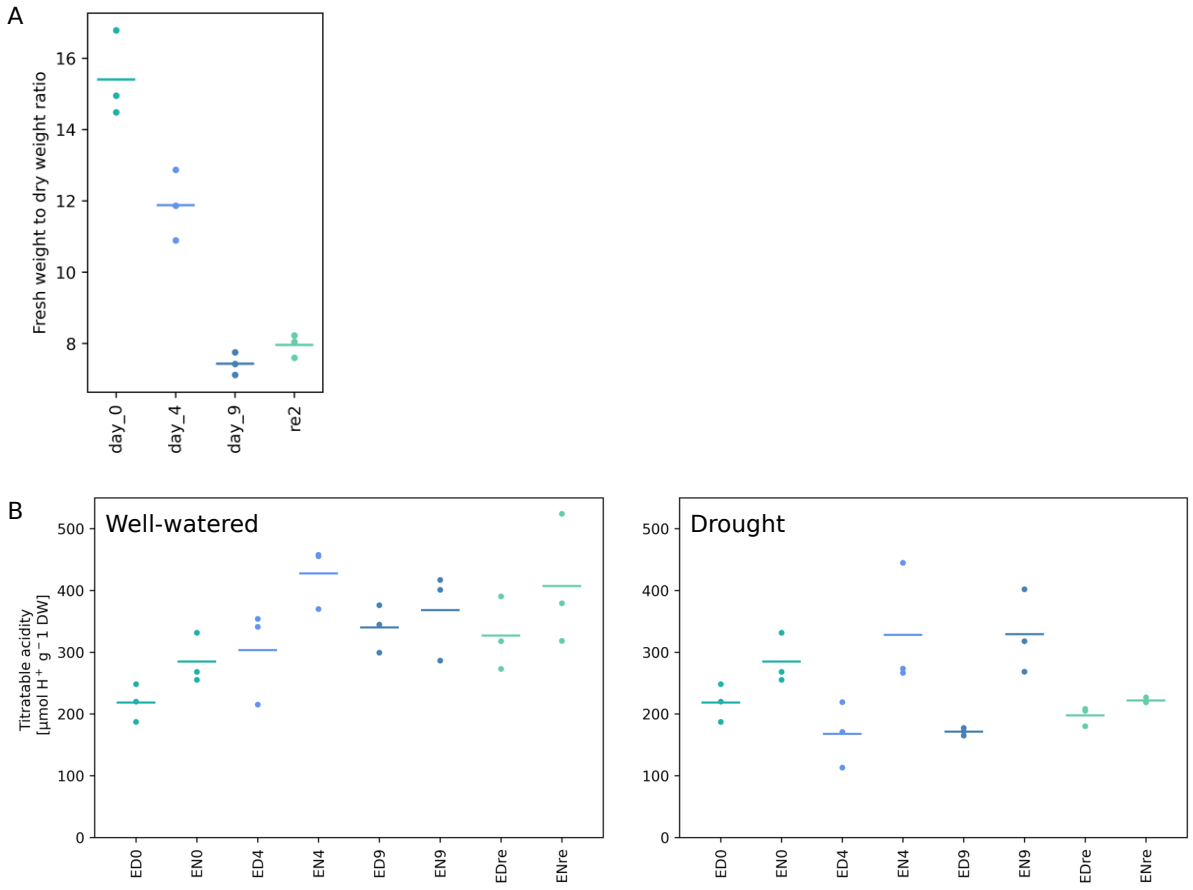

Figure 2: Changes in weight and titratable acidity levels during the time course.
A: Leaf weight of drought-stressed plants at day 0, day 4, day nine and 2 days after re-watering. 3 replicates and its mean are shown as fresh weight to dry weight ratios, B: Titratable acidity levels during the time course of well-watered and drought stressed plants. 3 individual replicates and the mean are shown for each time point.

Metabolic analysis of drought-stressed leaves

To understand the metabolic changes during the C_3-CAM transition, we analyzed metabolites from samples at day nine, where plants have either been watered on a regularly basis (WW) or on water-withhold (D). Timepoints of sampling were chosen two hours after dust or dawn.

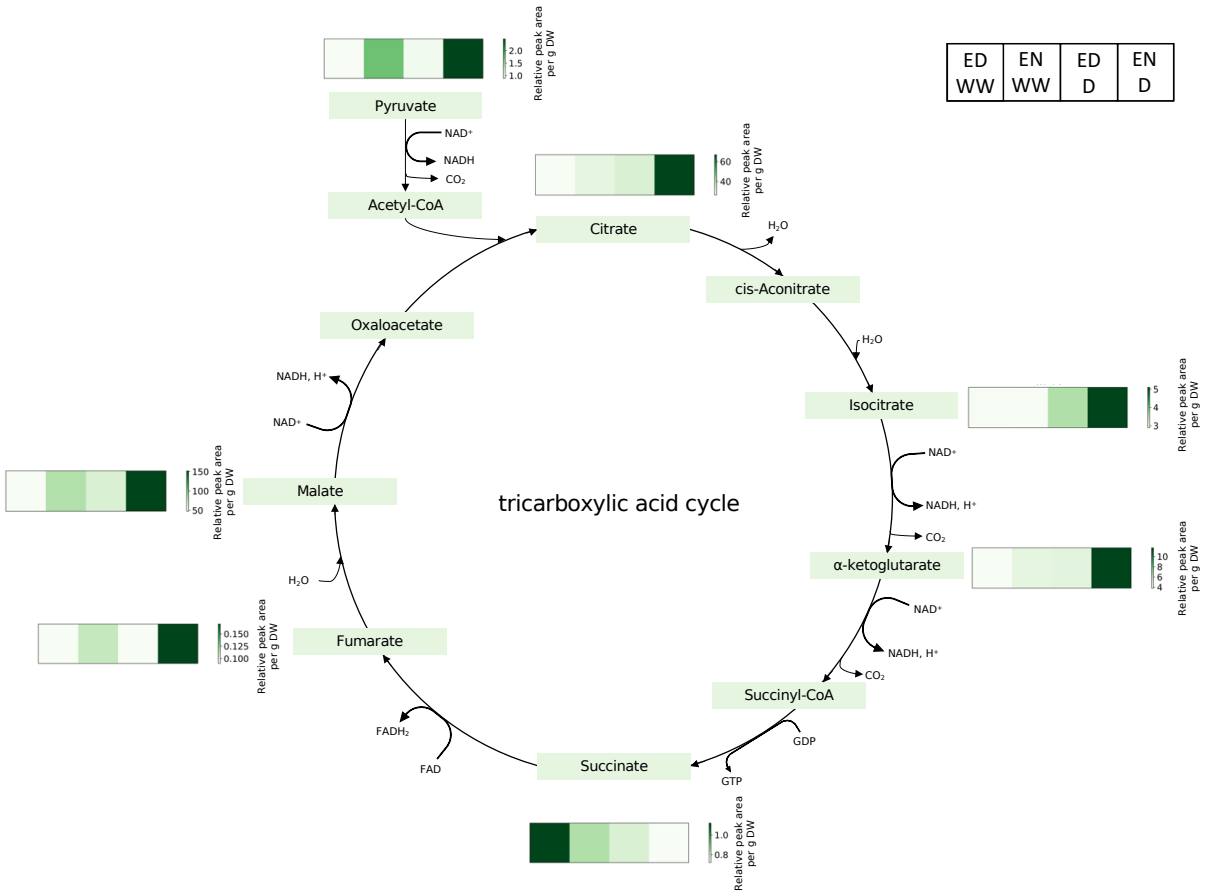

Figure 3: Metabolic changes of intermediates of the tricarboxylic acid cycle.
Boxes show mean values of well-watered (WW) and drought (D) stressed plants on day nine at the of the day (ED) or end of the night (EN) visualized by a color code. Darker colors indicate higher values, lighter colors indicate lower values. Values are calculated as the relative peak area per gram dry weight.

Figure 3 shows the components of the tricarboxylic acid cycle (TCA) and their metabolite levels indicated by heatmaps. Values shown represent the mean of five individual samples and are calculated as the relative peak area per gram dry weight. Boxes, from left to right, show data ED and EN samples, well-watered or drought, respectively. Darker colors indicate higher values, while lighter green colors represent lower values.

Pyruvate, citrate, isocitrate, α-ketoglutarate, fumarate and malate levels were increased at the end of the night (compare Figure 3 and Supplemental Table S 1). However, levels were higher for drought-stressed samples compared to well-watered plants. Except for pyruvate,

metabolite levels at the end of the night were significantly different (Supplemental Table S 1) between the different treatments. In contrast to that, succinate levels show increased values at the end of the day and levels are higher for well-watered plants. In conclusion we could observe changes in metabolites involved in the TCA cycle when plants have been drought-stressed. The changes of the organic acids described here, go hand in hand with the findings of the titratable acidity levels (compare Figure 2B).

Transcriptome analysis of *T. fruticosum* helps to understand the regulation of facultative CAM

To understand the genetic regulation behind the phenotypic and physiological adjustments observed in response to water withdrawal, we performed whole-mRNA transcriptome sequencing for 34 samples of different treatments during a time course.

RNA-seq analyzes was used to conduct principal component analysis (PCA), gene expression clusters and more detailed analysis of genes and potential transcription factor binding motifs.

Comparative expression dynamics in *T. fruticosum* in response to drought stress

In an initial PCA on the mapped transcriptome data for the drought-treated samples, 45% of the variance were explained by the first principal component and 30.5% by the second. Two main clusters in the PCA separated EN and ED samples along the first principal component. In the EN cluster, day nine samples were distinct from day zero, day four and re-watered samples. The ED cluster also showed differences for samples throughout the time course, however, samples of day nine are closer to re-watered samples as seen in the EN cluster.

PCA analysis across all samples (Supplemental Figure S 2.) as well led to a cluster separation between end of day and end of night samples. Here, the first principal component explained 43%, the second principal component explained 35% of the variance. Within the clusters, a tendency towards a separation by sampling time-points could be observed. In the cluster containing EN, the timepoints were dispersed further compared to the second cluster. Within the EN cluster, samples from day zero were in close proximity to day four and re-watering samples, as well as well-watered plant samples from day nine. Drought-stressed plant samples taken on day nine separated from the others within the cluster. Samples in the ED cluster were less spread, however day nine drought samples were also slightly distinct. PCA analysis

visualized time course data and could show differences between end of day and end of night sampling points, but also for plants under drought stress.

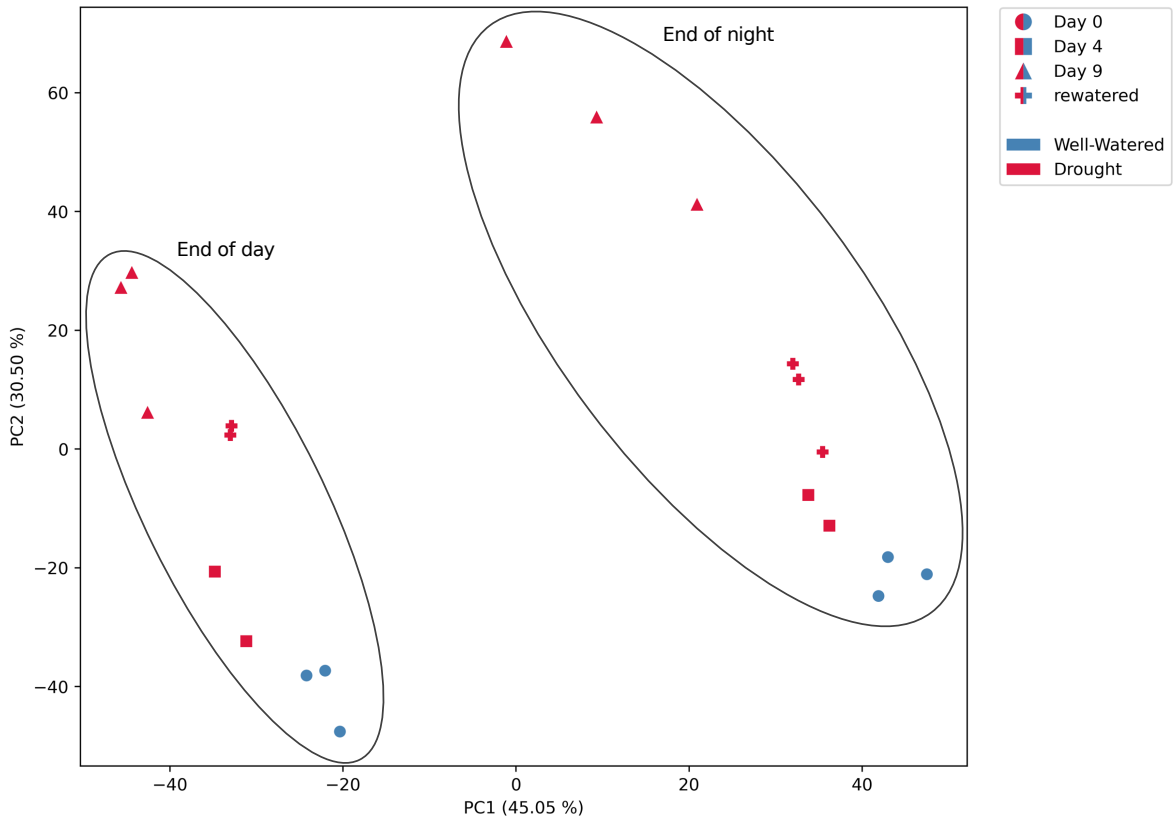

Figure 4: PCA analysis to visualize comparative expression dynamics.
Each dot represents an individual sample of a drought-stressed plant during the time course. Different symbols are used to highlight sampling timepoints. Red colors indicate drought stressed plants, blur colors well-watered plants. The two principal components are shown on the axes, where the first one explains 45% and the second one 30% of the variance.

Analysis of co-expression gene clusters

In the time-course transcriptomic data, we looked for co-expressed gene clusters especially in the drought datasets. Using *Clust* (Abu-Jamous and Kelly, 2018) coordinately behaving and putatively co-expressed genes can be identified and extracted. Using *Clust*, we could identify five different clusters from our time course data of drought stressed samples (Figure 5).

Cluster 1 contained 4290 genes, cluster 2 3669 genes and 3853, 1213 and 1267 genes could be associated to cluster 3, 4 and 5, respectivley. Cluster 1 and 3 show a diurnal expression pattern, where either end of night or end of day timepoints showed upregulation of expression, respectively. Cluster 2 contained genes which showed lower expression at day nine. Genes

that were upregulated under drought were associated to cluster 5. Cluster 4 showed a diurnal pattern with slight increase in normalized transcript levels on day nine.

We utilized Mercator (Schwacke et al., 2019) to functionally annotate the reference *T. fruticosum* transcriptome using *MapMan* bins. Genes associated with the MapMan bins "coenzyme metabolism", "photosynthesis" and "nutrient uptake" were statistically enriched, determined using Fisher´s test, in cluster 1. In addition to that we also identified genes associated to cluster 1 associated to "plant reproduction", "solute transport" and "cytoskeleton organisation". Cluster 3, which showed a diurnal expression pattern included enriched genes associated with the bins "clade-specific metabolism", "external stimuli response", "RNA processing", "carbohydrate metabolism" and "protein modification". Cluster 2 and 5 showed up- or downregulation at day nine under drought-stress, respectivley. Cluster 2 included enriched genes associated with the bins "clade-specific metabolism", "photosynthesis" and "protein biosynthesis genes". Moreover, we could identify genes related to the MapMan codes "cell wall organisation", "coenzyme metabolism" and "cell division" in this cluster. Genes related to cluster 5, showing downregulation at day nine, are quite different. The genes from this cluster are asoociated with the bins "protein homeostasis", "multi-process regulation", "chromatin organisation", "lipid metabolism", "redox homeostasis" and "vesicle trafficking". Cluster 4 shows genes associated with the MapMan bins "vesicle trafficking", "external stimuli response" and "multi-process regulation", as well as "protein homeostasis", "cellular respiration" and "RNA biosynthesis".

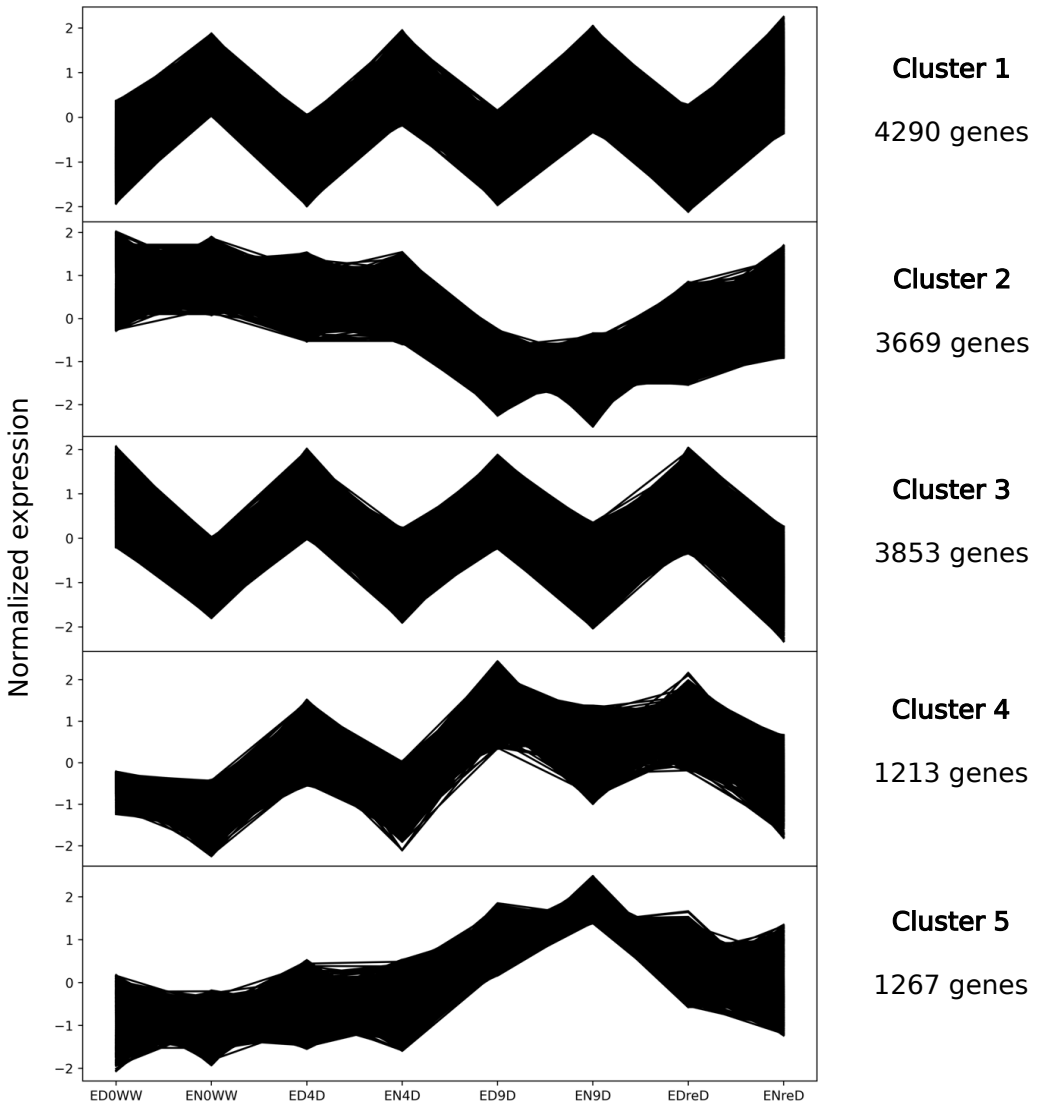

Figure 5: Cluster analysis of transcriptome data from drought-stressed plants throughout the time course, using *Clust*.
Genes have been automatically clustered leading to five clusters. Normalized expression is shown for well-watered plants (WW) and drought stressed plants (D) sampled at the end of night (EN) and end of day (ED) of day zero (ED0WW/EN0WW), four (ED4D/EN4D) and nine (ED9D/EN9D) as well as two days after re-watering (EDreD/ENreD).

To get a closer look into the set of genes involved in the transcriptional reprogramming after drought, we used *REVIGO*, a web based tool to visualize gene ontology (GO) terms enriched in the clusters (Supek et al., 2011). The algorithm is based on measurements of semantic similarities and reduces dimensionality of the enriched GO terms by multidimensional scaling. The hue of the scatter depicts the p-value after Fisher's exact test for GO term enrichment (Figure 6). In cluster 2, which shows downregulation at day nine under drought, we found highly enriched GO terms belonging to the terms "ubiquitin-dependent protein catabolic

processes" and "biosynthetic processes of plant cell wall" (Fig. 6). In addition to that, "response to water deprivation" was highly enriched in cluster 2. In cluster 5, which showed upregulation under drought at day nine, besides others, we could identify an enrichment of GO terms of "trehalose biosynthetic processes" and "acetyl-CoA biosynthetic processes". Moreover, genes with the GO term "negative regulation of absisic acid-activated signaling pathway" are highly enriched. Diurnal patterns in cluster 1 and 3 showed enriched transcripts related to "fatty acid processes" (Supplemental Figure S 4). Additionaly, we could find an enrichment of "cellular responses to light stimulus" and "chlorophyll biosynthetic processes" in cluster 1. "Sucrose catabolic processes", "RNA modifications" and "spermidine biosynthetic processes" are significantly changed in cluster 3. "Floral organ morphogenesis" and "embryo development ending in seed dormancy", as well as "positive regulation of gibberellic acid mediated signaling pathways" are enriched GO in cluster 4, where besides a diurnal pattern a slight upregualtion under drought can be found.

Clust analysis of well-watered samples led to two clusters of putatively co-expressed genes (Supplemental Figure S 3). Cluster 1 contained 5126 and cluster 2 4473 genes. Both showed diurnal patterns, while cluster 1 showed upregulation at the end of the night and cluster 2 higher expression for genes at the end of the day. Genes of cluster 1 were involved in "photosynthesis" and "coenzyme metabolism", as well as "nutrient uptake", "plant reproduction" and "lipid metabolism". In cluster 2 genes from "polyamine and carbohydrate metabolism", "external stimuli response", "RNA processing" and "protein modificaiton" can could be found. Using *Clust* and *REVIGO* led to clustering of go-expressed genes, as well as identification of enriched GO terms within the clusters. A full list of genes can be found in the dataplant repository.

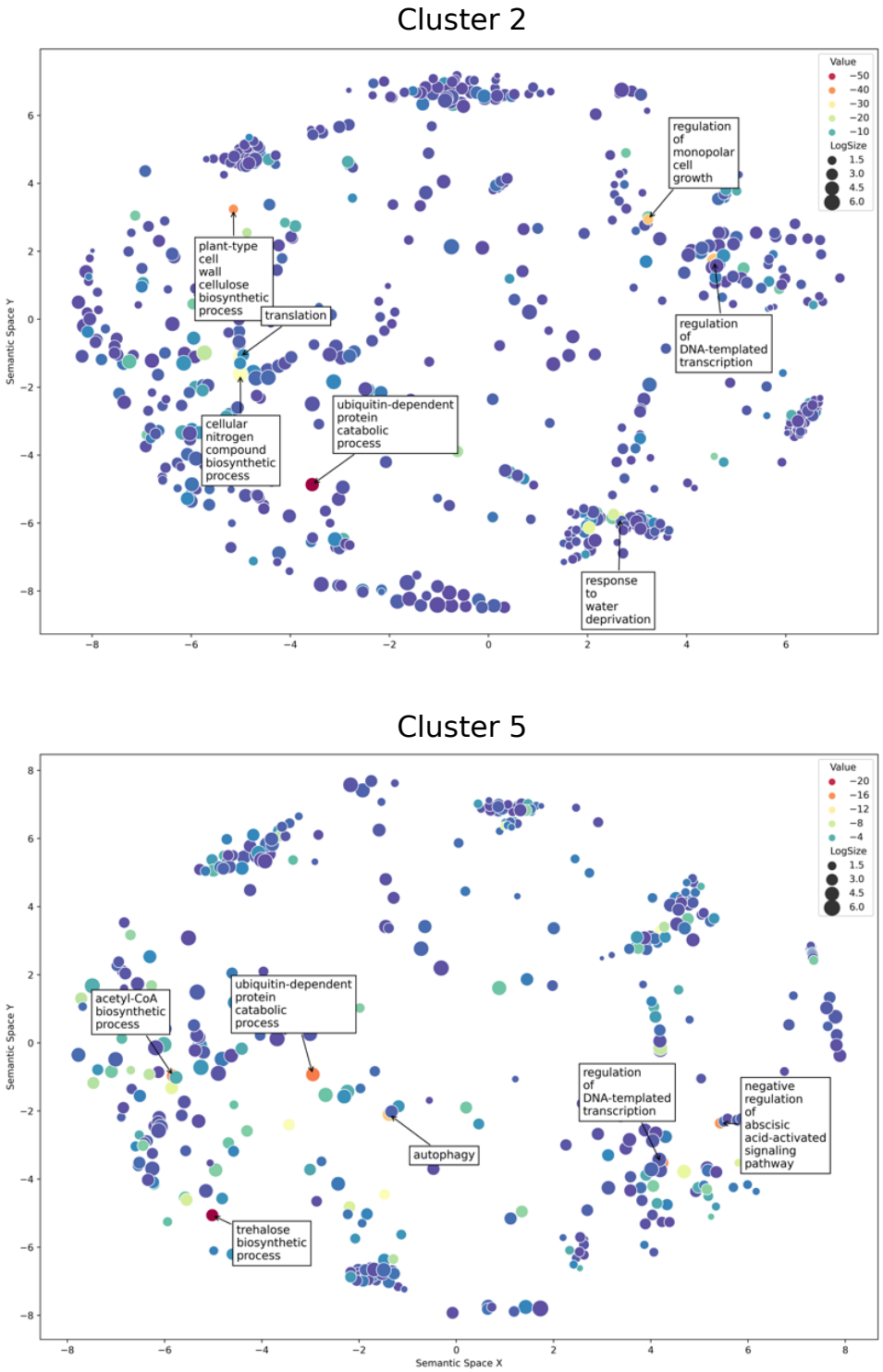

Figure 6: Scatter plot depicting the GO term enrichment after multidimensional scaling. Enriched GO terms are shown for cluster 2 and 5. Multidimensional scaling was performed to reduce dimensionality and semantic similarities are used to group GO terms. Axes are scaled as semantic space. Dots represent the GO terms found in each cluster. Dot color and size represent enrichment significance after Fisher's exact test, where red colors indicate more significantly enriched GO terms than blue colored dots. The number of genes within the GO term is depicted by the dot size.

PEPC plays an important role in CAM photosynthesis

PEPC plays an important role in the primary CO_2 fixation. As photosynthesis is separated in a temporal manner, the components of the CAM machinery need to be precisely regulated by the circadian clock (Bräutigam et al., 2014). *PEPC* fixes CO_2 in form of bicarbonate together with PEP to oxaloacetate. In further steps, malate is formed, which is stored as malic acid in the vacuole during the night. Six genes have been identified in the major *PEPC* orthogroup (OG0001398) in *T. fruticosum* (Brilhaus et al., 2023). Four *PEPC* genes reside together in close proximity to each other on the same scaffold, presumably originating from a tandem duplication event. The genes do not only differ in their amino acid sequence (Brilhaus et al., 2023), but also show differences in their transcript abundance (Supplemental Figure S 5.). We confirmed that the genes with the IDs Tf_contig_062_000128 and Tf_contig_062_000130 show basic level of expression under all conditions and time points. However, a slight increase in transcript abundance on day nine after water-withhold can be observed. For Tf_contig_062_000130, the upregulation is limited to samples taken at the end of the day. In contrast to this, Tf_contig_062_000129 and Tf_contig_062_000131 show almost no transcript abundance in the well-watered samples, but expression is increased nine days of drought stress. Upregulation of Tf_contig_062_000129 can be observed at the end of the night (EN9D), while expression of Tf_contig_062_000131 is both increased at the end of the day and end of the night (ED/EN9D).

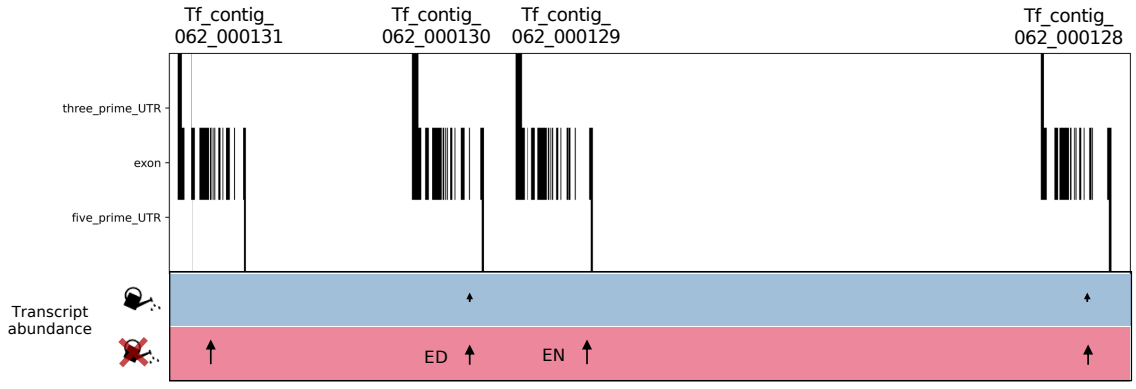

Figure 7: Overview of four *PEPC*s on same scaffold and how their transcript abundance changes in response to drought.
Schematic overview of gene region of Tf_contig_062_000128, Tf_contig_062_000129, Tf_contig_062_000130 and Tf_contig_062_000131 is shown. Arrows indicate upregulation, smaller arrows less upregulation than bigger arrows. Transcript abundance behavior is shown under well-watered (blue) and drought (red) conditions.

Potential TF candidates of transcriptional regulation

Transcriptional regulation steps are often mediated by transcription factors (TFs), which can target specific *cis*-regions and recruit additional proteins if needed. Enhancers, short DNA sequenced to which TFs can bind, are needed to activate transcription to a higher level (Strader et al., 2022). In CAM photosynthesis, differentiation of regulatory *cis*-elements might play a major role in gene regulation (Monson, 2012).

To investigate transcription factor candidates which might play a role in the adaptation to drought in *T. fruticosum*, we analyzed gene expression of a selected set of TFs during the time course. The set of TFs was selected based on previous motif binding studies to *PEPC* (Maleckova, PhD thesis, 2020). Read coverage plots showed the transcript abundance for each of three selected TFs at along the analyzed time course (Fig. 8). Tf_contig_016_000497 was identified as a homolog to the *A. thaliana* genes AT2G27990, AT5G02030, both encoding for proteins belonging to the BEL1-LIKE HOMEODOMAIN (BLH) family. In all our samples, BLH was highly expressed. Transcript abundance was similar between samples of drought stressed as well as well-watered plants. Moreover, the expression values were similar for samples taken at the ED and EN timepoints. Tf_contig_037_000016 has Arabidopsis homolog to AT2G31180 (MYB14) and AT1G06180 (MYB13). Both belong to the family of MYB TFs, involved in a variety of plant processes (Ambawat et al., 2013). In our data, the MYB14 TF showed higher transcript abundance for samples taken at ED compared to EN samples. Expression could be observed for both well-watered and drought stressed plants. However, transcript abundance was highest at day nine. The homolog of Tf_contig_015_000048 in *A. thaliana* was identified as TF RESPONSIVE TO DESICCATION (RD26) (AT4G27410). Transcript abundance for this gene was highly increased under drought at the end of day of day nine. Transcript abundance was only slightly upregulated at the end of day four and two days after re-watering for both WW and D samples. Here, we have shown expression for three representative TFs throughout the time-course, which show different responses to drought stress and time of the day in *T. fruticosum*.

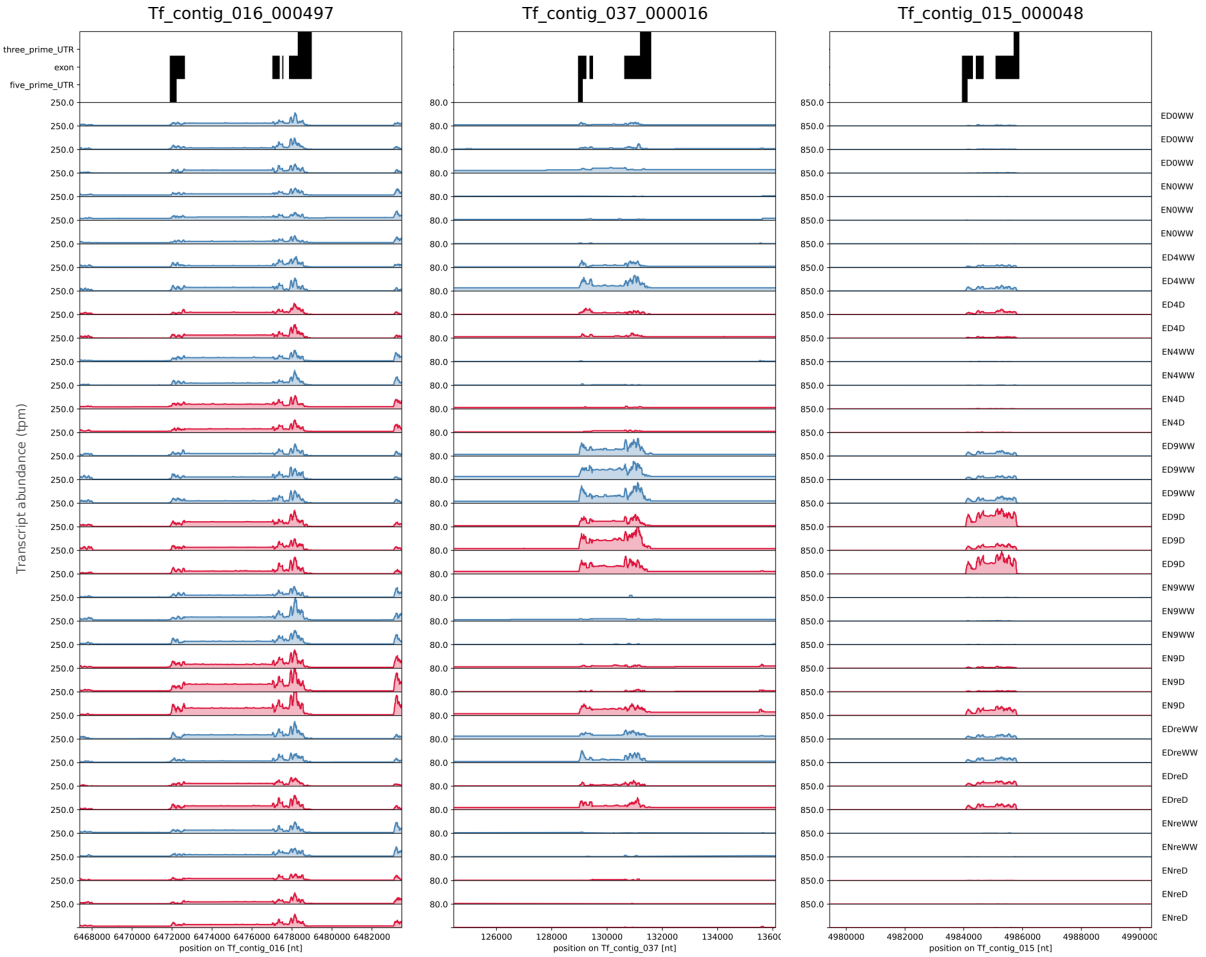

Figure 8: Expression coverage plot of transcription factor Tf_contig_016_000497, Tf_contig_037_000016 and Tf_contig_015_000048.
Transcript abundance of the individual gene region is shown. Time points (end of day (ED), end of night (EN)) at each sampling day (0, 4, 9, re-watered(re)) and replicates are represented individually. Blue or red color indicates samples of well-watered (WW) or drought stressed (D) plants, respectively.

Mammalian cells as an orthogonal system to study gene regulation

Based on previous experiments and our time-course transcriptome profiling, we performed a deep investigation of the interplay between three TFs and three *PEPC* homologs. The co-expression data and *in-silico* predictions of binding motifs (Maleckova, PhD thesis, 2020) suggest a potential connection between these TFs and the regulatory regions of the *PEPC* homologs.

For fast and easy identification and confirmation of TF binding to their predicted binding regions, we established a synthetic biology approach using heterologous expression in an orthogonal system. We chose the mammalian cell line Chinese ovary hamster-K1 (CHO) to test interactions between the heterologously expressed TF candidates and a secreted alkaline phosphatase (SEAP) reporter system under control of the target Tf_*PEPC cis*-regions fused to

a minimal promoter. Mammalian cells were co-transfected with constructs, carrying either the *PEPC* upstream region or the coding sequence of the TF of interested. The 1.1 kbp *PEPC* upstream region was cloned upstream of a P_{CMW} minimal promoter. The promoter controls expression of the SEAP, which was measured photometrically and was used as an assay read-out. The individual TF gene was either cloned with or without the C-terminal *transactivator domain Virus Protein 16 (VP16)*, which can facilitate TF binding in the mammalian cell (Müller et al., 2014). 24 h after transfection, the SEAP activity was measured in a plate-reader. The signal was then used as an output to determine potential interactions between the putative *cis*-region and the TFs, that are suggested to function as enhancers. Based on analysis of the RNA-seq dataset, we chose a variety of TFs, which are predicted to bind to motifs found in the upstream *PEPC* regions and show differences in their expression profile between the conditions tested (Figure 8). We focused on the 1.1 kb upstream regions of three *PEPC* orthologs, Tf_contig_062_000128, Tf_contig_062_000129 and Tf_contig_062_000131 as these *PEPC* orthologs show different transcript abundance. Due to their transcript abundance pattern, we assume that they function mainly in CAM (Tf_contig_062_000129 and Tf_contig_062_000131) or in C_3 (Tf_contig_062_000128) photosynthesis. Here we are testing the three TFs, Tf_contig_016_000497 (BHL), Tf_contig_037_000016 (MYB), Tf_contig_015_000048 (RD26) as discussed above. The experiment has been repeated three times individually.

Figure 9 shows the SEAP activity [U/L] of the mammalian cell lines expressing the respective TFs co-transfected with the upstream region of one of the *PEPC* homologs. Negative controls are indicated by 131 (-), 129 (-) and 128 (-) for the individual genes, respectively. As a negative control, upstream *PEPC* regions were co-transfected with a non-specific polycistronic-cassette construct. The upstream regions of the two predicted CAM isoforms Tf_contig_062_000129 and Tf_contig_062_000131 did not show SEAP activity, while signal could be observed for Tf_contig_062_000128. Interactions of MYB and RD26 were tested with Tf_contig_062_000131. SEAP expression was observable for the MYB ortholog and significantly higher signal for the RD26 ortholog when compared to the negative control. Fusion of the transactivator domain VP16 to RD26 seemed to be needed for significantly increased expression. Detection of SEAP signal can be used as a read-out for TF-DNA interaction, as SEAP activity can only occur when its promoter is switched on due to enhancer binding. The BHL, MYB and RD26 homologs from *T. fruticosum* were tested for their interaction with Tf_contig_062_000129. For all three TFs an

increase in SEAP activity could be observed. However, the signal was strongest for the RD26 and lowest for BHL TFs. In addition to that, increase in signal could also be observed when the TF was fused to the transactivator domain. BHL was co-transfected with Tf_contig_062_000128. A strong SEAP expression could be found, also increased when the TF was fused to VP16. However, the negative control also showed an observable signal which might indicate leakiness in the test system. We could still identify a highly significant SEAP activity of the Tf_contig_062_000128 upstream region and BHL interaction compared to the negative control of the Tf_contig_062_000128 upstream region.

Using the orthogonal test system., we could confirm the binding of TFs that showed a transcription pattern correlating with the *PEPC* transcript pattern. However, to verify that the system is suitable to test predicted interaction pairs, we designed positive controls for the assay. There are *bona fide* no closely related plant species to *T. fruticosum* with already confirmed interaction pairs known in literature to date. Therefore, we developed a CRISPR/dCas9 system based on polycistronic tRNA+sgRNA (PTG) together with a dead Cas9, fused to C-terminal transcription factors. The catalytically inactive dCas9 can still target the DNA-sequence, but cannot cleave it (Brezgin et al., 2019). The PTGs are used as a guide for the dCas9-transactivator domain to achieve binding of the dCas9/sgRNA complex to the target signal and initiate gene expression. The PTG constructs were based on single guides chosen based on the *PEPC* upstream regions. Its final design and virtual construction were done using the PolyGEN software (Urquiza-Garcia, unpublished). The predicted primers were used to amplify the fragments needed, followed by GoldenBraid assembly to create the final construct. When the plasmids are transformed into mammalian cells, the endogenous cell system will process the PTG and release the gRNA needed. Both PTG constructs tested within the system, one PTG using single guides of a representative CAM *PEPC* (here Tf_contig_062_000131) and the other one of Tf_contig_062_000128, show high expression, indicated by SEAP levels. Values were even higher for the putative C_3 *PEPC*, Tf_contig_062_000128. High SEAP level indicate successful performance of positive control. As an assay control itself, we used a constitutive expression of SEAP, which indicated if the assay is technically working. Using this method, we could create specific controls to receive a reliable read-out if our synthetic approach is suitable to confirm interaction pairs. Moreover, we established a method to identify and confirm TF/*cis*-element interaction of *T. fruticosum* in an orthogonal system.

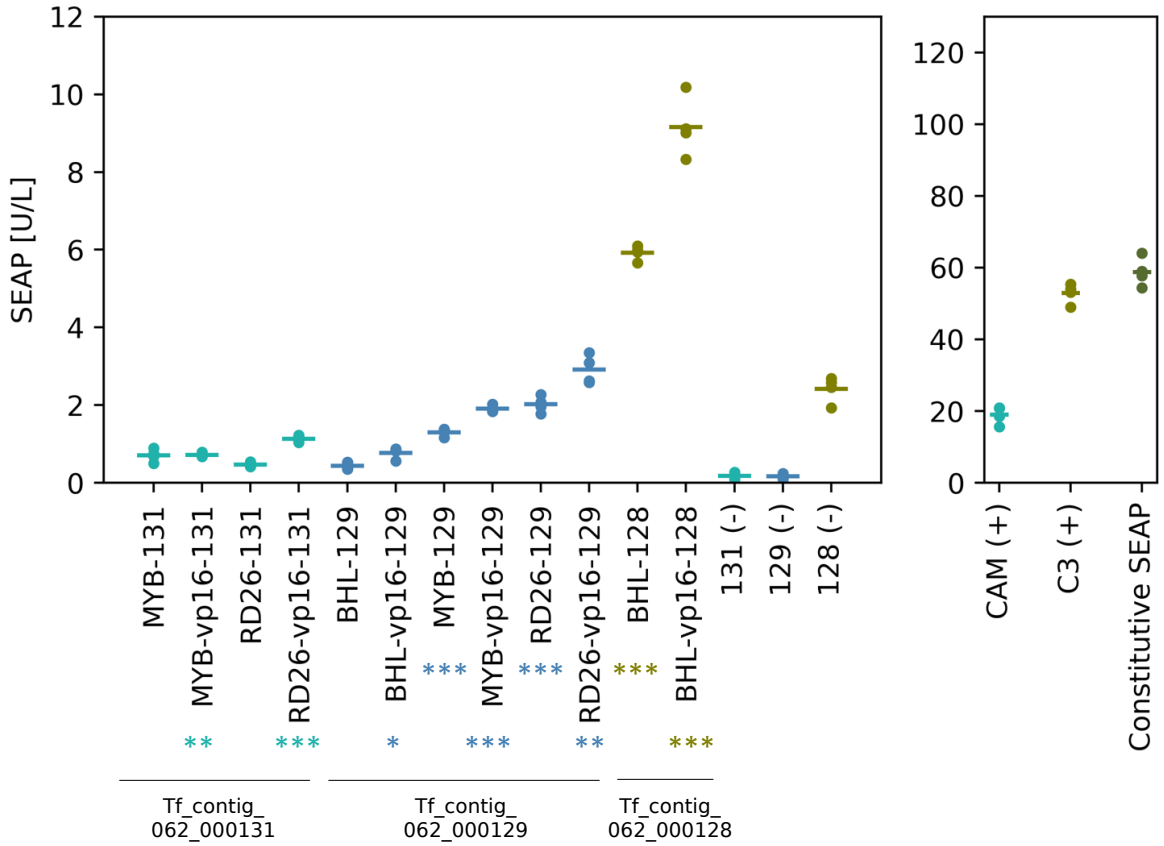

Figure 9: Interaction of TFs and three *PEPC* upstream regions have been tested in mammalian CHO cells.
Secreted alkaline phosphatase assay has been used as detection assay. Four individual replicate and their mean is plotted. BHL represents Tf_contig_016_000497, MYB represents Tf_contig_037_000016 and RD26 represents Tf_contig_015_000048. Colors indicate measurements or TF interactions with Tf_contig_062_000131 (turquoise), Tf_contig_062_000129 (blue) or Tf_contig_062_000128 (olive) or the respective negative (-) or positive (+) control. Constitutive expression of SEAP is measured as a positive control for the assay. Asterixis underneath the indicate significance level when compared to it regarding *PEPC* upstream region negative control. Statistics have been calculated using Bonferroni corrected post-hoc test; p-values: * $p < 0.05$, ** $p < 0.01$, *** $p < 0.001$.

Transcription factor analysis reveals further potential candidates that might play a role in adapting to environmental changes in *T. fruticosum*

To identify further TF candidates that might play a role in facultative CAM, we analyzed the scaffold region containing the four *PEPC*s in more detail. As discussed before, the four genes are in close proximity on the same scaffold (Tf_contig_062), but show differences in their transcript abundance (compare Figure 7, Supplemental Figure S 5) and amino acid sequence (Brilhaus et al., 2023). The potential tandem duplication event leading to potential sub-or neofunctionalization makes them an interesting target to study facultative CAM.

We used the *Find Individual Motif Occurrence (FIMO)* tool (Grant et al., 2011) to identify putative TF binding sites (TFBS) in the region of the four *PEPC*s on contig 62. *FIMO* scans for known

motifs from the JASPAR database, using the *Arabidopsis thaliana* TF set and individual sequence matches in the *T. fruticosum* query contig.

We identified 61 TFs, for which potential TFBS were found in the selected *PEPC* region (Figure 10). The upper square of Figure 10 shows the helixer annotation of the four *PEPC*s, as described before (compare Figure 7). The middle part of the figure shows the location of the TF motif. TFs are distributed based on their q-value. We identified a high number of TFBS in the upstream region and in the 5´UTR of TF_contig_062_000131. However, there is an even high number of TFBS found in the upstream region of TF_contig_062_000129, but almost none in the short intergenic sequence directly upstream of TF_contig_062_000130 and TF_contig_062_000128. There are a lot of TFBS found in relatively close proximity upstream of TF_contig_062_000129, but a high number is also found even further upstream. In the set of predicted TFBS, we identified binding motifs of TFs that belong to the family of EHTYLENE RESPONSE FACTORS (ERF). Moreover, we identified a number of TFBS for BASIC PENTACYSTEINE (BPC).

Besides transcriptomics and TFBS prediction, the influence of epigenetics on the drought response of *T. fruticosum* cannot be ruled out. However, the lack of any epigenomic data for *T. fruticosum* or closely related species makes it challenging to make any assumptions about the influence of epigenetics on the analyzed phenotypes. To get an insight into the dynamics of the heterochromatic state of the *T. fruticosum* genome during the C_3-CAM transition, we employed *predomoter*, a novel deep neural network-based platform to predict Assay for Transposase-Accessible Chromatin using sequencing (ATAC-seq) and Chromatin Immunoprecipitation DNA-Sequencing (ChIP-seq) read coverage along our analyzed scaffold. *Predmoter* was trained and validated with data from a variety ATAC and ChIP-seq data of monocot and dicot plants, as well as from other photosynthetic organisms. Here we show the predicted ATAC-seq (blue colored line) and ChIP-seq (orange line) coverage for the gene region of the four *PEPC*s (Figure 10). ChIP-seq is experimentally used to analyze protein-DNA interactions. Using *predmoter* to predict these regions in our gene region of interest, we could find a number of ChIP-seq peaks. Interestingly, the predicted TFBS and the predicted ChIP-seq peaks correlate quite precisely. These peaks are found in the regions of *FIMO* predicted TF motifs. Looking for ATAC-seq predictions, we could find a peak in the upstream region of TF_contig_062_000129. Suggesting an open chromatin region upstream of a number of *FIMO* predicted TF motifs.

To further analyze for TFs, we selected seven regions, which will be called "bin" (compare Figure 10) with predicted TF binding regions based on *FIMO* ChIP-seq prediction. Within the regions, we selected four TFs each with the highest difference between its transcript abundance pattern of well-watered and drought stressed plants (Supplemental Figure S 6). In bin 1, which is found in the region of the 5'-UTR of TF_contig_062_000131, we found TF with Arabidopsis homologs to ARABIDOPSIS THALIANA HOMEOBOX 7 (ATHB-7) and ABA-RESPONSIVE KINASE SUBSTRATE 1 (BHLH122) with strong transcript abundance increase at day nine of drought (ED/EN9). We also identified SUPPRESSOR OF OVEREXPRESSION OF CO 1 (SOC1) and LATE ELONGATED HYPOCOTYL 1 (LHY) in bin 1, showing a smaller difference in drought to well-watered samples. BHLH122 was also found in bin 2 and SOC1 in bin 2 and 3. We selected bin 2 further upstream of TF_contig_062_000131 and identified also ETHYLENE RESPONSE FACTOR 73 (ERF073) and ARABIDOPSIS NAC DOMAIN CONTAINING PROTEIN 78 (NAC078). Bin 3 to 7 were selected in the region of the 5'-UTR of TF_contig_062_000129, as well as regions further upstream. ETHYLENE RESPONSE FACTOR 74 (RAP2) were found in bin 3, 4 and 7. ERF073 was found in bin 5 and 6. We also identified SOC1 and TELOMERE REPEAT BINDING FACTOR 1 (TRB1) in bin 3 and the TFs ABSCISIC ACID RESPONSIVE ELEMENTS-BINDING FACTOR 3 (ABF3) and HOMEOBOX PROTEIN 23 (ZHD9) in bin 4. TRB1 and WRKY DNA-BINDING PROTEIN 23 (WRKY23) could be found in bin 5. LHY and TRB1 were identified in bin 6, while bin 7 also unravels TFs ATHB-7. These TFs identified showed differences in their expression pattern during drought and were found in close proximity to the putative CAM PEPCs of *T. fruticosum*.

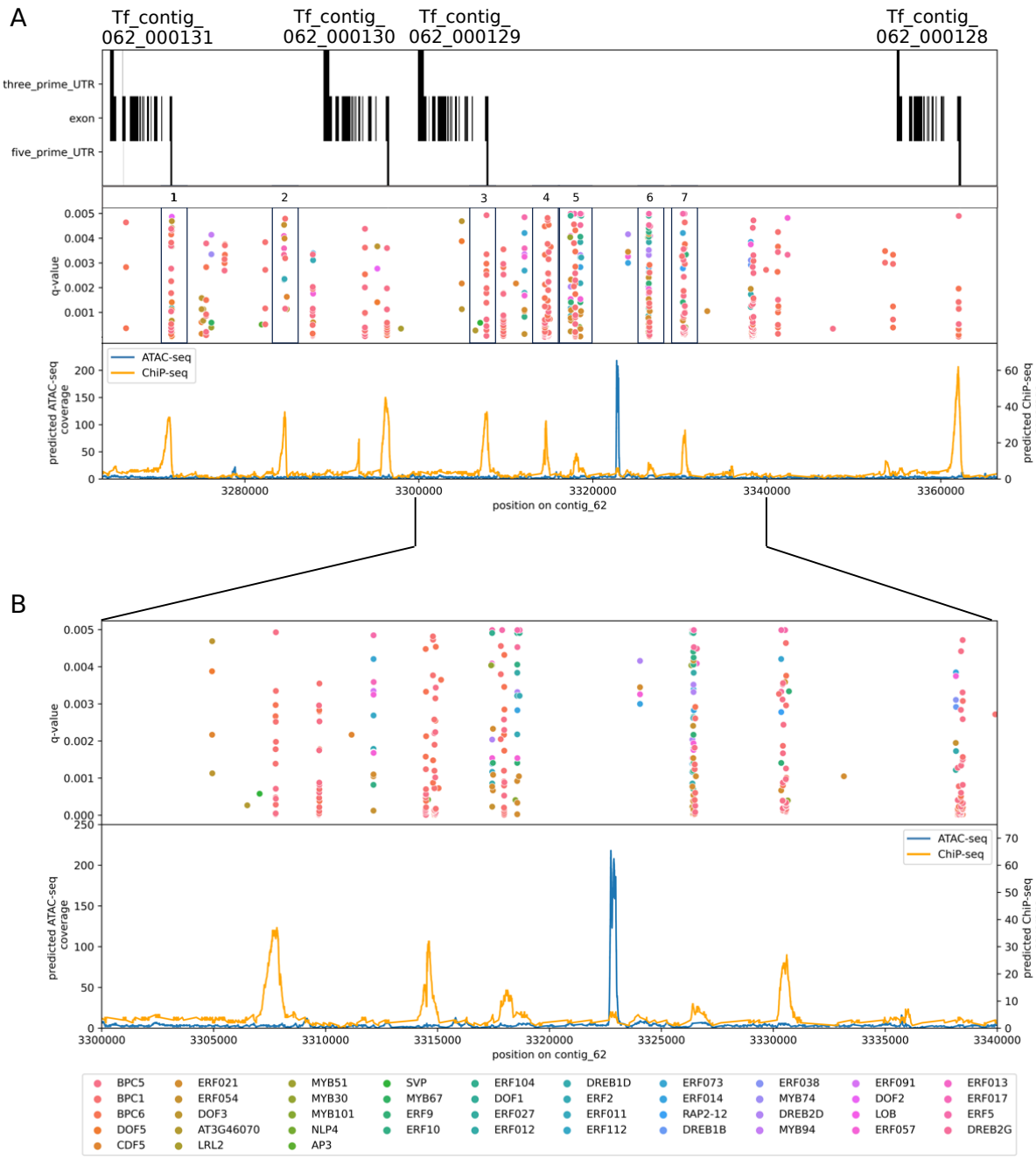

Figure 10: *FIMO* analysis, ATAC and ChIP-seq predictions of *PEPC* region on scaffold 62.
The exact gene position is plotted on the x-axis. A: Helixer annotations with three and five prime regions are shown in the upper part. *FIMO* predictions are plotted in the middle part. *FIMO* performs Benjamini-Hochberg multiple testing correction as part of the motif search functionality. TFs are distributed by their calculated q-value. The lower part shows ATAC predictions, represented by the blue colored line and predicted coverage is shown on the left y-axis. ChIP-seq predictions are plotted in orange with predicated coverage indicated on the y-axis on the right-hand side. B: A zoom-in plot of the gene region from 3300000-3340000 bp on scaffold 62. Shown are the *FIMO* (upper part), ATAC-seq (blue line, lower part) and ChIP-seq (orange line, lower part) predictions.

Discussion

Environmental changes can be a severe challenge for sessile organisms such as plants. Here we investigated the facultative CAM plant *Talinum fruticosum* that can transition between C_3 and CAM photosynthesis. This strategy helps to adapt to environmental changes, like drought. Plants performing CAM photosynthesis separate the photosynthetic steps throughout the day. After CO_2 is taken up and converted to oxaloacetate malate is store as malic acid, together with citric acids, in the vacuole during the night. These acids are transported out of the vacuole at the next day and will be used as a pre-component in the Calvin-Benson Cycle. Thus, increasing levels of a titratable acidity are used as an indicator of CAM activity (Winter and Smith, 2022).

In our study, we could observe increasing acidification of the leaves at the end of the night when plants have been on water-withhold and decreased when water has been re-supplied. We observe more similar titratable acidity levels on day zero and after two days of re-watering, which can give hints about performance of C_3 photosynthesis. Changes in the acidity level (Figure 2B) and measurable organic acids (Figure 3) indicate that *T. fruticosum* adapts it photosynthetic strategy to drought stress. Therefore, it can be assumed that *T. fruticosum* performs CAM during dry periods, but can switch back to C_3 when water is re-supplied. The data collected from the growth chamber in Germany confirm the measurements of the experiment performed in the Republic of Panama (compare (Brilhaus et al., 2016)). However, we could also observe a general increase of titratable acidity levels over time, when plants have been well-watered. One explanation could be a developmental effect of basic expression of CAM, where acidity levels are higher when the plant is fully developed. A correlation of CAM and phenotypic plasticity has also been found in other plants (Winter et al., 2008). We also found the leaf rosette rather closed during drought, which might reduce water loss as the leaves are less exposed to sun light. Phenotypic findings and acidification during drought go hand in hand with previous observations from Brilhaus et al., 2016.

Within the study, we observed that data of well-watered plants from day nine was less similar to day zero, four and re-watered than expected. This is can for example be seen in the principal component analysis, where day nine well-watered samples cluster relatively close to day nine drought samples (Supplemental Figure S 2). This is also true for transcript abundance levels of the *PEPC*-CAM isoforms (Tf_contig_062_000129, Tf_contig_062_000131). A tendency of

increase can be observed at day nine, while transcript abundance seems to decrease at re-watering. One possible explanation for a weak stress response found in well-watered plants could be, the close spatial proximity between drought stressed and well-watered plants in the growth chamber during the experiment. It is known, that plants can signal, as well as sense stress responses to their neighboring plants. One mechanism used are the emission of volatile organic compounds (VOCs), which are known to influence not only gene regulation and metabolism, but also stress responses (Brosset and Blande, 2022). During water-withhold, *T. fruticosum* plants respond by activating drought stress responses. It might be assumed that the stressed plants transmit a signal to their neighboring plants, so they can prepare for a potential upcoming drought period. However, we did not observe a strong stress response in the well-watered plants, it is likely that these plants sense the signal, but as access to water is given, no strong stress response was activated. As seen in Supplemental Figure S 1, growth conditions were stable during the experiment. Since we did not detect changes in light intensity, humidity or temperature we might evaluate growth conditions as a rather unlikely reason for the plants stress response.

Metabolite analysis showed that, besides succinate, all measured components of the TCA cycle were increased at the end of the night of drought stressed samples (Figure 3). Succinate showed higher amounts not only at the end of the day, but also in well-watered plants. One explanation might be that the TCA cycle represents only one pathway and regulation might therefore also be dependent on alternative fluxes in the plant (Sweetlove et al., 2010). However, as *T. fruticosum* transitions to CAM photosynthesis upon drought stress, the plant seems to adapt its TCA cycle. Intermediates and organic acid could be found in higher levels two hours after dawn. Metabolic changes of malate and citrate could also be shown for other facultative plants (Lüttge, 2002; Winter and Smith, 1996) and in previous studies (Brilhaus et al., 2016).
Metabolic regulation involves cross-talk between photosynthesis and mitochondrial respiration. Complex II, succinate dehydrogenase (SDH), is not only part of the electron transport chain (ETC), but also involved in the TCA. Assembly of a fully functional SDH complex requires insertion of cofactors and presence of subunits. In *A. thaliana* SDH1 and SDH2 form the catalytic site of SDH of complex II, where electrons are transferred to FAD. It is known that lacking of one these requirements lead to decrease of enzymatic activity of SDH (Li et al., 2022). In our study, SDH1-2 and SDH3-1 show higher transcript levels under drought

(Supplemental Figure S 7). It is known from other plant species such as *Ilex paraguariensis*, that SDH1, that SDH1, the flavoprotein subunit, is upregulated under drought stress and ABA treatment. This could indicate that that *T. fruticosum* has a higher enzyme abundance of SDH under C_3 to the CAM state, which might be required for an osmotically adjustment. This might lead to a faster conversion from succinate to fumarate during a process to sustain metabolic adjustment and to recover after water is re-supplied (Acevedo et al., 2013).

Analysis of RNA-seq data gave new insights into the mechanism of the facultative CAM plant *T. fruticosum* and unraveled additional players in the gene regulatory network that might be investigated further. PCA for drought samples only and for both drought and control conditions showed separation of end of day and end of night samples, indicating a strong diurnal transcriptional regulation. Moreover, close proximity of samples from day zero, four and re-watering indicate that there might be many genes, which return back to normal expression relatively quick after re-watering. This observation could also be made in other plant species, like in the desiccation plant *Craterostigma* (VanBuren et al., 2023). Therefore, it could be assumed that the plants can adapt relatively quick to environmental changes using a complex and quick gene regulatory mechanism, to use the most efficient growth and survival strategy possible. PCA analysis showed a slight tendency for sample separation across the samples taken during the experimental time-course. This could reveal a developmental separation, like simple aging of the plant during the course of the experiment, since the trend was also visible in control, well-watered plants. However, samples from drought-treated species cluster distinct along the both principal components, indicating a stronger influence of drought on the transcriptional patterns than aging. It is known that for some CAM species, like *Kalanchoë pinnata*, that the extent of the CAM cycle is dependent on plant age (Winter et al., 2008), which might also be true for *T. fruticosum*. In addition to that, the data showed that EN9D were more distinct than ED9D in their respective cluster. This might suggest that gene expression of CAM-related genes is more differentiated at the end of the night than at the end of the day when plants face drought stress. This indicates that differential gene regulation of CAM-related genes may take place mostly during the night. Temporally differentiated gene expression has been observed for a variety of CAM species including *Yucca* (Heyduk et al., 2019) and *Kalanchoë* (Yang et al., 2017).

By analyzing specific GO terms, which have been grouped by semantic similarities in the identified clusters, we could also see differences in the underlying gene regulation of CAM. While photosynthetic regulation, such as biosynthesis of chlorophyll, but also fatty acid synthesis was found to follow diurnal rhythms, we identified stress responsive- and general cellular and gene regulatory transcripts in clusters showing drought responses. Cluster 2, which shows downregulated transcripts under drought, shows an enrichment of transcripts involved in growth and development.

In phenotypic observations, we observed that biomass was gained slower during CAM photosynthetic activity. Enriched transcripts found in cluster two confirmed the assumption that development is slowed down during drought. This characteristic was also found in other plant species and might indicate a trade-off towards survival under non-favorable environmental conditions (Winter, 2019). Cluster 1, which follows a diurnal pattern, shows enrichment of transcript involved in proline biosynthesis. Proline has been found in salt-stressed ice plants, following a diurnal rhythm (Sanada et al., 1995). Besides playing a role as an osmoprotectant, it was suggested that proline supports carbon fixation through citrate synthesis. This is done by supplying 2-oxoglutarate through proline degradation during the night (Töpfer et al., 2020). We have found enrichment of proline biosynthesis-related transcripts at the end of the night, which indicates a similar role in *T. fruticosum* plants during drought.

One of the key players of CAM photosynthesis, PEPC, shows transcripts of different expression patterns in *T. fruticosum*. Four *PEPC*s are found on the same scaffold in close proximity within 100 kbp. Differences in transcript abundance suggest that the different isoforms might play specialized roles in response to drought stress. Gene duplications have also been found in other CAM families, like the Agavoideae, where a duplication event in the *PEPC1* tree was observed (Heyduk et al., 2022). Differentiation in *PEPC* expression might be needed for adaptation to environmental changes and tight regulation of *PEPC* through the circadian clock. *PEPC1* knockdowns in *Kalanchoë laxiflora* led to changes in its oscillation patterns (Boxall et al., 2020), suggesting a strong importance of the clock implementation to the CAM pathway. It might be assumed that the presence of a variety of *PEPC* copies is needed for (time-)specific photosynthetic responses and regulation.

In addition to the *PEPC* genes, we investigated three TFs of interested that were predicted to bind certain *PEPC* upstream regions (Maleckova, PhD thesis, 2020). Tf_contig_016_000497 has Arabidopsis orthologs to BHL8 and BHL9, Tf_contig_037_000016 to MYB13 and MYB14 and Tf_contig_015_000048 to RD26. BHL TFs play a role in morphogenesis and meristem maintenance (Ung and Smith, 2011). It can be assumed that this TF is needed to maintain growth and development. Even though they play an important role, it is not surprising that we did not observe a difference in transcript abundance pattern between well-watered and drought-stressed plants as its gene regulatory role might be needed during both conditions. ATMYB13 and ATMYB14 are known to be involved in flower development and responses to cold, respectively (Ding et al., 2013). We observed increased transcript abundance for plants of both conditions, indicating that Tf_contig_037_000016 plays both a role in C_3 and CAM photosynthesis. However, we found increased gene expression at the end of the day. Therefore, in contrast to BHL, the MYB TF shows no difference after treatment, but seems to be regulated in a time-specific manner. RD26 shows both, treatment and time-specific expression. Transcript abundance is increased under drought-stress at the end of the day. RD26 has also been identified in a study by Song et al., 2016, where the complex transcriptional network in *Arabidopsis thaliana* in response to environmental changes was investigated. In their approach, the authors applied the hormone ABA to analyze water limited stress. Using chromatin immunoprecipitation, they identified 21 TFs that were ABA pathway-related, one of them was RD26. As this TF could also be identified in water-limited stress response incurred by ABA, there is high confidence to see an effect after water withhold in *T. fruticosum*.

Transcriptome analysis can unravel the complex molecular mechanisms behind drought adaptations, however, little is investigated in experimental confirmation of predicted gene regulation. Studying gene regulation *in planta* can be difficult and time-consuming. Especially yet non-model plants might be challenging, as only a few techniques are established and their special characteristics might complicate molecular work. The facultative CAM plant *T. fruticosum* has waxy and slight succulent leaves containing a lot of secondary metabolites, which makes handling challenging. Therefore, it is difficult for *T. fruticosum*, but might also be true for other plant species, to confirm predicted protein-DNA interaction pairs *in planta*.
Here we could establish a standardized test system for testing transcriptional activation using a synthetic approach. It can be used to study predicted TF-DNA interaction pairs from

T. fruticosum in a mammalian cell line. As a proof-of-concept, we tested interactions of the upstream regions of three *PEPC*s with a selected set of three TFs reported in Maleckova, PhD thesis, 2020 and discussed above. Although we observed leakiness of the potential C_3 *PEPC* homologs, we still could see interaction with the BHL TF. Negative controls of the two CAM *PEPC*s upstream regions did not show leakiness and interaction could be observed for MYB and RD26 with TF_contig_062_000131 and for all three TFs with TF_contig_062_000129. The signal was even stronger when the TF was fused to the transactivation domain, suggesting its support in inducing gene transcription. Additionally, we could also establish positive controls, based on the CRISPR/dCas9 system (Brezgin et al., 2019), to verify that the approach is suitable and reliable. Construction of the PTGs needed for a multiplexed test design can be done in an automated way, by using PolyGEN (Urquize-Garcia, unpublished) and the modular cloning approach GoldenBraid (Sarrion-Perdigones et al., 2013). These advantages make the system easy-to-use and applicable to a great number of laboratories. Implementation of synthetic biological approaches into plant science can facilitate the understanding of complex gene regulation and signaling network. As *in planta* approaches are challenging for *T. fruticosum* and other CAM species, due to its morphology and specific growth conditions, the established assay can improve fast screening and identification of gene regulatory candidates. In addition to using mammalian cells as an orthogonal system, we attempted to transform *A. thaliana* protoplasts. Therefore, we cloned genes from *T. fruticosum* into vector, which were introduced into the plant cells, to look for potential interactions (Supplemental Figure S 8). The positive controls, also using the CRISPR/dCas9 system, showed high functionality. However, the negative controls of the *PEPC* upstream regions also led to a high signal, indicating leakiness of the system. This might be due to binding of other transcription factors found in *A. thaliana* protoplast, which in turn stresses the advantages of a highly distant orthogonal test system. A disadvantage of the highly orthogonal system is that downstream analysis, such as analyzing the impact of external factors like ABA treatment, cannot easily be conducted using the mammalian test chassis. In this case, studies in the native plant need to be performed. To this end, we suggest transformation of *T. fruticosum* protoplast, to receive a less noisy background for interaction studies (see Manuscript I of this PhD thesis).

Being a proof-of concept exercise, our synthetic reconstruction study was limited to three tested transcription factors reported in Maleckova, PhD thesis, 2020. To identify further

candidates in the transition from C3 to CAM photosynthesis, we scanned for novel TFBS in the 100 kbp region containing the four *PEPC* homologs using the *FIMO* tool. In addition, we used predmoter, a currently developed machine learning software to predict ATAC and ChIP-seq coverage across this sequence. It has to be noted that both tools are treatment-agnostic and cannot distinguish between well-watered and drought-treated samples. Using a combination of both tools, we reduced a large set of transcription factors to a few TFs that showed TFBS in predicted regions of open chromatin and, in addition, showed an upregulation under drought compared to the control state.

In this set, among others, we identified TFs that belong to the family of ERFs. These could be found with lower q-values especially in the upstream region of TF_contig_062_000129. ERFs play a role in a variety of biological processes. Not only are they important for growth and plant development, but they are also involved in transcriptional regulation in response to environmental stimuli (Nakano et al., 2006). Moreover, we identified a number of motifs for BPC TFs. BPCs play a role in developmental processes, regulation of phytohormones, as cytokinin and signaling pathways (Shanks et al., 2018). In addition to that, we found members of the large MYB TF family in the upstream regions of the *PEPC*s. MYBs also play a role in a variety of cellular processes, including response to biotic and abiotic stress. While MYB51 and MYB30 are involved in pathogen response, MYB60, MYB74 and MYB101 are connected to drought and ABA-mediated responses (Ambawat et al., 2013). Analysis of the TFs indicate that regions of the two predicted CAM-*PEPC* genes (TF_contig_062_000131 and TF_contig_062_000129) show binding motifs for a variety of TFs. The identified TFs play not only a role in growth and development, but also in drought and ABA-mediated responses, suggesting a tight regulation of expression of the CAM-*PEPC* genes in response to environmental stimuli, presumably through a complex array of interacting *trans*-factors. To further analyze the *PEPC* intergenic regions, we used the currently developed deep learning software *predmoter*. It predicts ChIP-seq and ATAC-seq read coverage and by this can give hints on the heterochromatic state of the respective upstream regions. *Predmoter* was trained with publicly available datasets from a variety of plant species and other photosynthetic organisms and *Brassica rapa* has been used as a dicot representative for validation of prediction accuracy of the trained model. Here we show both predictions for ChIP-seq and ATAC-seq in the *T. fruticosum PEPC* region of interest.

The peaks predicted by *predmoter* likely to contain TF binding sites, since euchromatic regions are accessible to transcription factors and often hint at sites of active transcription. It is highly remarkable that the *in silico* predicted ChIP-seq based peaks found in the *PEPC* intergenic region of interest correlate almost perfectly with the *in silico* predicted TFBS identified by *FIMO*, suggesting a strong confidence of actual TF binding regions, as evidence comes from two independent methodologies. ATAC-seq predictions can unravel accessible chromatin regions (Buenrostro et al., 2016) and might therefore be a suitable addition to ChIP-seq prediction. Here we identified one ATAC-seq peak upstream of TF_contig_062_000129. This might suggest an open chromatin region, which is needed for gene regulation, upstream of three *PEPC*s (Figure 10).

It might be assumed that the *PEPC* region on contig 62 is of high interest for further evaluation to understand the regulatory mechanisms of environmental adaptations. Combination of *FIMO* analysis and ChIP-seq and ATAC-seq prediction showed to be a powerful tool to identify those regions and candidates involved in key steps of genetic regulation. More precise evaluation of the candidates will help to be able to choose fewer targets that could be verified using for example orthogonal systems. Not only does the *PEPC* region exhibit four presumably subfunctionalized and specialized *PEPC* homologs, we could also narrow down a set of potential *trans*-acting interaction partners that show confident binding motifs in euchromatic regions and expression patterns matching the *PEPC* transcripts (Figure 10, Supplemental Figure S 6).

To this end, we used the *in silico* predictions to narrow down the set of predicted TFs to upregulated TFs under drought-stress. We defined seven bins, each 2000-2500 bp in size, in the upstream or 5′ UTR of the CAM-*PEPC* homologs TF_contig_062_000131 and TF_contig_062_000129. To narrow down the set of potentially binding TFs, we selected for the ones with highest difference in their transcript abundance between well-watered and drought from day zero to day nine. Therefore, we used the slopes of the expression levels instead of a quantitative statistics selection, as too many comparative t-test with a large false discovery (FDR) rate would exclude potential candidates after FDR correction. Even though our approach does not quantify significant co-expression, our analysis revealed a set interesting candidates. However, due to the lack of statistical corrections, this set is possibly inflated by false-positive hits, which is, however, not an issue for an unbiased selection of targets for downstream experimental validation.

In all bins, except bin 1, we identified members of the ERF family, which we have also identified through *FIMO* analysis (Figure 10, Supplemental Figure S 6). Within the ERF family, we found two *A. thaliana* homologs, RAP2 and ERF073, which are both known to be involved in hypoxia and salt stress responses (Seok et al., 2022), indicating that these TFs might play a role in stress responses in *T. fruticosum* and potential regulation of the CAM-*PEPC*s. Tf_contig_057_000556 found in to bind in bin 1 and 2, has an *A. thaliana* homolog to ABA-RESPONSIVE KINASE SUBSTRATE 1. This TF has also been found in the study by Song et al., 2016, which has been discussed above and also indicates involvement of the TF in ABA-mediated stress responses in *T. fruticosum*. Tf_contig_042_000188 could be found in bin 1, in the start region of TF_contig_062_000131 and in bin 7, upstream of TF_contig_062_000129. It shows weak gene expression under well-watered conditions and for the first four days of drought treatment. However, the transcript abundance highly increased at day nine under water-withhold. Its *A. thaliana* homolog, ATHB-7, is known to be induced under water-deficit and its regulation follows an ABA-dependent pathway (Söderman et al., 1996). ATHB-7 is a positive regulator of the protein phosphatase type 2C and *in vivo* promoter-reporter gene assays unraveled its role as a transcriptional activator (Valdés et al., 2012). A role of Tf_contig_042_000188 during drought stress in *T. fruticosum* might therefore be likely.
As these TFs are found close to the CAM-*PEPC*s it might be suggested that they could play a role in CAM photosynthesis, as a stress response of *T. fruticosum*. We suggest that these candidates could be important to understand mechanisms of CAM photosynthesis and should therefore be further investigated experimentally, for instance using synthetic approaches.

Identification and analysis of protein-DNA interaction partners by using different approaches can give a reliable analysis of candidates, which might play an important role in environmental adaptation and gene regulation. These candidates need to be verified in future studies by using the synthetic reconstruction approach established in this study. Our established method for *T. fruticosum*, will help to understand the complex regulation and intricate signaling pathways during the C_3-CAM transition. The fast and modular synthetic biology approach follows a rapid design-build-test cycle and will make it easier to unravel genetic building blocks and their role in genetic regulation.
Our analysis workflow, merging expression analysis, TFBS prediction, machine-learning-based epigenome profiling with a highly modular and robust *in vivo* validation platform is a

highly promising platform to further study the complex regulatory network of behind complex traits such as inducible CAM photosynthesis in the non-model species *T. fruticosum*.

Acknowledgment:

We would like to thanks Stefanie Kuschel from the Institute of Synthetic Biology for technical support in maintaining and preparing cell cultures; Katrin Weber, Maria Graf and Elisabeth Klemp from the CEPLAS Metabolomics facility for technical assistance in metabolic measurements, Dr. Thorsten Wachtmeister and his team from Biologisch-medizinisch-Forschungszentrum for library preparation and sequencing and the Institute for Biological Data Science for functional annotation of the T. *fruticosum* transcriptome using *Mercator*.

References

Abu-Jamous, B., Kelly, S., 2018. Clust: automatic extraction of optimal co-expressed gene clusters from gene expression data. Genome Biol 19. https://doi.org/10.1186/s13059-018-1536-8

Acevedo, R.M., Maiale, S.J., Pessino, S.C., Bottini, R., Ruiz, O.A., Sansberro, P.A., 2013. A succinate dehydrogenase flavoprotein subunit-like transcript is upregulated in Ilex paraguariensis leaves in response to water deficit and abscisic acid. Plant Physiology and Biochemistry 65, 48–54. https://doi.org/10.1016/J.PLAPHY.2012.12.016

Adams, K.J., Pratt, B., Bose, N., Dubois, L.G., St. John-Williams, L., Perrott, K.M., Ky, K., Kapahi, P., Sharma, V., Maccoss, M.J., Moseley, M.A., Colton, C.A., Maclean, B.X., Schilling, B., Thompson, J.W., 2020. Skyline for Small Molecules: A Unifying Software Package for Quantitative Metabolomics. J Proteome Res 19, 1447–1458. https://doi.org/10.1021/ACS.JPROTEOME.9B00640/SUPPL_FILE/PR9B00640_SI_001.PDF

Ambawat, S., Sharma, P., Yadav, N.R., Yadav, R.C., 2013. MYB transcription factor genes as regulators for plant responses: An overview. Physiology and Molecular Biology of Plants. https://doi.org/10.1007/s12298-013-0179-1

Baaske, J., Gonschorek, P., Engesser, R., Dominguez-Monedero, A., Raute, K., Fischbach, P., Müller, K., Cachat, E., Schamel, W.W.A., Minguet, S., Davies, J.A., Timmer, J., Weber, W., Zurbriggen, M.D., 2018. Dual-controlled optogenetic system for the rapid down-regulation of protein levels in mammalian cells. Sci Rep 8, 1–10. https://doi.org/10.1038/s41598-018-32929-7

Bailey, T.L., Johnson, J., Grant, C.E., Noble, W.S., 2015. The MEME Suite. Nucleic Acids Res 43, W39–W49. https://doi.org/10.1093/nar/gkv416

Berardini, T.Z., Reiser, L., Li, D., Mezheritsky, Y., Muller, R., Strait, E., Huala, E., 2015. The arabidopsis information resource: Making and mining the "gold standard" annotated reference plant genome. Genesis 53, 474–485. https://doi.org/10.1002/dvg.22877

Bolger, A.M., Lohse, M., Usadel, B., 2014. Trimmomatic: A flexible trimmer for Illumina sequence data. Bioinformatics 30, 2114–2120. https://doi.org/10.1093/bioinformatics/btu170

Boxall, S.F., Kadu, N., Dever, L. V, Knerova, J., Waller, J.L., Gould, P.D., Hartwell, J., 2020. Kalanchoë PPC1 is Essential for Crassulacean Acid Metabolism and the Regulation of

Core Circadian Clock and Guard Cell Signaling Genes. Plant Cell. https://doi.org/10.1105/tpc.19.00481

Bräutigam, A., Schliesky, S., Külahoglu, C., Osborne, C.P., Weber, A.P.M., 2014. Towards an integrative model of C4 photosynthetic subtypes: Insights from comparative transcriptome analysis of NAD-ME, NADP-ME, and PEP-CK C4 species. J Exp Bot 65, 3579–3593. https://doi.org/10.1093/jxb/eru100

Bray, N.L., Pimentel, H., Melsted, P., Pachter, L., 2016. Near-optimal probabilistic RNA-seq quantification. Nat Biotechnol 34, 525–527. https://doi.org/10.1038/nbt.3519

Brezgin, S., Kostyusheva, A., Kostyushev, D., Chulanov, V., 2019. Dead Cas Systems: Types, Principles, and Applications. Int J Mol Sci 20. https://doi.org/10.3390/IJMS20236041

Brilhaus, D., Bräutigam, A., Mettler-Altmann, T., Winter, K., Weber, A.P.M., 2016. Reversible Burst of Transcriptional Changes during Induction of Crassulacean Acid Metabolism in Talinum triangulare . Plant Physiol 170, 102–122. https://doi.org/10.1104/pp.15.01076

Brilhaus, D., Denton, A.K., Maleckova, E., Reichel-Deland, V., Weber, A.P.M., 2023. The genome of Talinum fruticosum. BioRxiv. https://doi.org/10.1101/2023.04.20.537669

Brosset, A., Blande, J.D., 2022. Volatile-mediated plant–plant interactions: volatile organic compounds as modulators of receiver plant defence, growth, and reproduction. J Exp Bot 73, 511. https://doi.org/10.1093/JXB/ERAB487

Buenrostro, J., Wu, B., Chang, H., Greenleaf, W., 2016. ATAC-seq method. Curr Protoc Mol Biol 2015, 1–10. https://doi.org/10.1002/0471142727.mb2129s109.ATAC-seq

Christin, P.A., Arakaki, M., Osborne, C.P., Bräutigam, A., Sage, R.F., Hibberd, J.M., Kelly, S., Covshoff, S., Wong, G.K.S., Hancock, L., Edwards, E.J., 2014. Shared origins of a key enzyme during the evolution of C4 and CAM metabolism. J Exp Bot 65, 3609–3621. https://doi.org/10.1093/jxb/eru087

Curien, G., Lyska, D., Guglielmino, E., Westhoff, P., Janetzko, J., Tardif, M., Hallopeau, C., Brugière, S., Dal Bo, D., Decelle, J., Gallet, B., Falconet, D., Carone, M., Remacle, C., Ferro, M., Weber, A.P.M., Finazzi, G., 2021. Mixotrophic growth of the extremophile Galdieria sulphuraria reveals the flexibility of its carbon assimilation metabolism. New Phytologist 231, 326–338. https://doi.org/10.1111/NPH.17359

Deng, H., Zhang, L.S., Zhang, G.Q., Zheng, B.Q., Liu, Z.J., Wang, Y., 2016. Evolutionary history of PEPC genes in green plants: Implications for the evolution of CAM in orchids. Mol Phylogenet Evol 94, 559–564. https://doi.org/10.1016/j.ympev.2015.10.007

Ding, Y., Liu, N., Virlouvet, L., Riethoven, J.J., Fromm, M., Avramova, Z., 2013. Four distinct types of dehydration stress memory genes in Arabidopsis thaliana. BMC Plant Biol 13, 1–11. https://doi.org/10.1186/1471-2229-13-229/FIGURES/4

Dobin, A., Davis, C.A., Schlesinger, F., Drenkow, J., Zaleski, C., Jha, S., Batut, P., Chaisson, M., Gingeras, T.R., 2013. STAR: Ultrafast universal RNA-seq aligner. Bioinformatics 29, 15–21. https://doi.org/10.1093/bioinformatics/bts635

Drennan, P.M., Nobel, P.S., 2000. Responses of CAM species to increasing atmospheric CO2 concentrations. Plant Cell Environ 23, 767–781. https://doi.org/10.1046/j.1365-3040.2000.00588.x

Ehleringer, J.R., Sage, R.F., Flanagan, L.B., Pearcy, R.W., 1991. Climate change and the evolution of C4 photosynthesis. Trends Ecol Evol 6, 95–99. https://doi.org/10.1016/0169-5347(91)90183-X

Figueroa, C.M., Feil, R., Ishihara, H., Watanabe, M., Kölling, K., Krause, U., Höhne, M., Encke, B., Plaxton, W.C., Zeeman, S.C., Li, Z., Schulze, W.X., Hoefgen, R., Stitt, M., Lunn, J.E., 2016. Trehalose 6–phosphate coordinates organic and amino acid metabolism with carbon availability. The Plant Journal 85, 410–423. https://doi.org/10.1111/TPJ.13114

Flügel, F., Timm, S., Arrivault, S., Florian, A., Stitt, M., Fernie, A.R., Bauwe, H., 2017. The Photorespiratory Metabolite 2-Phosphoglycolate Regulates Photosynthesis and Starch Accumulation in Arabidopsis. Plant Cell 29, 2537. https://doi.org/10.1105/TPC.17.00256

Gibson, D.G., Young, L., Chuang, R.Y., Venter, J.C., Hutchison, C.A., Smith, H.O., 2009. Enzymatic assembly of DNA molecules up to several hundred kilobases. Nat Methods 6, 343–345. https://doi.org/10.1038/nmeth.1318

Grant, C.E., Bailey, T.L., Noble, W.S., 2011. FIMO: Scanning for occurrences of a given motif. Bioinformatics 27, 1017–1018. https://doi.org/10.1093/bioinformatics/btr064

Haug-Baltzell, A., Stephens, S.A., Davey, S., Scheidegger, C.E., Lyons, E., 2017. SynMap2 and SynMap3D: Web-based whole-genome synteny browsers, in: Bioinformatics. Oxford University Press, pp. 2197–2198. https://doi.org/10.1093/bioinformatics/btx144

Herrera, A., 2009. Crassulacean acid metabolism and fitness under water deficit stress: If not for carbon gain, what is facultative CAM good for? Ann Bot 103, 645–653. https://doi.org/10.1093/aob/mcn145

Herrera, A., Ballestrini, C., Montes, E., 2015. What is the potential for dark CO2 fixation in the facultative crassulacean acid metabolism species Talinum triangulare? J Plant Physiol 174, 55–61. https://doi.org/10.1016/j.jplph.2014.10.006

Heyduk, K., McAssey, E. V., Leebens-Mack, J., 2022. Differential timing of gene expression and recruitment in independent origins of CAM in the Agavoideae (Asparagaceae). New Phytologist 235, 2111–2126. https://doi.org/10.1111/nph.18267

Heyduk, K., Ray, J.N., Ayyampalayam, S., Moledina, N., Borland, A., Harding, S.A., Tsai, C.J., Leebens-Mack, J., 2019. Shared expression of crassulacean acid metabolism (CAM) genes pre-dates the origin of CAM in the genus Yucca. J Exp Bot 70, 6597–6609. https://doi.org/10.1093/jxb/erz105

Holst, F., Bolger, A., Günther, C., Maß, J., Triesch, S., Kindel, F., Kiel, N., Saadat, N., Ebenhöh, O., Usadel, B., Schwacke, R., Bolger, M., Weber, A.P.M., Denton, A.K., 2023. Helixer–de novo Prediction of Primary Eukaryotic Gene Models Combining Deep Learning and a Hidden Markov Model. bioRxiv 2023.02.06.527280. https://doi.org/10.1101/2023.02.06.527280

Li, Y., Belt, K., Alqahtani, S.F., Saha, S., Fenske, R., Van Aken, O., Whelan, J., Millar, A.H., Murcha, M.W., Huang, S., 2022. The mitochondrial LYR protein SDHAF1 is required for succinate dehydrogenase activity in Arabidopsis. The Plant Journal 110, 499–512. https://doi.org/10.1111/TPJ.15684

Lunn, J.E., Feil, R., Hm Hendriks, J., Gibon, Y., Morcuende, R., Osuna, D., Scheible, W.-R., Carillo, P., Hajirezaei, M.-R., Stitt, M., 2006. Sugar-induced increases in trehalose 6-phosphate are correlated with redox activation of ADPglucose pyrophosphorylase and higher rates of starch synthesis in Arabidopsis thaliana. Arabidopsis thaliana. Biochemical Journal 397. https://doi.org/10.1042/BJ20060083ï

Lüttge, U., 2002. CO2-concentrating: Consequences in crassulacean acid metabolism. J Exp Bot. https://doi.org/10.1093/jxb/erf081

Lüttge, U., Ball, E., 1980. 2H+:1 malate2− stoichiometry during Crassulacean Acid Metabolism is unaffected by lipophilic cations. Plant Cell Environ 3, 195–200. https://doi.org/10.1111/1365-3040.ep11581541

Maleckova, E., Brilhaus, D., Wrobel, T.J., Weber, A.P.M., 2019. Transcript and metabolite changes during the early phase of abscisic acid-mediated induction of crassulacean acid

metabolism in Talinum triangulare. J Exp Bot 70, 6581–6596. https://doi.org/10.1093/jxb/erz189

Monson, R.K., 2012. Gene Duplication , Neofunctionalization , and the Evolution of C4 Photosynthesis Author (s): Russell K . Monson Reviewed work (s): Source : International Journal of Plant Sciences , Vol . 164 , No . S3 , Evolution of Functional Traits in Plants (May 164.

Müller, K., Zurbriggen, M.D., Weber, W., 2014. Control of gene expression using a red- and far-red light-responsive bi-stable toggle switch. Nat Protoc 9, 622–632. https://doi.org/10.1038/nprot.2014.038

Nakano, T., Suzuki, K., Fujimura, T., Shinshi, H., 2006. Genome-wide analysis of the ERF gene family in arabidopsis and rice. Plant Physiol 140, 411–432. https://doi.org/10.1104/pp.105.073783

Ochoa-Fernandez, R., Abel, N.B., Wieland, F.G., Schlegel, J., Koch, L.A., Miller, J.B., Engesser, R., Giuriani, G., Brandl, S.M., Timmer, J., Weber, W., Ott, T., Simon, R., Zurbriggen, M.D., 2020. Optogenetic control of gene expression in plants in the presence of ambient white light. Nat Methods 17, 717–725. https://doi.org/10.1038/s41592-020-0868-y

Osmond, C.B., 1978. Crassulacean Acid Metabolism: A Curiosity in Context. Annu Rev Plant Physiol 29, 379–414. https://doi.org/10.1146/annurev.pp.29.060178.002115

Sanada, Y., Ueda, H., Kuribayashi, K., Andoh, T., Hayashi, F., Tamai, N., Wada, K., 1995. Novel Light-Dark Change of Proline Levels in Halophyte (Mesembryanthemum crystallinum L.) and Glycophytes (Hordeum vulgare L. and Triticum aestivum L.) Leaves and Roots under Salt Stress. Plant Cell Physiol 36, 965–970. https://doi.org/10.1093/OXFORDJOURNALS.PCP.A078867

Sarrion-Perdigones, A., Vazquez-Vilar, M., Palací, J., Castelijns, B., Forment, J., Ziarsolo, P., Blanca, J., Granell, A., Orzaez, D., 2013. Goldenbraid 2.0: A comprehensive DNA assembly framework for plant synthetic biology. Plant Physiol 162, 1618–1631. https://doi.org/10.1104/pp.113.217661

Schwacke, R., Ponce-Soto, G.Y., Krause, K., Bolger, A.M., Arsova, B., Hallab, A., Gruden, K., Stitt, M., Bolger, M.E., Usadel, B., 2019. MapMan4: A Refined Protein Classification and Annotation Framework Applicable to Multi-Omics Data Analysis. Mol Plant 12, 879–892. https://doi.org/10.1016/j.molp.2019.01.003

Seok, H.Y., Tran, H.T., Lee, S.Y., Moon, Y.H., 2022. AtERF71/HRE2, an Arabidopsis AP2/ERF Transcription Factor Gene, Contains Both Positive and Negative Cis-Regulatory Elements in Its Promoter Region Involved in Hypoxia and Salt Stress Responses. Int J Mol Sci 23, 5310. https://doi.org/10.3390/IJMS23105310/S1

Shanks, C.M., Hecker, A., Cheng, C.Y., Brand, L., Collani, S., Schmid, M., Schaller, G.E., Wanke, D., Harter, K., Kieber, J.J., 2018. Role of BASIC PENTACYSTEINE transcription factors in a subset of cytokinin signaling responses. Plant Journal 95, 458–473. https://doi.org/10.1111/tpj.13962

Söderman, E., Mattsson, J., Engström, P., 1996. The Arabidopsis homeobox gene ATHB-7 is induced by water deficit and by abscisic acid. Plant J 10, 375–381. https://doi.org/10.1046/J.1365-313X.1996.10020375.X

Song, L., Huang, S.S.C., Wise, A., Castanoz, R., Nery, J.R., Chen, H., Watanabe, M., Thomas, J., Bar-Joseph, Z., Ecker, J.R., 2016. A transcription factor hierarchy defines an environmental stress response network. Science (1979) 354. https://doi.org/10.1126/science.aag1550

Strader, L., Weijers, D., Wagner, D., 2022. Plant transcription factors — being in the right place with the right company. Curr Opin Plant Biol 65, 102136. https://doi.org/10.1016/j.pbi.2021.102136

Supek, F., Bošnjak, M., Škunca, N., Šmuc, T., 2011. Revigo summarizes and visualizes long lists of gene ontology terms. PLoS One 6. https://doi.org/10.1371/journal.pone.0021800

Sweetlove, L.J., Beard, K.F.M., Nunes-Nesi, A., Fernie, A.R., Ratcliffe, R.G., 2010. Not just a circle: Flux modes in the plant TCA cycle. Trends Plant Sci 15, 462–470. https://doi.org/10.1016/j.tplants.2010.05.006

Taisma, M.A., Herrera, A., 1998. A relationship between fecundity, survival, and the operation of crassulacean acid metabolism in Talinum triangulare.

Töpfer, N., Braam, T., Shameer, S., Ratcliffe, R.G., Sweetlove, L.J., 2020. Alternative Crassulacean Acid Metabolism Modes Provide Environment-Specific Water-Saving Benefits in a Leaf Metabolic Model. Plant Cell 32, 3689–3705. https://doi.org/10.1105/TPC.20.00132

Ung, N., Smith, H.M.S., 2011. Regulation of shoot meristem integrity during Arabidopsis vegetative development. https://doi.org/10.4161/psb.6.8.16462 6, 1250–1252. https://doi.org/10.4161/PSB.6.8.16462

Valdés, A.E., Övernäs, E., Johansson, H., Rada-Iglesias, A., Engström, P., 2012. The homeodomain-leucine zipper (HD-Zip) class I transcription factors ATHB7 and ATHB12 modulate abscisic acid signalling by regulating protein phosphatase 2C and abscisic acid receptor gene activities. Plant Mol Biol 80, 405–418. https://doi.org/10.1007/S11103-012-9956-4/FIGURES/7

VanBuren, R., Wai, C.M., Giarola, V., Župunski, M., Pardo, J., Kalinowski, M., Grossmann, G., Bartels, D., 2023. Core cellular and tissue-specific mechanisms enable desiccation tolerance in Craterostigma. The Plant Journal 114, 231–245. https://doi.org/10.1111/TPJ.16165

Walker, B.J., Vanloocke, A., Bernacchi, C.J., Ort, D.R., 2016. The Costs of Photorespiration to Food Production Now and in the Future. Annu Rev Plant Biol 67, 107–129. https://doi.org/10.1146/annurev-arplant-043015-111709

West-eberhard, M.J., Smith, J.A.C., Winter, K., 2011. Photosynthesis, Reorganized 332.

Winter, K., 2019. Ecophysiology of constitutive and facultative CAM photosynthesis. J Exp Bot. https://doi.org/10.1093/jxb/erz002

Winter, K., Garcia, M., Holtum, J.A.M., 2008. On the nature of facultative and constitutive CAM: Environmental and developmental control of CAM expression during early growth of Clusia, Kalanchoë, and Opuntia, in: Journal of Experimental Botany. pp. 1829–1840. https://doi.org/10.1093/jxb/ern080

Winter, K., Holtum, J.A.M., 2014. Facultative crassulacean acid metabolism (CAM) plants: powerful tools for unravelling the functional elements of CAM photosynthesis. J Exp Bot 65, 3425–3441. https://doi.org/10.1093/jxb/eru063

Winter, K., Holtum, J.A.M., Smith, J.A.C., 2015. Crassulacean acid metabolism: A continuous or discrete trait? New Phytologist. https://doi.org/10.1111/nph.13446

Winter, K., Smith, J.A.C., 2022. CAM photosynthesis: the acid test. New Phytologist. https://doi.org/10.1111/nph.17790

Winter, K., Smith, J.A.C., 1996. An Introduction to Crassulacean Acid Metabolism. Biochemical Principles and Ecological Diversity 1–13. https://doi.org/10.1007/978-3-642-79060-7_1

Yang, X., Cushman, J.C., Borland, A.M., Liu, Q., 2020. Editorial: Systems Biology and Synthetic Biology in Relation to Drought Tolerance or Avoidance in Plants. Front Plant Sci. https://doi.org/10.3389/fpls.2020.00394

Yang, X., Hu, R., Yin, H., Jenkins, J., Shu, S., Tang, H., Liu, D., Weighill, D.A., Cheol Yim, W., Ha, J., Heyduk, K., Goodstein, D.M., Guo, H.B., Moseley, R.C., Fitzek, E., Jawdy, S., Zhang, Z., Xie, M., Hartwell, J., Grimwood, J., Abraham, P.E., Mewalal, R., Beltrán, J.D., Boxall, S.F., Dever, L. V., Palla, K.J., Albion, R., Garcia, T., Mayer, J.A., Don Lim, S., Man Wai, C., Peluso, P., Van Buren, R., De Paoli, H.C., Borland, A.M., Guo, H., Chen, J.G., Muchero, W., Yin, Y., Jacobson, D.A., Tschaplinski, T.J., Hettich, R.L., Ming, R., Winter, K., Leebens-Mack, J.H., Smith, J.A.C., Cushman, J.C., Schmutz, J., Tuskan, G.A., 2017. The Kalanchoë genome provides insights into convergent evolution and building blocks of crassulacean acid metabolism. Nat Commun 8. https://doi.org/10.1038/s41467-017-01491-7

Zhu, J.K., 2002. Salt and drought stress signal transduction in plants. Annu Rev Plant Biol. https://doi.org/10.1146/annurev.arplant.53.091401.143329

Supplemental Information

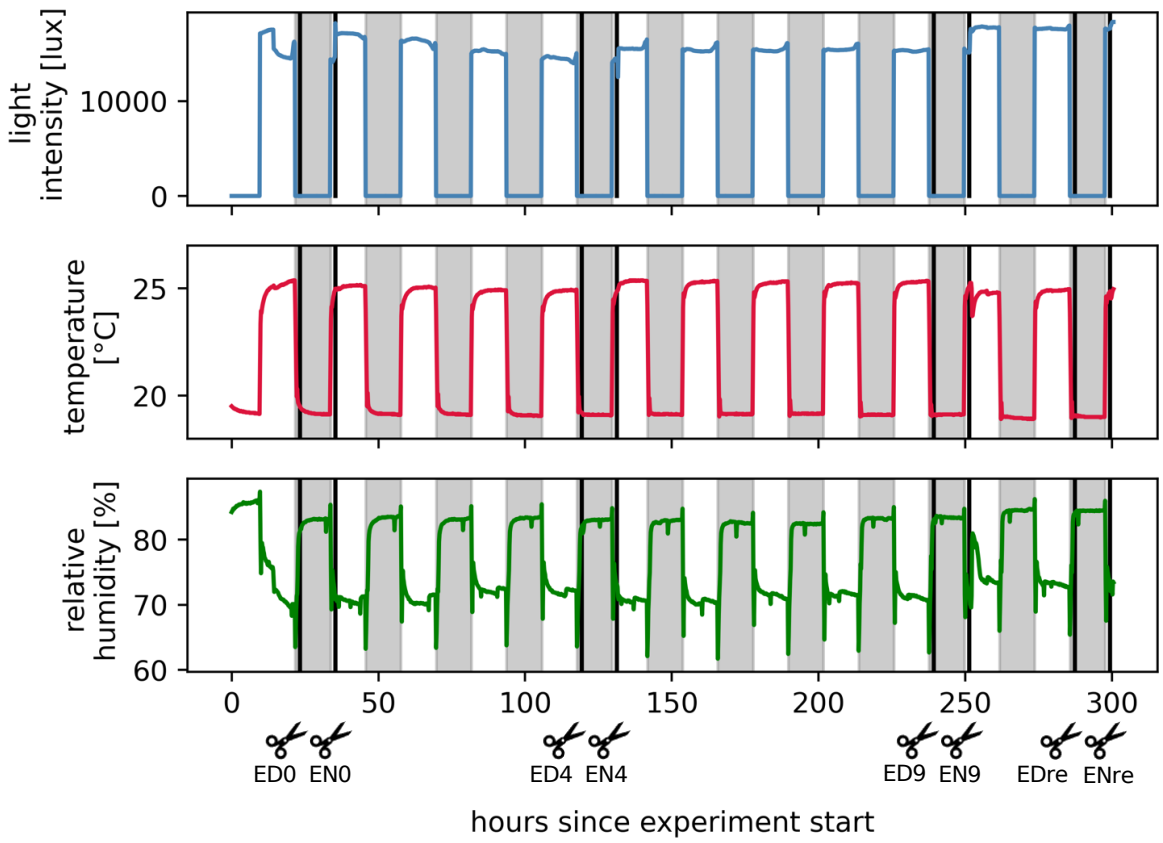

Supplemental Figure S 1: Growth condition and harvesting points during time course.
Light intensity, temperature and relative humidity have been recorded throughout the experiment using a HOBO Data Logger. Grey background in the plot represent night, white background the day. Leaves have been harvested at day 0, 4, 9 and two days after re-watering for further analysis.

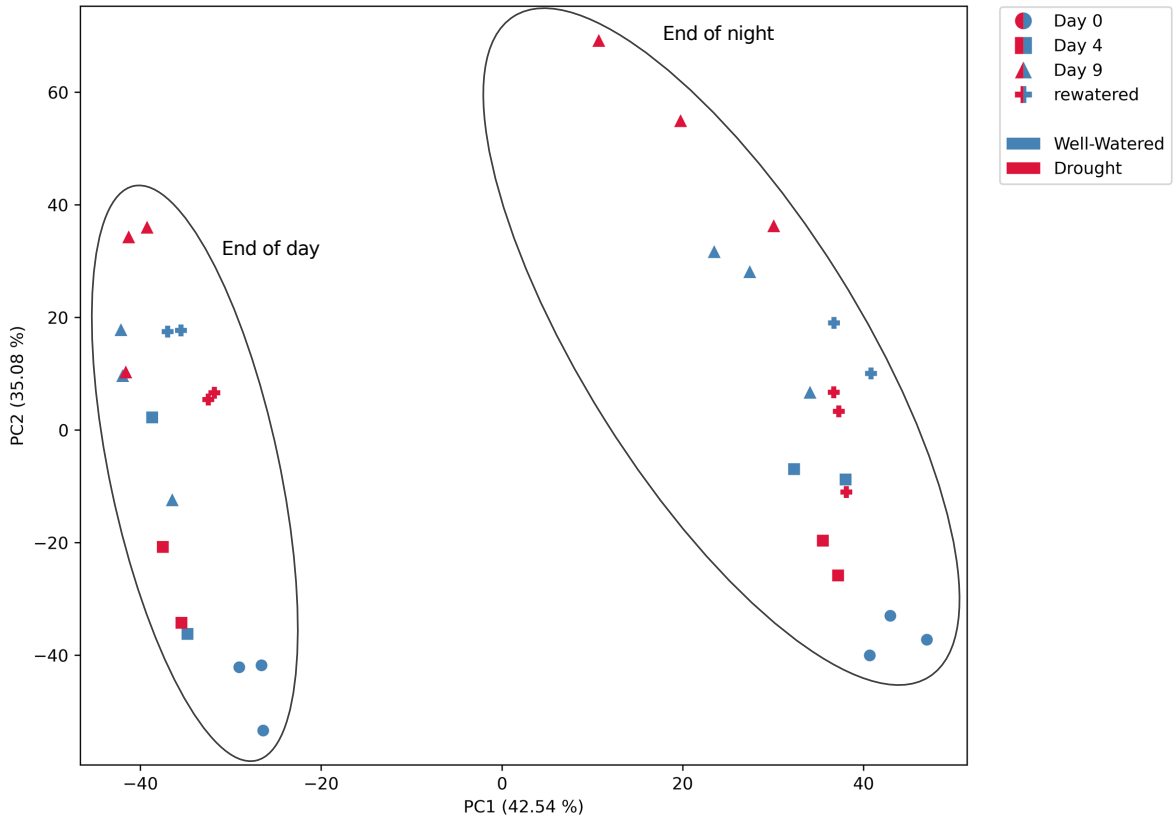

Supplemental Figure S 2: PCA analysis of drought-stressed and well-watered plants.
Blue colors represent well-watered samples, while samples of drought stressed plants are indicated by red color. Different symbols are used to highlight sampling timepoints. Each dot represents an individual sample of a drought-stressed plant during the time course. Symbols indicate different days of sampling. Red colors indicate drought stressed plants, blur colors well-watered plants. The two principal components are shown on the axes, where the first one explains 45% and the second one 30% of the variance.

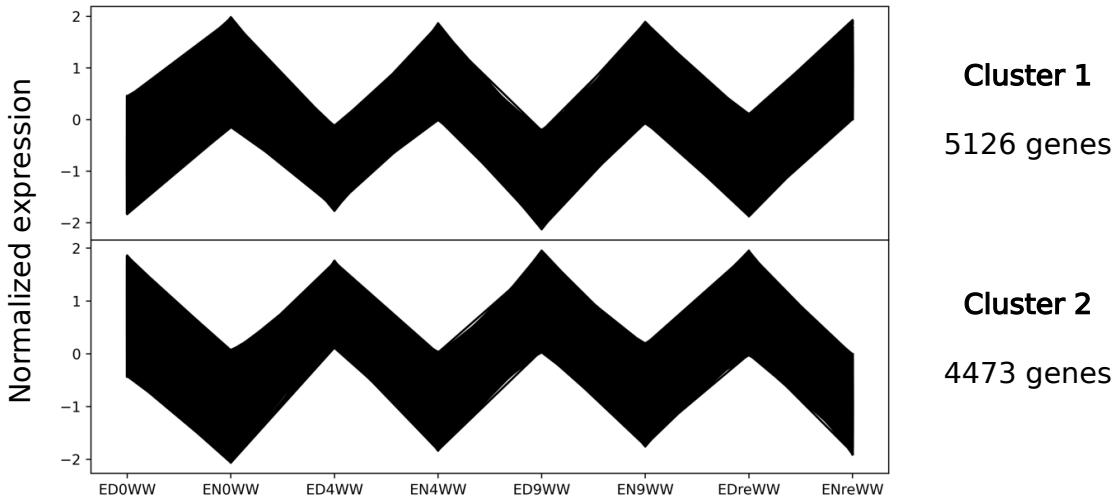

Supplemental Figure S 3: *Clust* analysis of well-watered samples throughout time course.
Normalized expression values are plotted against the time points. Two clusters were identified and consist of 5126 and 4473 genes, respectively.

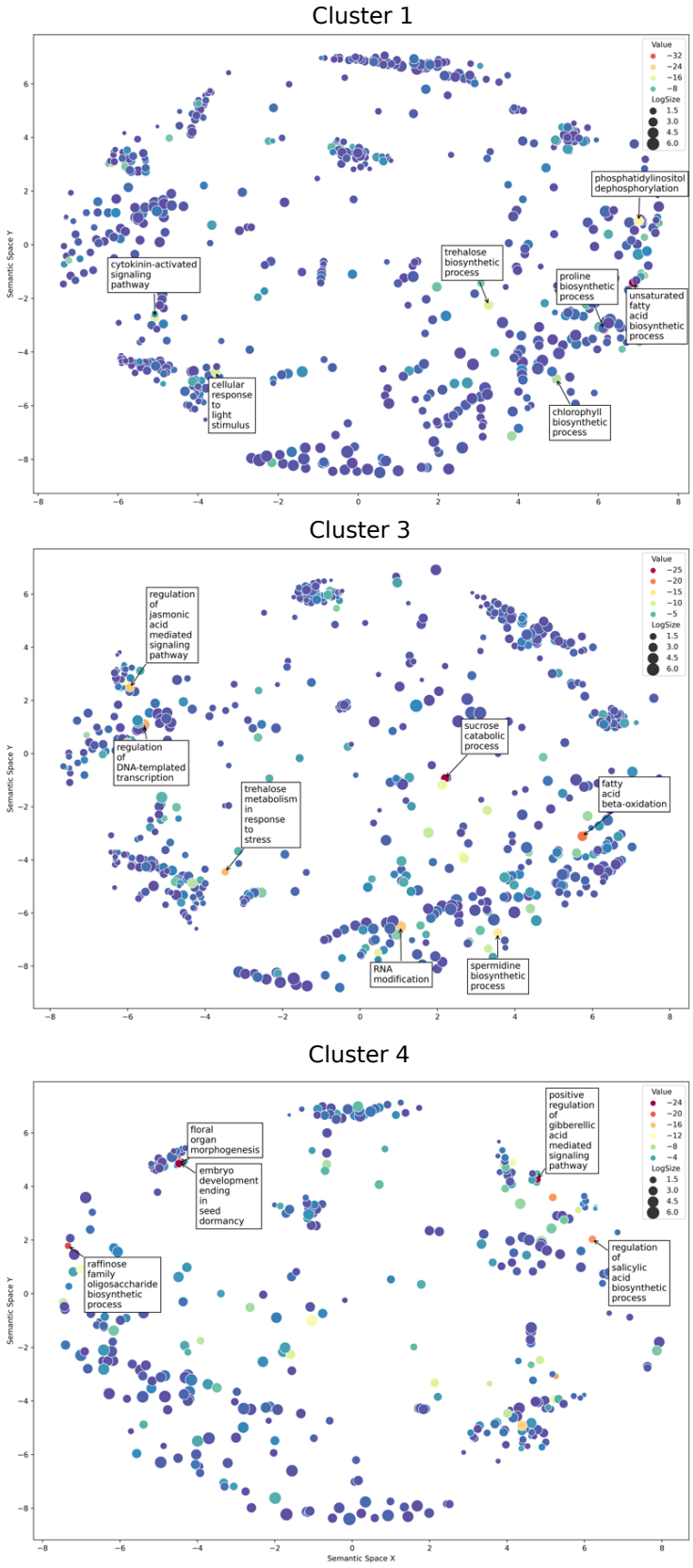

Supplemental Figure S 4: Dynamics of gene co-expression.
Enriched GO terms are shown for cluster 1, 3 and 5. Multidimensional scaling is performed to reduce dimensionality and semantic similarities are used to group GO terms. Axes are scaled as semantic space. Dots represent GO terms found in each cluster. Dot color and size represent significance, where red colors indicate more enriched GO terms than blue colored dots. Number of genes correlate with dot size.

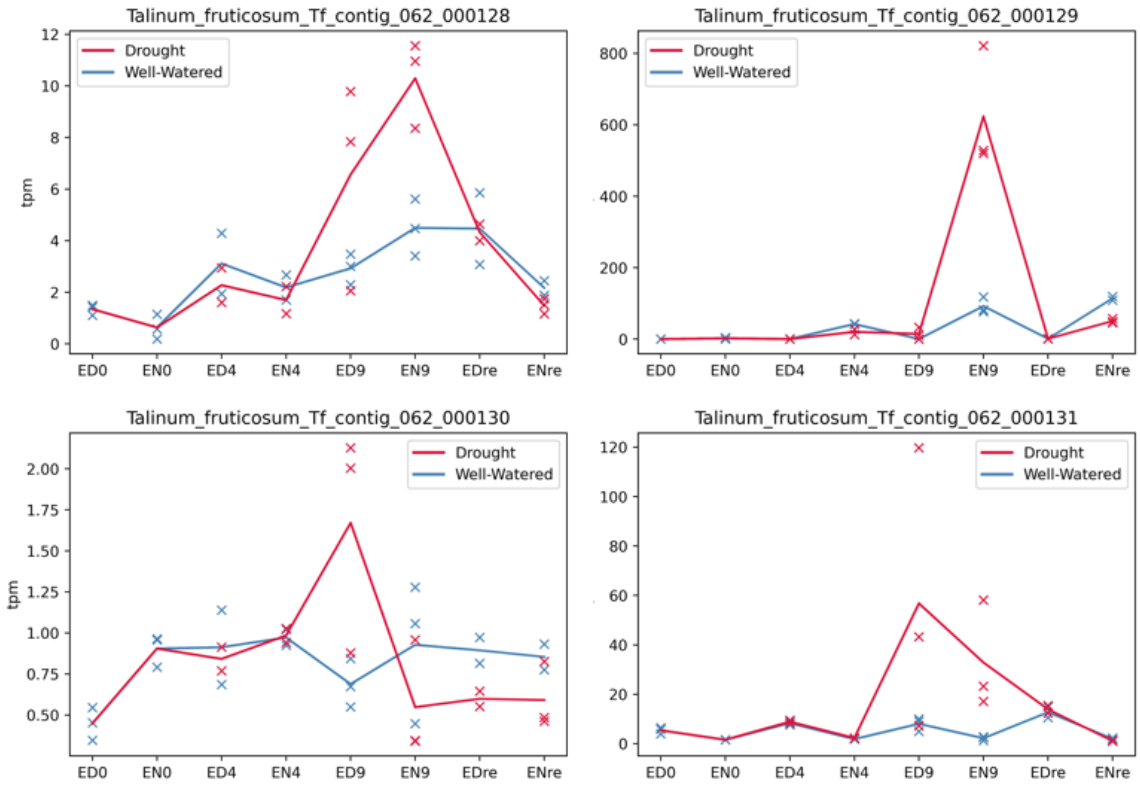

Supplemental Figure S 5: Transcript abundance of four identified *PEPC*s.
Transcript abundance (tpm) is plotted against the time course of the experiment. Grey background represents the night, white background represents the day. Individual samples are shown as dots. Well-watered samples are shown in blue color, samples of drought stressed plants are represented in red.

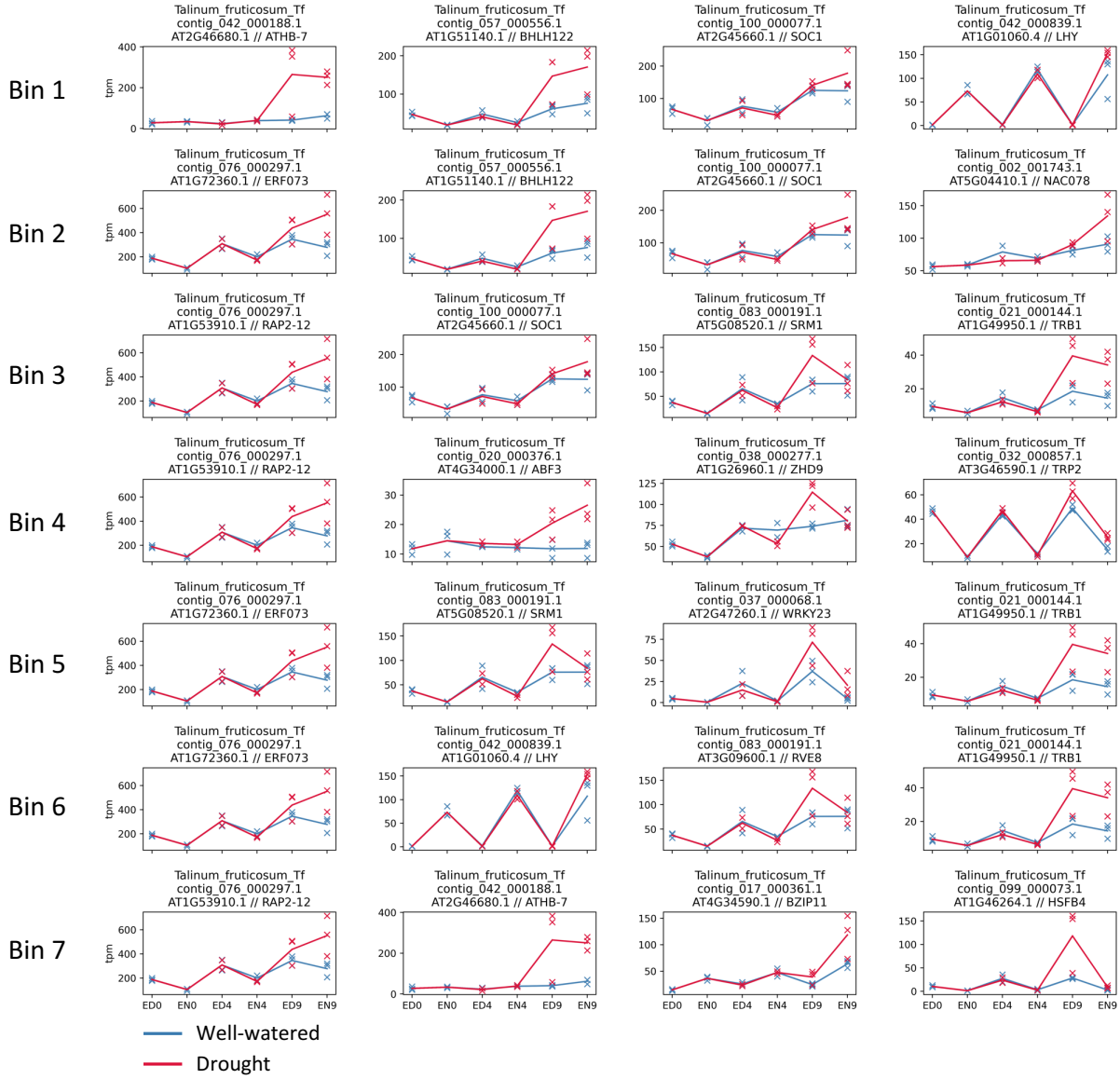

Supplemental Figure S 6: Transcript abundance (tpm) of the four best TF hits from each bin, based on *FIMO*/ChIP-seq data.

We selected seven bins, where *FIMO* and ChIP-seq predicted binding of TFs in the *PEPC* region (compare Figure 10). TF candidates have been selected based on the highest difference in their slope until day nine between drought and well-watered plants. Time course is plotted on the x-axis and colors indicate individual data points and mean for drought (red) or well-watered samples (blue).

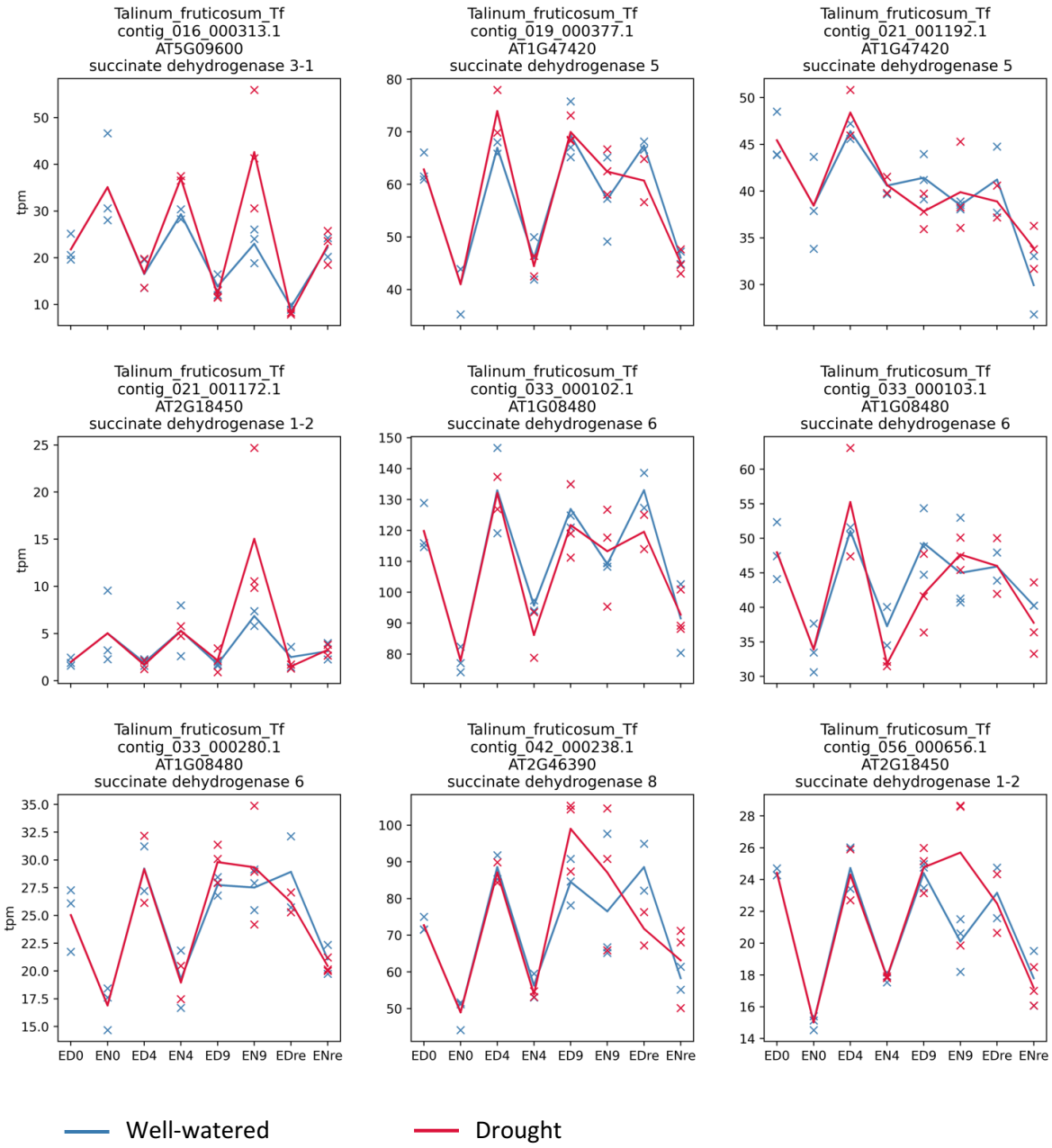

Supplemental Figure S 7: Transcript abundance (tpm) of parts of the SDH complex.
Gene expression is shown over the time course for the individual replicates and the mean. Red colors indicate drought samples, blue colors represent well-watered samples.

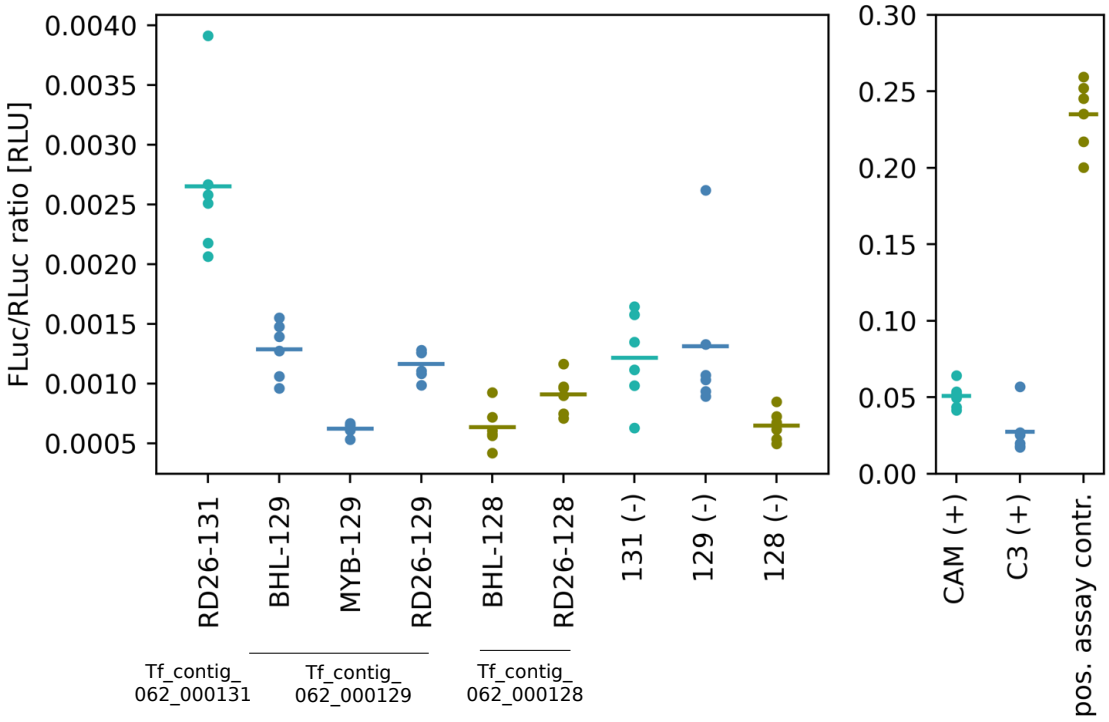

Supplemental Figure S 8: Arabidopsis thaliana protoplast as an orthogonal system to study mechanisms in gene regulation.
Interaction of TFs and PEPC upstream regions, as discussed above, were tested. Firefly/Renilla [relative light units] ratio is calculated as an indicator for interaction. Five replicates and the mean is plotted. 131 (-), 129 (-) and 128 (-) represent the negative control for the PEPC upstream region Tf_contig_062_000131, Tf_contig_062_000129 and Tf_contig_062_000128, respectively. Positive CRISPR/dCas9 controls are shown on the right, as well as a positive assay control.

Supplemental Table S 1 Metabolic measurements of day nine samples.
Metabolites of the citric acid cycle are shown for end of day (ED) and end of night (EN) of well-watered (WW) or drought (D) samples at day nine. The calculated mean (relative peak area/g DW) of five replicates is shown, as well as t-test between the conditions.

	Pyruvate		Citrate		Isocitrate		alpha-ketoglutarate		Succinate		Fumarate		Malate	
	Mean	t-test	Mean	t-test	Mean	t-test	Mean	t-test	Mean	t-test	Mean	t-test	Mean	t-test
ED9WW	0,8941	0,7412	26,2856	0,2677	2,8963	0,2376	3,8108	0,1495	1,1156	0,2359	0,0928	0,7515	47,8993	0,0396
ED9D	0,9529		33,3703		3,6030		4,8383		0,7917		0,0898		66,1844	
EN9WW	1,7016	0,0512	31,2431	0,0085	2,8864	0,0054	4,7847	0,0003	0,8513	0,4191	0,1134	0,0311	81,1229	0,0005
EN9D	2,4658		66,8803		5,1005		11,6990		0,7195		0,1682		152,7872	

Mean: [relative peak area/g DW]

Supplemental Table S 2: Constructs used in this study.

Plasmid name	Description	Backbone	Cloning procedure	Reference
pVRD007	PSV40:Tf_contig_016_000497:pA	pMZ333	pMZ333 was linearized with NotI and XbaI, Fragment assembly by using Gibson	This work
pVRD008	PSV40:Tf_contig_016_000497:vp16:pA	pJA032	pJA032 was linearized with NotI and EcoRI, Fragment assembly by using Gibson	This work
pVRD009	PSV40:Tf_contig_037_000016:pA	pMZ333	pMZ333 was linearized with NotI and XbaI, Fragment assembly by using Gibson	This work
pVRD010	PSV40:Tf_contig_037_000016:vp16:pA	pJA032	pJA032 was linearized with NotI and EcoRI, Fragment assembly by using Gibson	This work
pVRD028	PSV40:Tf_contig_037_000016:pA		pGEN was PCR amplified, Fragment assembly by using Gibson	This work
pVRD052	PSV40:Tf_contig_015_000048:pA		pGEN was PCR amplified, Fragment assembly by using Gibson	This work
pVRD053	1.1 kb upstream region of Tf_contig_062_000131	pJA045	pJA045 was linearized by NheI and EcoRV, Fragment assembly by using Gibson	This work
pVRD056	1.1 kb upstream region of Tf_contig_062_000129	pJA045	pJA045 was linearized by NheI and EcoRV, Fragment assembly by using Gibson	This work
pVRD058	1.1 kb upstream region of Tf_contig_062_000128	pJA045	pJA045 was linearized by NheI and EcoRV, Fragment assembly by using Gibson	This work
pVRD060	PSV40:Tf_contig_015_000048:pA	pMZ333	pMZ333 was linearized with NotI and XbaI, Fragment assembly by using Gibson	This work
pVRD061	PSV40:Tf_contig_015_000048:vp16:pA	pJA032	pJA032 was linearized with NotI and EcoRI, Fragment assembly by using Gibson	This work
pVRD062	UBQ10:sgRNA polycistron of 1.1 kb upstream region of Tf_contig_062_000131:Tnos, lvl 0	pDGB3a2	GoldenBraid	This work
pVRD065	UBQ10:sgRNA polycistron of 1.1 kb upstream region of Tf_contig_062_000128:Tnos, lvl 0	pDGB3a2	GoldenBraid	This work
pVRD066	sgRNA polycistron of 1.1 kb upstream region of Tf_contig_062_000131, lvl 2; pKT307, pVRD062, pKT310	pUU256	GoldenBraid	This work
pVRD069	sgRNA polycistron of 1.1 kb upstream region of Tf_contig_062_000128, lvl 2; pKT307, pVRD065, pKT310	pUU256	GoldenBraid	This work
pVRD070	pSa:1.1 kb upstream region of Tf_contig_062_000131		pROF206 was PCR amplified, Fragment assembly by using Gibson	This work
pVRD071	pSa:1.1 kb upstream region of Tf_contig_062_000129		pROF206 was PCR amplified, Fragment assembly by using Gibson	This work
pVRD072	pSa:1.1 kb upstream region of Tf_contig_062_000128		pROF206 was PCR amplified, Fragment assembly by using Gibson	This work
pVRD073	GB0223_pVRD062_GB0037_UBQ10		GoldenBraid	This work
pVRD075	GB0223_pVRD064_GB0037_UBQ10		GoldenBraid	This work
pVRD078	PSV40:Tf_contig_016_000497:pA		pGEN was PCR amplified, Fragment assembly by using Gibson	This work
pKT310	pUPD2_lvl0_			Tang, HHU, unpublished
pUU256	pUDP2_lvl0_UBQ10i(BpiI-BpiI)NL3F10H			Urquiza-Garcia, HHU, unpublished
pMZ333	PSV40-PhyB(1-908)-L-mCherry-pA			Beyer et al., 2015
pJA045	(pifO)4-pCMVmin-SEAP-pA; PSV40-Gaussia-SV40TA			Dissertation Jennifer Andres, HHU, 2019

Supplemental Table S 3: Oligonucleotides used in this study.

Oligonucleotide name	Sequence 5'->3'
oVRD015	ATGGAAGAGGCTCTGGGC
oVRD016	TCACTGTTTTGCCAGCCAAA
oVRD017	ATGGGGAGAGCTCCGTGCTGT
oVRD018	CTATAATGCTATTTCTGAAAATTCTGGCAATTCATTAGAAGGTC
oVRD038	TCTTTTATTTCAGGTCCCGGATCGAATTGCATGGAAGAGGCTCTGGGC
oVRD039	CTGGATCGAAGCTTGGGCTGCAGGTCGACTTCACTGTTTTGCCAGCCAAAATG
oVRD040	CACTACCAGCACTACCAGCACTATCGAATTCCTGTTTTGCCAGCCAAAATGGT
oVRD041	TCTTTTATTTCAGGTCCCGGATCGAATTGCATGGGGAGAGCTCCGTGC
oVRD042	CTGGATCGAAGCTTGGGCTGCAGGTCGACTCTATAATGCTATTTCTGAAAATTCTGGCAATTC
oVRD043	CACTACCAGCACTACCAGCACTATCGAATTCTAATGCTATTTCTGAAAATTCTGGCAATTCATT
oVRD136	CACCTGACGTCGTCGACGATCTAGGTGTGCCAGAAAAAATTGACA
oVRD137	CGAGCTCTGCTTATATAGGGTGAACTTGACTTATTTTAAAAATTTGAGTAAAC
oVRD141	CACCTGACGTCGTCGACGATGGGATTAAGGAAGAGGACCAAGA
oVRD142	CGAGCTCTGCTTATATAGGGCAAAGTTGACTTACTCAAATTTAAAAACT
oVRD144	CACCTGACGTCGTCGACGATTAATCAAAACTTTTTGGATGCTCTTCTTC
oVRD145	CGAGCTCTGCTTATATAGGGCTCTCTCTCTCTCTCTCTCTCTCT
oVRD147	CAGGTCCCGGATCGAATTGCATGGGAATGCAAGAAAAGGATCC
oVRD148	GCTTGGGCTGCAGGTCGACTTCATTGTCCGAACCCGAATC
oVRD149	CAGGTCCCGGATCGAATTGCATGGGAATGCAAGAAAAGGATCC
oVRD150	CTACCAGCACTATCGAATTCTCATTGTCCGAACCCGAATC
oVRD153	TTGAAGACTTGGCAAACAAAGCACCAGTGGTCTAGT
oVRD154	TTGAAGACTTGGAATACTTCGAGTTTATATGCACCAGCCGGGAATCG
oVRD155	TTGAAGACTTTTCCCGTTTTAGAGCTAGAAATAGCAAGTTAA
oVRD156	TTGAAGACTTGACAATGCACCAGCCGGGAATCG
oVRD157	TTGAAGACTTTGTCAAATTGCTATTTGGTGTTTTAGAGCTAGAAATAGCAAGTTAA
oVRD158	TTGAAGACTTGTCAATATTATGCACCAGCCGGGAATCG
oVRD159	TTGAAGACTTTGACAAGCAACCAAGTTTTAGAGCTAGAAATAGCAAGTTAA
oVRD160	TTGAAGACTTAAACTGCACCAGCCGGGAATCG
oVRD178	TTGAAGACTTAACTTCAGGGCATGTATTGCACCAGCCGGGAATCG
oVRD179	TTGAAGACTTAGTTACTGTTTTAGAGCTAGAAATAGCAAGTTAA
oVRD180	TTGAAGACTTAGAATAGGGATGCACCAGCCGGGAATCG
oVRD181	TTGAAGACTTTTCTAGAACCCAAAGTTTTAGAGCTAGAAATAGCAAGTTAA
oVRD182	TTGAAGACTTATGAGGGGGTTGAATTGTGCACCAGCCGGGAATCG
oVRD183	TTGAAGACTTTCATTTGGTTTTAGAGCTAGAAATAGCAAGTTAA
oVRD184	TTCGTCTCAGGAGGGCAGAGAAGCTAGGTGTGCCAGAAAAAATTG
oVRD185	GAAGGGTCTTGCGAAGGGGATCTGAACTTGACTTATTTTAAAAATTTGAGTAAAC
oVRD186	TCGTCTCAGGAGGGCAGAGAAGGGGATTAAGGAAGAGGACCAA
oVRD187	GGAAGGGTCTTGCGAAGGGGATCCAAAGTTGACTTACTCAAATTTAAAAACT
oVRD188	TTCGTCTCAGGAGGGCAGAGAAGTAATCAAAACTTTTTGGATGCTCTTCTTC
oVRD189	AGGAAGGGTCTTGCGAAGGGGATCCTCTCTCTCTCTCTCTCTCTCTCA
oVRD190	GACTCTAGCGCTACCGGTCGCCACCATGGGAATGCAAGAAAAGGATCCG
oVRD191	GGGGAAATTCGCCTCGAGATCAGTTATCATTGTCCGAACCCGAATCC
oVRD192	GAATTAGAGATCTTGGCAGGAT
oVRD193	CCTCTCCAAATGAAATGAACTTC

Addendum

Coleus amboinicus – a new model plant to understand CAM photosynthesis?

V.R.-D. designed, planned and performed the experiments, analyzed the data and wrote the Addendum.

Coleus amboinicus – a new model plant to understand CAM photosynthesis?

Coleus amboinicus is a semi-succulent plant that can be used to study and understand Crassulacean acid metabolism (CAM). It belongs to the group of Lamiaceae, where CAM plants can be found in close phylogenetic proximity to C_3 plants. *C. amboinicus*, also called Cuban oregano or Mexican mint is spread throughout parts or Africa and in the (sub-)tropics. It is used as an oregano substitute and as an herb in traditional medicine (Arumugam et al., 2016). However, as in the mint family CAM plants can only be found in the *Plectrantinae* subtribe, not a lot is known about its photosynthesis.

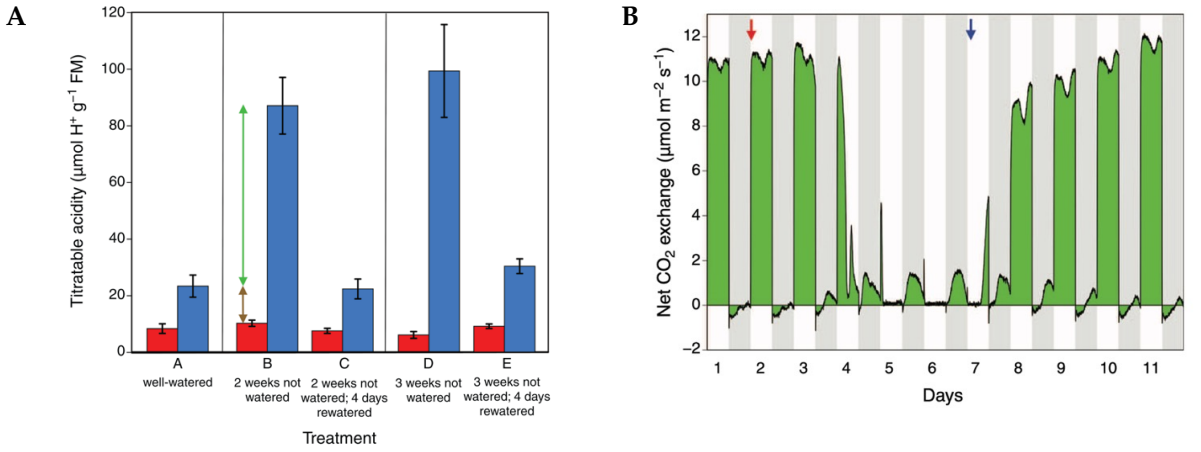

Figure 1: Physiological effects of stressed *C. amboinicus* plants.
Titratable acidity levels (A) and net CO2 exchange pattern for *C. amboinicus* plants under drought stress. Figure modified from (Winter et al., 2021) Figure 3 and 2.

Winter et al., 2021 could show that *C. amboinicus* exhibits a weak constitutive CAM expression, which is enhanced under drought conditions, but in a reversible manner. In their study, the authors grew the plants from 5 cm tall stem cuttings in pots underneath a rain shelter with about 30% solar radiation in the Republic of Panama (Winter et al., 2021). Measurements of acidity and gas exchange have been performed with plants about 20-30 cm height. The authors could observe that *C. amboinicus* plants show increased nocturnal acidity levels of leaf tissue when plants have been on water withheld. However, plants revert back to a slight nocturnal acidity increase after re-watering for 4 days (compare Figure 1A). These findings go hand in hand with the pattern of the gas measurements they observed. Net CO_2 fixation dropped to almost zero during drought stress in the light, while an upregulation could be observed during the night. When plants were re-watered the CO_2 fixation in the light recovered (compare

Figure 1B). Therefore, it is suggested that *C. amboinicus* can be considered to show a co-occurrence of constitutive and facultative CAM expression (Winter et al., 2021).

Growth conditions and physiological parameters

Induction of flowering

C. amboinicus plants used in this study were kindly provided by Prof. Klaus Winter from the Smithsonian Tropical Research Institute, Panama. Plants were propagated by stem cuttings and grown in the greenhouse (24 °C day temperature with 16 h light and 8 h dark, 20°C night temperature). *C. amboinicus* did not show flowering under these conditions. However, further studies could investigate research questions in the field of genomics, so production of seeds might be necessary. We hypothesized that the plants might produce seeds under rather unfavorable conditions and therefore moved them to a short day (8 h light, 16 h dark) and lower temperature (15/15 °C) greenhouse. After two to three month, flowering was induced and plants grew inflorescences (compare Figure 2). These inflorescences grew big with a high number of small flowers. Induction of flowering has been repeated several times and showed a reproducibility of inflorescence growth under colder and short-day conditions. However, to date, no seeds could be harvested.

Figure 2: Flower development of *C. amboinicus*.
Plants produce small light pink flowers.

Net CO_2 exchange drops in the light as a drought response

As described in Winter et al., 2021, *C. amboinicus* shows an enhanced nocturnal leaf acidification as well as a change in the net CO_2 exchange when plants face drought. The group around Winter planted *C. amboinicus* under a rain shelter with ~30% daily solar radiation or under natural conditions in a garden box. As the climate conditions in Republic of Panama and the greenhouse in Düsseldorf, Germany are different, adaptations of the plant have been tested experimentally. Therefore, water-withhold experiments have been performed and CO_2 assimilation rate and titratable acidity have been measured. Three plants each have either been watered at regularly basis or water has been withheld for ten days continuously. On day ten, the assimilation for one leaf per plant has been measured with LI-COR-6800 after a ~30 min adaptation period (daytime of the measurement was ~9-13 h). For titratable acidity and metabolomic measurements, leaves have been harvested at the same day in the end of the day and on the following morning at the end of the night. Leaves were directly frozen in liquid nitrogen and stored at -80 °C until further processing.

Figure 3 shows the measured net CO_2 assimilation rate of the leaves after ten days of two individual experiments (A and B). One can see that the assimilation rate is lower for the plants which have been on water withhold compared to plants that were watered on a regular basis. This shows that less CO_2 is assimilated by the leaves of the drought stressed plants at the measured timepoint. Since CAM plants downregulate CO_2 uptake during the day, a lower assimilation rate is expected as for C_3 photosynthesis. The difference in assimilation under various conditions could be a hint for a changed carbon fixing strategy. Both individual experiments show the same pattern of assimilation. Winter et al. could also show that the net CO_2 fixation dropped to almost zero for drought stressed plants during the day. These findings go hand in hand with the results described here and indicate that *C. amboinicus* might be suitable as a study organism not only in its native region, but also in a greenhouse in central Europe. However, the measurement only shows one timepoint during the day and no time course throughout eleven days, as shown by Winter. An additional experiment could therefore be a 24 h measurement with a LI-COR device to analyze a complete day. For a CAM plant one would expect a difference in assimilation rate, stomata conductance and CO_2 concentration inside the leaf at day and night. Due to temporal separation of photosynthetic steps, this pattern is expected to be seen only if the plant has transitioned to CAM photosynthesis. This

result might strengthen the hypothesis that *C. amboinicus* can be used as model plant all over the world if grown under suitable conditions to receive reproducible data.

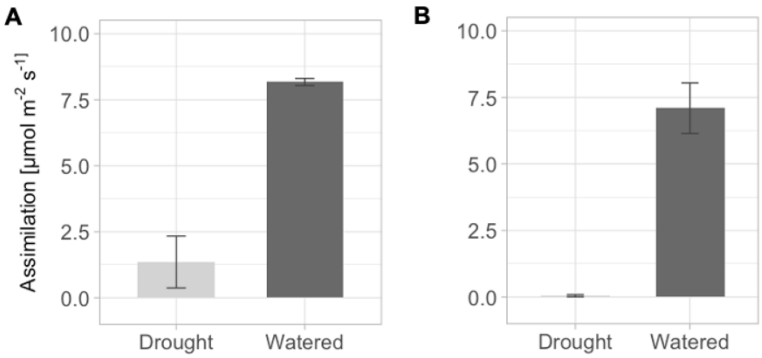

Figure 3: Assimilation rate of *C. amboinicus* plants.
Mean of the measured assimilation rate at drought stress or normal watered condition of two individual experiments (A and B). n=3, except for B, Drought condition (here n=2). Assimilation rate is increased for plants under watered conditions and drops under drought.

Titratable acidity indicates storage of acids in the vacuole

Moreover, Winter et al. could show that nocturnal acidity increased during the night when plants were not watered. However, this is reversible and an indication for the presence of facultative CAM (Winter and Holtum, 2014). To test whether this strategy can be observed in plants grown in the greenhouse in Düsseldorf, titratable acidity has been determined for plants ten day drought stressed plants and watered plants (compare Figure 4). Harvested leaves were flash frozen and ground to fine powder. About 500 mg were then boiled in 20 ml 50% MeOH/H_2O (v/v) until reduced to half of the volume. The solution was filled up to 20 ml with 50% MeOH/H_2O (v/v) and boiled again until half of the volume had evaporated. The solution was cooled to room temperature and filled with dH_2O to 20 ml. Titration was performed with 1 mM NaOH to pH 6.5. The measurements were done for three individual experiments to exclude influence of growth or sampling conditions as well handling. During CAM photosynthesis, acids are stored in the vacuole, which can be measured. One can compare between the different conditions as drought and well-watered and also distinguish between the acidity at the different timepoints. At both conditions the acidity was low at the end of the day (about 5 µmol H^+/g FW). For well-watered plants the acidity only increased slightly for samples taken at the end of the night (about 8 µmol H^+/g FW). Plants that have been on water withhold showed an increase in acidity (about 29 µmol H^+/g FW). The three individual experiments showed a similar result regarding the differences in titratable acidity. The third

repetition showed a generally higher acidity level, which might be due to a longer storage time of the base and exposing to air and therefore a higher volume is needed for titration. However, tendencies were comparable to the other measurements. The increase of acidity indicates storage of acids in the vacuole and therefore indicates transition from C_3 to CAM metabolism for plants under water-withhold. However, one needs to keep in mind that drought plants have a low water content in the leaves and therefore probably store less acids regarding to the total fresh weight. The tendency of the titratable acidity change is comparable to what has been shown in (Winter et al., 2021). However, the total amounts are increased when experiments have been performed in the Republic of Panama. This could be due to growth conditions as well as performance of acid extraction and its measurement.

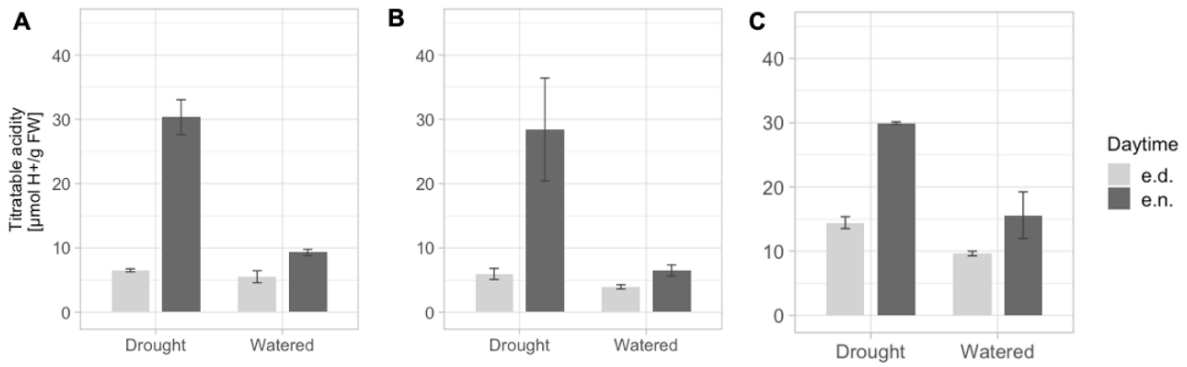

Figure 4: Titratable acidity at drought stress or watered condition.
Three individual experiments are shown (A, B, C, n=3). Titratable acidity shows similar values for leaves harvested at the end of the day for both conditions. Levels increase higher at the end of the night, when plants face drought.

Abscisic acid treatment might induce transition to CAM photosynthesis

CAM induction by drought cannot be done in a completely controlled manner. This is due to many aspects, including water content in the soil, capacity of pots, humidity and temperature. Therefore, other methods have been developed to induce CAM photosynthesis. Studies have been performed for example with salt treatment or abscisic acid (ABA), as the hormone is involved in drought response (Chu et al., 1990; Dai et al., 1994; Maleckova et al., 2019).

To receive a more precise reproducible test-system, CAM induction by ABA treatment was tested for *C. amboinicus* plants. To this end, leaves were dipped in either ABA or mock solution every morning for ten consecutive days. As ABA is dissolved in Methanol and Tween-20 is used as a wetting agent, a mock solution was used containing 0.095% MeOH and 0.2% Tween-20. After ten days the leaves were harvested and frozen in liquid nitrogen and stored at –80 °C

until further usage. The leaves were extracted and titration was performed as described before. Mock treated leaves did not show an increase in acidity level at the end of the night. A test series was performed to identify the ABA concentration needed for CAM induction, which does not lead to an unintended stress reaction. Concentrations of 10, 20, 50, 100 and 200 µM were used. Treatment with 100 µM ABA showed only a weak increase in titratable acidity overnight compared to drought stressed plants (Figure 5). Treatment with lower or higher concentrations did not show a difference in acidity levels. It was expected to see an increase in titratable acidity overnight after ABA treatment comparable to plants stressed by water-withhold (compare Taybi and Cushman, 2002, 1999). However, this result cannot be observed. Different explanations can be put forward trying to explain the lack of an increasing titratable acidity after ABA treatment. One explanation might be that ABA is not taken up by the plant. To test this hypothesis, leaves have been infiltrated with ABA solution. ABA concentration was decreased to 10 µM to avoid stressing the plant. 24 h or 48 h after treatment, plants did also not show an increase of titratable acidity. This might suggest that either the plant does not response to ABA with increasing levels of acidity or it is not measurable at this time point by using the method described. Other explanations such as activity of the hormone, size and age of the plant or residual storage of water in the soil or the plant itself should not be excluded in further research. It is suggested to try an alternative, such as salt treatment (Montero et al., 2018) to induce CAM induction in *C. amboinicus*, as it might be better reproducible than drought stress.

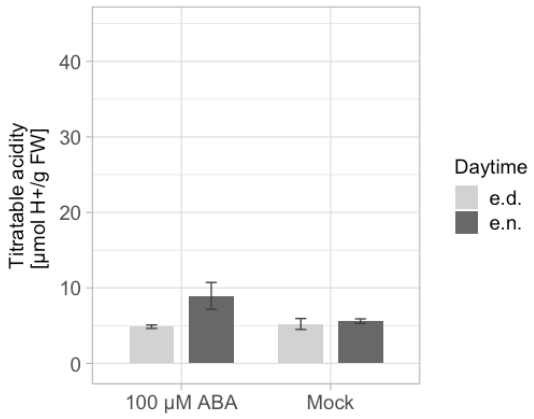

Figure 5: Titratable acidity after ABA treatment.
Shown is the mean of the titratable acidity for leaves dipped either in 100 µM ABA or mock solution for ten days in a row. Samples are either taken at the end of the day (e.d.) or at the end of the night (e.n.). ABA treatment only leads to a weak increase in titratable acidity levels.

Molecular tools to explore the genome, transcriptome and metabolome

Chromatography measurements can give insights into a plant's metabolome

Using *C. amboinicus*, a pilot study has been performed for metabolite analysis via gas chromatography-MS (GC-MS) and ion chromatography (IC). Towards that, leaves from four different treatments were analyzed. Treatment was done with 100 μM ABA (compare Figure 5) and drought (compare Figure 4A) and their controls (mock treatment or well-watered). Leaves were harvested at the end of the day and end of the night. The metabolite extraction from the leaves was performed with extraction buffer containing H_2O, methanol, and $CHCl_3$ in the ratio 1:2.5:1.

Isocitrate showed an increase for all treatments for samples taken at the end of the night. However, levels increased higher for drought stressed plants. In addition to that, malate levels of these plants are increased at the end of the night. These findings are true for both GC and IC measurements. Observation of both metabolites could indicate acid storage in the vacuole during CAM photosynthesis (compare Winter and Smith, 2022). The sugars glucose and fructose, as well as the photorespiratory metabolite glycerate showed decreased levels under drought, while raffinose levels increased. These findings go hand in hand with drought responses found in *T. fruticosum* studies (Brilhaus et al., 2016). Decreases in the sugars and glycerate might indicate differences in photosynthetic behavior between drought stressed and well-watered plants. IC data provide further insights into parts of the glycolysis pathway of *C. amboinicus*. Glucose-6-phosphate and 3-phosphoglycerate levels were decreased under drought stress (compare Figure 7), indicating a change in photosynthetic strategy compared to well-watered plants. These findings could also be observed in Abbey et al. (2023). However, the authors concentrated only on one time point and did not analyze temporal differences, which is the basis of CAM photosynthesis. Additional metabolites have been measured, but not all of them showed differences in their patterns (compare Figure 6 and Figure 7). Changes in metabolites for plants treated with ABA could not be shown, as expected to be similar to drought plants. Therefore, it is suggested to use drought as a method for CAM induction and normalize the metabolites on dry weight to learn more about CAM transition and its regulation in *C. amboinicus*.

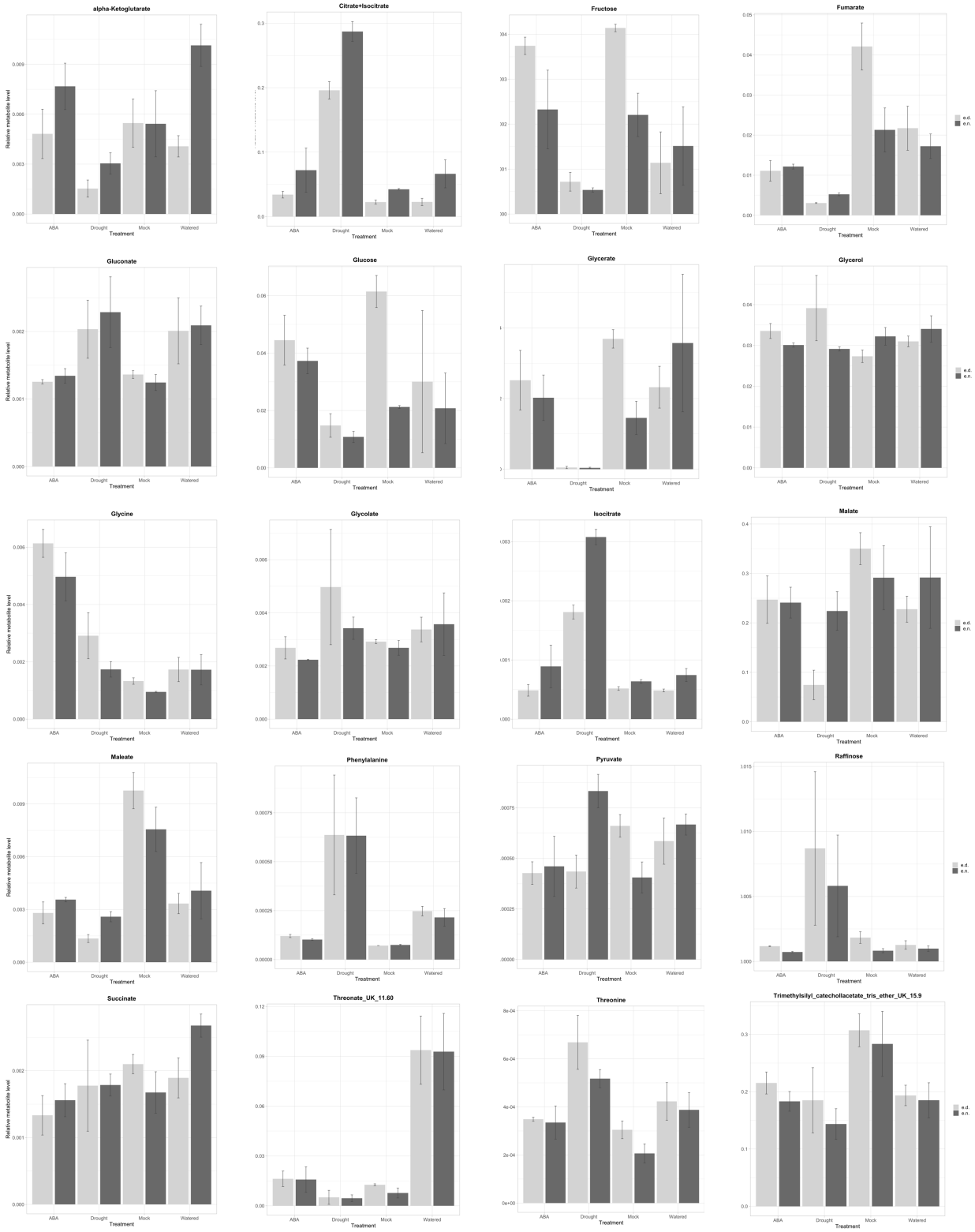

Figure 6: Metabolome analysis by GC-MS for ABA and drought treated *C. amboinicus* leaves. Metabolites were measured for ABA and drought treated samples, as well as mock and well-watered. Timepoints are end of day (ed) and end of night (en).

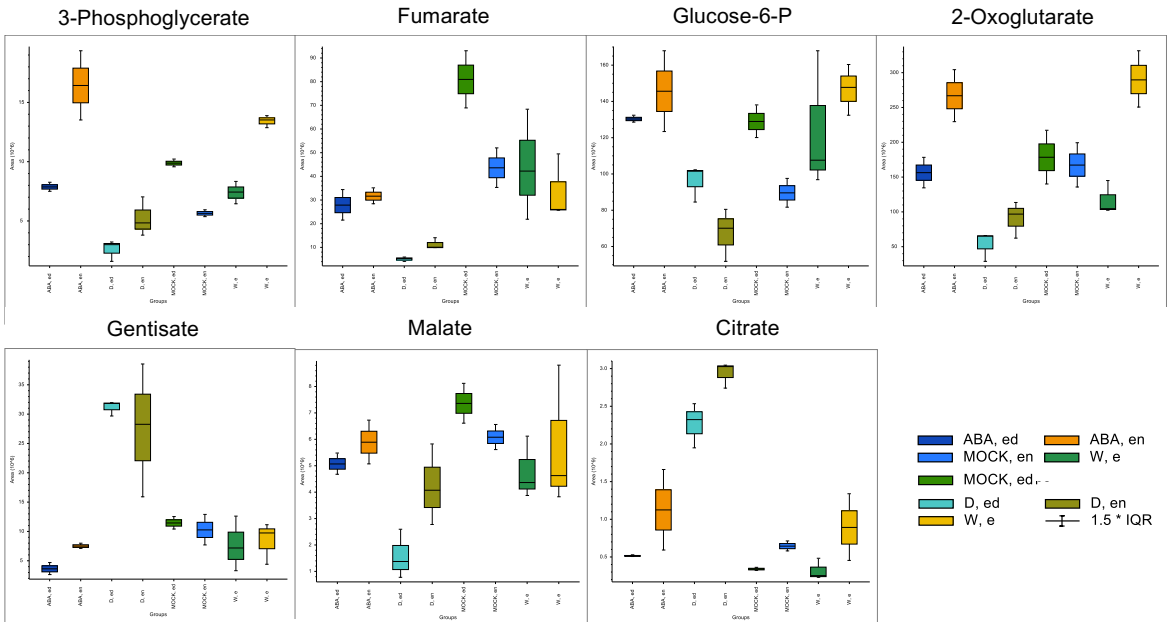

Figure 7: Metabolome analysis by IC-MS for ABA and drought treated *C. amboinicus* leaves.
Metabolites have been measured for ABA, mock and drought (D) treated samples, as well as well-watered (W). Timepoints are end of day (ed) and end of night (en).

Isolation of high-quality genomic DNA

Isolation of genomic DNA (gDNA) is the basis for further molecular genetic work. The protocol shown here can be used to isolate high-quality genomic DNA from *C. amboinicus*, which will be needed for genome sequencing. New genomes are the basis to understand molecular mechanisms of CAM photosynthesis and allow comparisons between species to gain a deeper knowledge (compare Winter, 2019). The protocol has been slightly modified from publications of Manikandan et al., 2017 and Sahu et al., 2012. Young *C. amboinicus* leaves were ground with Polyvinylpyrrolidone in a cold mortar. The powder was heated with suspension buffer (20 mM EDTA, 100 mM Tris-HCl, 1.5 M NaCl, 1 M sucrose, 2.5% Triton-X 100, 1.5% 2-Mercaptoethanol) and phase separation was performed using chloroform/isoamyl alcohol. DNA was precipitated with isopropanol and washed with ethanol. DNA barcoding was performed using oligonucleotides published in Manikandan et al., 2017. **Figure 8** A shows gDNA isolation from different *C. amboinicus* samples. gDNA can be identified on the top of the gel as a clear band. Manikandan and co-authors have used plant specific markers for barcoding. Here, the same oligos have been used to verify genomic DNA of *C. amboinicus*. Except for the oligo pair of MATURASE K (matK-1), gDNA bands could be verified. Additionally, RNAse treatment has been performed at 37 °C for 30 min (compare **Figure 8**C).

Samples treated with RNAse do not show a RNA band, but still a weak gDNA signal, while the control, without RNAse treatment still shows RNA contamination. Isolation, including RNAse treatment, as well as barcoding of genomic DNA from *C. amboinicus* could be successfully repeated using this slightly modified protocol.

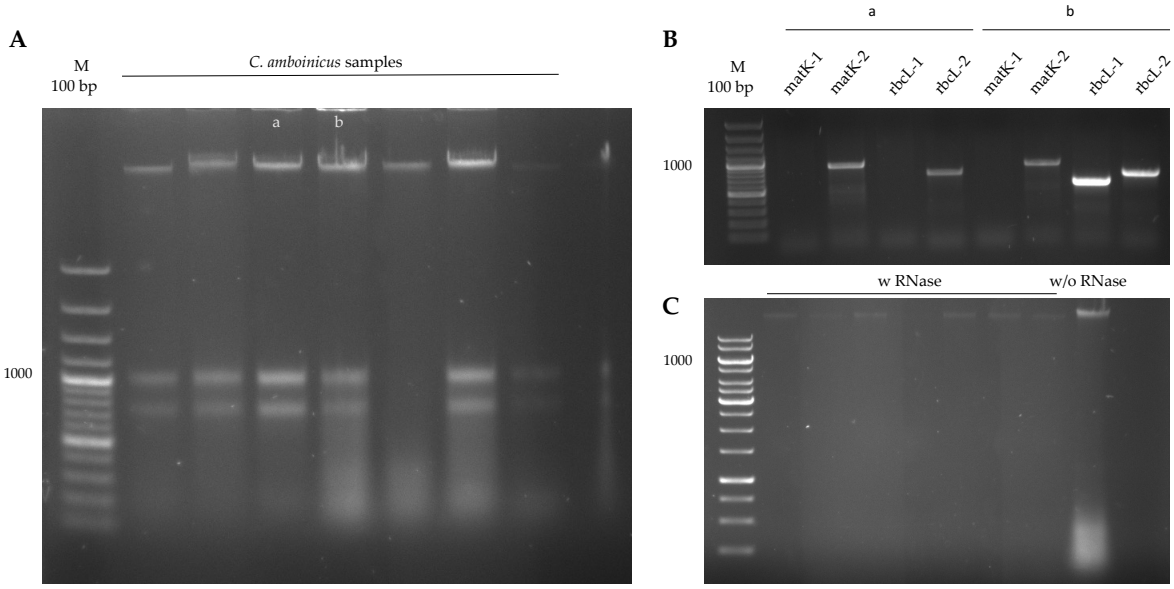

Figure 8: Isolation of genomic DNA from *C. amboinicus* leaves. A: gDNA visible as a clear band on top of the gel. B: Barcoding of gDNA samples a and b. C: gDNA after RNase treatment and without RNase treatment as a control.

Isolation of high-quality RNA

To dive deeper into exploring the genomic regulation and function of *C. amboinicus*, genomic material needs to be accessible. Therefore, a method for isolation of RNA had to be established in the lab. The Universal RNA Kit from Roboklon with DTT or beta-mercaptoethanol and Qiagen Rneasy Plant mini Kit have been tested, but did not lead to isolation of RNA. This might be due to the slightly succulent leaves and a high content of secondary metabolites, which could interfere with kit components or lead to a viscous solution, which might not pass through the columns. Using the Macherey-Nagel NucleoSpin RNA Plant and Fungi Mini kit (740120.50), following the manufacturer's instructions, led to successful RNA extraction. RNA samples have to be treated with DNAse, to eliminate contaminating DNA. Samples were treated with DNase for 1, 5, 10 or 30 min on ice, on room temperature (RT) or at 37 °C, respectively. RNA without DNase treatment was taken as a control. Samples were analysed on a Bioanalyser to evaluate the purity of the RNA. Figure 9 shows the Bioanalyser results of the different treatments. Treatment at 37 °C for 30 min showed only a weak DNA signal and almost no difference in RNA quality, while other treatments seem to decrease quality and not

remove DNA completely. To remove all DNA, DNAse treatment was prolonged to 1 h at 37 °C. An additional 10 min 75 °C inactivation step was needed to receive DNA-free RNA samples. PCR was performed to confirm the isolation of DNA-free RNA by using matK2-F and matK2-R oligos from Manikandan et al. 2017 as described before. A fragment could be amplified from gDNA and RNA samples without DNA treatment, but not for two RNA samples treated with DNase. No band is visible in the negative water control (neg) (compare Figure 10).

The protocol described here can be used to yield DNA-free RNA for RNA-seq studies, which can give new insights about the plant's transcriptome. RNA-seq data can help to understand the changing cellular transcriptome within a facultative CAM plant. Transcriptome studies in other CAM plants could already help to identify important regulators of CAM photosynthesis (compare Introduction). Candidates involved in circadian and diurnal rhythms found in *Erycina* species and *Kalanchoë fedtschenkoi* are suggested to be necessary in C_3-CAM transition (Heyduk et al., 2019; Moseley et al., 2018). Transcription factors and core CAM genes have been identified in RNA-seq studies of *Talinum fruticosum* (Brilhaus et al., 2016; Maleckova et al., 2019). However, in contrast to most studies available, RNA-seq analysis of *C. amboinicus* can give even deeper analysis. The advantage of using *C. amboinicus* lies in its closely related C_3 lineages. Therefore, comparisons between different photosynthetic types are more accurate and a deeper understanding of its regulation might be possible.

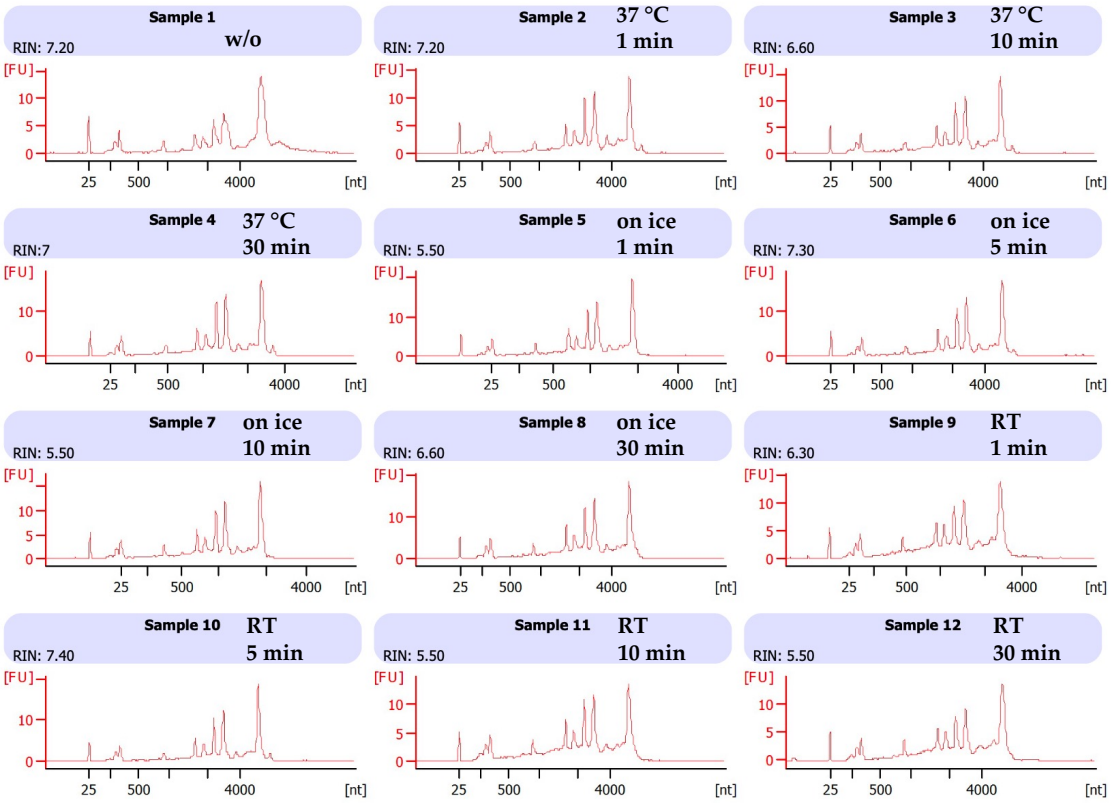

Figure 9: RNA analysis on a Bioanalyser. RNA samples have been treated with DNase for 1 to 30 min on ice, RT or at 37 °C. Incubation at 37 °C for 30 min shows almost no DNA signal and a high RNA quality.

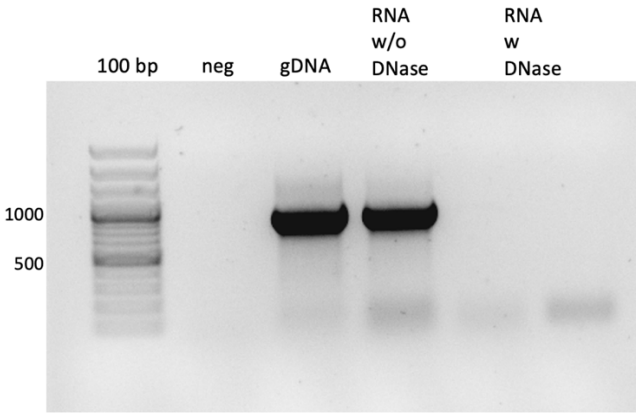

Figure 10: PCR amplification of isolated RNA and gDNA.
Oligonucleotides matK2-F and matK2-R from Manikandan et al., 2017 have been used. Negative water control (neg) and RNA treated with DNase do not show a band, while gDNA and RNA sample without treatment do show an amplification.

Coleus amboinicus as a model-plant to understand CAM photosynthesis

Drought stress leads to a transition from C_3 to CAM photosynthesis in *C. amboinicus*. Physiological responses could be observed not only in Panama, but also in a greenhouse in central Europe. We are now able to perform CAM induction by water withhold, metabolic analysis, gDNA and RNA extraction. This can support further studies in the inducible CAM plant *C. amboinicus*, which might aim to unravel key components of signaling pathway or gene regulatory networks. Even though no seeds were produced until now, flower induction was successful. Working with *C. amboinicus* might need additional effort in establishing a method to genetically modify it by plant tissue culture. This might be a relatively fast approach as *C. amboinicus* can easily be propagated by cuttings. As shown before, metabolites can be analyzed on GC-MS and IC-MS, which shows patterns comparable to previous studies for other CAM species (Brilhaus et al., 2016). Moreover, methods for genomic and transcriptomic work could be developed and confirmed in our laboratory environment. The induction of CAM transition with ABA treatment could not be shown so far. Therefore, development of an alternative method, such as salt treatment, is crucial to establish a reproducible protocol for CAM induction.

Taken together the new approaches and insights, this makes *C. amboinicus* a suitable model plant for CAM research, as comparisons between species can be drawn easily. As *C. amboinicus* has phylogenetically close relatives performing C_3 photosynthesis, conclusions between evolution and CAM transition could be drawn easier than for other established CAM model plants. Easy handling of the plant and available methods make it a suitable organism to study CAM photosynthesis.

Acknowledgment:

I would like Klaus Winter from the Smithsonian Tropical Research Institute, Republic of Panama for providing C. amboinicus plants, Philipp Westhoff for metabolite measurements and Samantha Flachbart for RNA analysis on the Bioanalyser.

References

Abbey, Lord, Ofoe, R., Wang, Z., Chada, S., 2023. How Central Carbon Metabolites of Mexican Mint (Plectranthus amboinicus) Plants Are Impacted under Different Watering Regimes. Metabolites 13. https://doi.org/10.3390/metabo13040539

Arumugam, G., Swamy, M.K., Sinniah, U.R., 2016. Plectranthus amboinicus (Lour.) Spreng: Botanical, Phytochemical, Pharmacological and Nutritional Significance. Molecules 21. https://doi.org/10.3390/molecules21040369

Brilhaus, D., Bräutigam, A., Mettler-Altmann, T., Winter, K., Weber, A.P.M., 2016. Reversible burst of transcriptional changes during induction of crassulacean acid metabolism in Talinum triangulare1[OPEN]. Plant Physiol 170, 102–122. https://doi.org/10.1104/pp.15.01076

Chu, C., Dai, Z., Ku, M.S.B., Edwards, G.E., 1990. Induction of Crassulacean Acid Metabolism in the Facultative Halophyte Mesembryanthemum crystallinum by Abscisic Acid1, Plant Physiol.

Dai, Z., Ku, M.S.B., Zhang, D., Edwards, G.E., 1994. Effects of growth regulators on the induction of Crassulacean acid metabolism in the facultative halophyte Mesembryanthemum crystallinum L, Planta.

Heyduk, K., Moreno-Villena, J.J., Gilman, I.S., Christin, P.A., Edwards, E.J., 2019. The genetics of convergent evolution: insights from plant photosynthesis. Nat Rev Genet 20, 485–493. https://doi.org/10.1038/s41576-019-0107-5

Maleckova, E., Brilhaus, D., Wrobel, T.J., Weber, A.P.M., 2019. Transcript and metabolite changes during the early phase of abscisic acid-mediated induction of crassulacean acid metabolism in Talinum triangulare. J Exp Bot 70, 6581–6596. https://doi.org/10.1093/jxb/erz189

Manikandan, S., Ansarali, S., Alagu Lakshmanan, G.M., 2017. Optimizing the pure genomic DNA isolation procedure for Plectranthus amboinicus DNA – A prerequisite for further genomic Studies. Journal of Applied and Advanced Research 2, 249–255. https://doi.org/10.21839/jaar.2017.v2i4.97

Montero, E., Francisco, A.M., Montes, E., Herrera, A., 2018. Salinity induction of recycling Crassulacean acid metabolism and salt tolerance in plants of Talinum triangulare. Ann Bot 121, 1333–1342. https://doi.org/10.1093/aob/mcy030

Moseley, R.C., Mewalal, R., Motta, F., Tuskan, G.A., Haase, S., Yang, X., 2018. Conservation and diversification of circadian rhythmicity between a model crassulacean acid metabolism plant kalanchoë fedtschenkoi and a model C3 photosynthesis plant arabidopsis thaliana. Front Plant Sci 871. https://doi.org/10.3389/fpls.2018.01757

Sahu, S.K., Thangaraj, M., Kathiresan, K., 2012. DNA Extraction Protocol for Plants with High Levels of Secondary Metabolites and Polysaccharides without Using Liquid Nitrogen and Phenol. ISRN Mol Biol 2012, 1–6. https://doi.org/10.5402/2012/205049

Taybi, T., Cushman, J.C., 2002. Abscisic acid signaling and protein synthesis requirements for phosphoenolpyruvate carboxylase transcript induction in the common ice plant. J Plant Physiol 159, 1235–1243. https://doi.org/10.1078/0176-1617-00834

Taybi, T., Cushman, J.C., 1999. Signaling Events Leading to Crassulacean Acid Metabolism Induction in the Common Ice Plant 1.

Winter, K., 2019. Ecophysiology of constitutive and facultative CAM photosynthesis. J Exp Bot. https://doi.org/10.1093/jxb/erz002

Winter, K., Holtum, J.A.M., 2014. Facultative crassulacean acid metabolism (CAM) plants: Powerful tools for unravelling the functional elements of CAM photosynthesis. J Exp Bot 65, 3425–3441. https://doi.org/10.1093/jxb/eru063

Winter, K., Smith, J.A.C., 2022. CAM photosynthesis: the acid test. New Phytologist. https://doi.org/10.1111/nph.17790

Winter, K., Virgo, A., Garcia, M., Aranda, J., Holtum, J.A.M., 2021. Constitutive and facultative crassulacean acid metabolism (CAM) in Cuban oregano, Coleus amboinicus (Lamiaceae). Functional Plant Biology 48, 647–654. https://doi.org/10.1071/FP20127

Journal version of published Manuscript I

Photorespiration is the solution, not the problem

Journal of Plant Physiology 282 (2023) 153928

Contents lists available at ScienceDirect

Journal of Plant Physiology

journal homepage: www.elsevier.com/locate/jplph

Photorespiration is the solution, not the problem

Laia Segura Broncano [1], Krzysztof Robin Pukacz [1], Vanessa Reichel-Deland [1], Urte Schlüter [1], Sebastian Triesch [1], Andreas P.M. Weber [*,1]

Institute of Plant Biochemistry, Cluster of Excellence on Plant Science (CEPLAS), Universitätsstraße 1, 40225 Düsseldorf, Germany

A B S T R A C T

The entry of carbon dioxide from the atmosphere into the biosphere is mediated by the enzyme Rubisco, which catalyzes the carboxylation of ribulose 1,5-bisphosphate (RuBP) as the entry reaction of the Calvin Benson Bassham cycle (CBBC), leading to the formation of 2 molecules of 3-phosphoglyceric acid (3PGA) per CO_2 fixed. 3PGA is reduced to triose phosphates at the expense of NADPH + H^+ and ATP that are provided by the photosynthetic light reactions. Triose phosphates are the principal products of the CBBC and the precursors for almost any compound in the biosphere.

Every year, in the order of 150 Gt of carbon are transferred from the atmosphere to the biosphere by the Rubisco reaction (Jian et al., 2022). The current atmosphere contains approx. 900 Gt C (Friedlingstein et al., 2022), which means that every six to seven years, the entire atmospheric carbon pool is routed once through Rubisco in plants, algae, and cyanobacteria.

However, the acronym Rubisco stands for RuBP carboxylase/oxygenase, specifying that Rubisco does not only carboxylate but also oxidize RuBP. The oxygenation reaction leads to the formation of 2-phosphoglycolic acid (2PG), which is an inhibitor of some CBBC enzymes and hence 2PG must be efficiently removed to avoid blockage of the CBBC by the oxygenation product of Rubisco. Further, 2PG must be transformed into molecules that are compatible with plant metabolism. This is achieved by a metabolic repair pathway called photorespiration.

Bauwe (2023) provides an authoritative account of photorespiration, with a particular emphasis on the involved enzymes, starting with the different forms of Rubisco and Rubisco-like proteins and their evolutionary history, and moving on to the "Magnificent Ten", the core set of enzymes in chloroplasts, peroxisomes, mitochondria and cytoplasm that jointly convert 2PG to 3PGA. Figure 4 in Bauwe (2023) shows the entire pathway, hence we refer to this figure for the details. A unique strength of this review is its focus on the enzyme components of the pathway, their structures (where available), and their catalytic mechanisms. Thereby Bauwe (2023) develops a detailed picture of how deeply photorespiration is embedded in plant metabolism, beyond its immediate role in enabling oxygenic photosynthesis.

Photorespiration is frequently portrayed as a wasteful pathway that reduces the efficiency of photosynthesis. Indeed, the removal of 2PG and its conversion to 3PGA requires energy and redox power and it leads to the release of previously fixed CO_2 and ammonia. Bauwe's review stands out by emphasizing that photorespiration is the solution to a problem (i.e., the oxygenation reaction of Rubisco), and not the problem itself. In fact, photosynthesis in an oxygen-containing environment would not be possible without photorespiration. Even cyanobacteria that utilize very efficient carbon concentrating mechanisms (CCMs) have multiple, partially redundant routes for detoxification of 2PG and their deletion is lethal. The same holds for C_4 plants – mutations in the photorespiratory pathway are lethal or lead to severe growth retardation, indicating that carbon concentrating mechanisms are insufficient to fully suppress the oxygenation reaction (Levey et al., 2019; Zelitch et al., 2009).

1. Integration of photorespiration into leaf nitrogen network

Bauwe reminds us that photorespiration serves multiple functions beyond the detoxification of 2PG. In the C3 leaf, photorespiration considerably contributes to balancing of C, N and energy metabolism. The photorespiratory cycle does not just work as a closed system, but is interlinked with the metabolic network of the leaf and is dynamically redirecting C and N from the CBBC to a range of other pathways. Indeed, in C3 plants, photorespiration serves as the major source for Serine (Ser). Fu et al. (2022) recently measured the rate of amino acid export from photorespiration and found that between 27 and 39% of Ser was exported from the pathway under ambient O_2 and CO_2 conditions (Fig. 1). Although Ser can also be produced by the phosphorylated Ser biosynthesis pathway that is essential for plant growth and survival (Zimmermann et al., 2021), it seems to be advantageous for the C3 leaf

* Corresponding author.
E-mail address: aweber@hhu.de (A.P.M. Weber).
[1] All authors equally contributed to this commentary.

https://doi.org/10.1016/j.jplph.2023.153928
Received 17 January 2023; Accepted 22 January 2023
Available online 28 January 2023
0176-1617/© 2023 Elsevier GmbH. All rights reserved.

to meet serine demands during the day mainly from photorespiration. Photorespiratory Ser serves also as dominant precursor for O-acetylserine and subsequent cysteine synthesis connecting photorespiration to Sulfur metabolism of the leaf (Samuilov et al., 2018). Ser derived compounds such as dehydrins, glutathione, glycine betaines or glucosinolates can also improve stress tolerance of the leaf (Busch, 2020).

Glycine (Gly), like Ser, can also directly feed into protein biosynthesis. Gly to Ser conversion in mitochondria during photorespiration is also deeply interlinked with C1 metabolism. Draining of glycine and C1 compounds from photorespiration alters the amount of CO_2 released from the oxygenase reaction of Rubisco (Busch, 2020). Fu et al. (2022) suggest that photorespiratory Gly serves as a dynamic, metabolically largely benign buffer that can store photorespiration-derived carbon and nitrogen until it can be further processed in the downstream pathways. Bauwe (2023) also highlights the substrate promiscuity of the peroxisomal serine:glyoxylate aminotransferase, which can use alanine (Ala) instead of Ser as an amino donor, thereby affording metabolic flexibility and balancing of leaf amino acid metabolism upon withdrawal of Ser or

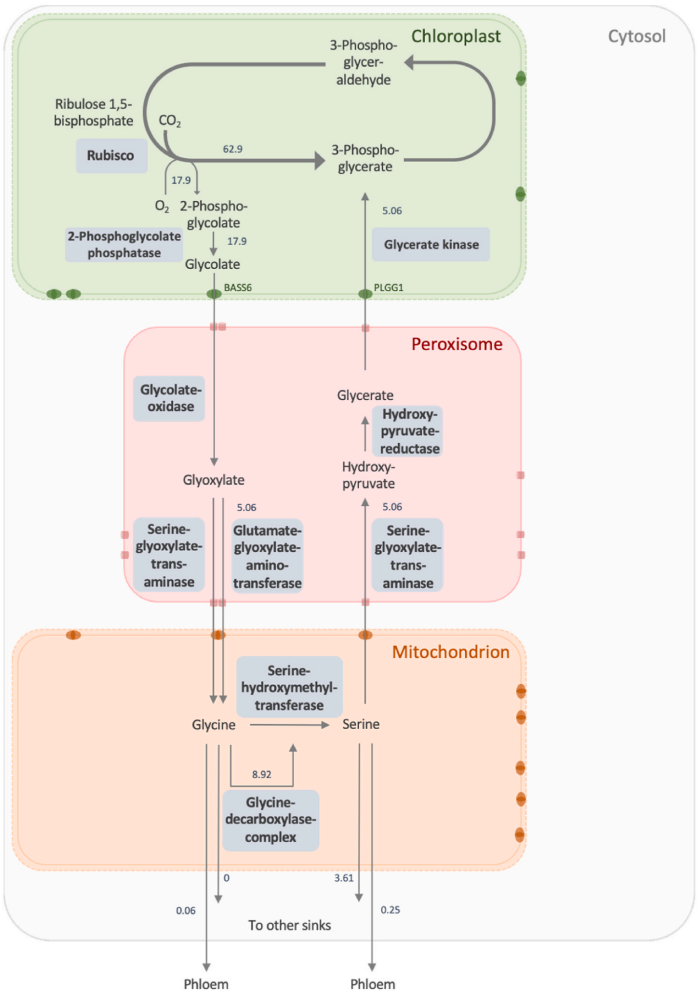

Fig. 1. (A) Simplified scheme of the ten key enzymatic steps ("Magnificent Ten") and central metabolites of photorespiration in a single plant cell.Photorespiration in plants is distributed between the chloroplast, the peroxisome and the mitochondrion. The relative fluxes are taken from modelling approaches described in Fu et al. (2022) assuming an atmospheric O_2 concentration of 21%. Glycine and serine leave the mitochondria either via passive diffusion or transporters and to a substantial degree enter amino acid metabolism.
(B) Simplified scheme of the nine key enzymatic steps and central metabolites of photorespiration in a single *Chlamydomonas reinhardtii* cell.In contrast to land plants, where glycolate processing takes place in the peroxisome, photorespiration in *C. reinhardtii* is limited to the chloroplast and mitochondrion. As a result, parts of the pathway are catalysed by different enzymes. Glycine and serine are transported to the cytosol and are fed into amino acid metabolism as well as other pathways.

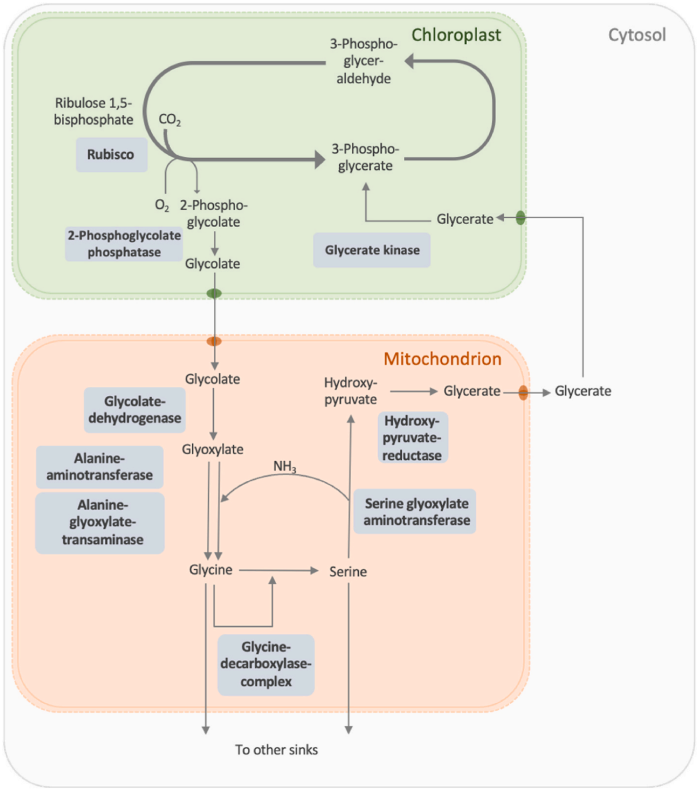

Fig. 1. (*continued*).

Gly from the pathway.

Photorespiration correlated positively to rates of N uptake and assimilation (Rachmilevitch et al., 2004). The mechanisms underpinning this phenomenon are not yet resolved, but withdrawal of amino acids from photorespiration increases the demand for *de novo* N assimilation (Busch et al., 2018). Lower rates of photosynthesis during photorespiratory conditions could also improve availability of ferredoxin for N assimilation in the plastids (Huma et al., 2018; Rachmilevitch et al., 2004). Influence of photorespiration on whole plant performance is mainly discussed under the aspect of C and energy loss, but photorespiration can also have positive effects on plant composition and fitness (Rachmilevitch et al., 2004; Busch et al., 2018). Under elevated CO_2 concentrations, C3 species show a reduction in N content (Bloom et al., 2010). With the evolution of CO_2 concentrating mechanisms in land plants, such as C4, N metabolism apparently adjusted to the reduced rates of photorespiration in C4 leaves. Interestingly, C4 plants have lower rates of N assimilation compared to C3. This can be explained by lower demand for proteins in the assimilatory machinery of the leaf. Recent modelling studies, however, suggest that N metabolism and availability played an important role during evolution of C4 photosynthesis (Blätke and Bräutigam, 2019; Sundermann et al., 2021). In terms of resource allocation, phenotypic plasticity of C4 plants could be reduced (Sundermann et al., 2021).

2. Evolutionary origins of photorespiration

Being an integral part of the core heterotrophic metabolism, photorespiration was subject to rapid evolutionary turnovers. Bauwe (2023) reconstructs the ancient origins of photorespiration: while core enzymes were recruited from alpha-proteobacterial carbon metabolism, PGLP seems to originate from archaea and GLYK seems to be of cyanobacterial origin. PGLP, GS and SHMT can even be found in the minimal set of 102 gene families that are thought to be present in the last universal common ancestor (LUCA). The gene products might have played a role in the autotrophic methanogenic lifestyle of LUCA, e.g. in Gly and Ser biogenesis (Weiss et al., 2016, 2018). Bauwe (2023) goes even further back in time and reminds us that lower-molecular photorespiratory intermediates such as glycolate, glycine, sugars and even nucleobases can also be formed via ZnS-catalysis in abiotic environments (Omran et al., 2020).

Oxygenic photosynthesis arose with the emergence of heterodimeric PSII clusters with oxygen evolving complexes in cyanobacteria (Allen and Martin, 2007). Photorespiration in these organisms was likely built upon pre-existing metabolic modules. The peroxisome likely evolved concomitantly with the installation of a mitochondrion as the result of an endosymbiosis event between an archaeal host and an alpha-proteobacterium. The installation of a chloroplast likely involved

a eukaryotic cell with an endosymbiotic cyanobacterium. Glycolate excreted from the nascent plastid may have contributed to the carbon flux from endosymbiont to the host cell.

Apart from its evolution as a detoxification pathway for 2PG, photorespiration can also be seen as a keystone for further evolutionary progress: Bauwe (2023) points out that high levels of photorespiration reduce photosynthetic efficiency, which may have provided a selective force for the evolution of CCMs. In nature these mechanisms take the form of pyrenoids or carboxysomes in algae and cyanobacteria, respectively, or CAM and C4 photosynthesis in land plants. Bauwe (2023) highlights that in the evolution of C4 photosynthesis, photorespiration was initially split up between mesophyll and bundle-sheath cells, installing a photorespiratory glycine shuttle. Interestingly, this glycine shuttle created an N-imbalance between both cell types which required the installation of what today can be observed as a full C4 photosynthetic pathway (Mallmann et al., 2014).

3. The photorespiratory pathway in green algae differs from that of land plants

Recent work has also suggested an important role for photorespiration in algae. Most green algae have a reduced rate of photorespiration thanks to their CO_2 concentrating mechanism, which is based on the active transport of inorganic carbon into a phase-separated Rubisco condensate known as the pyrenoid. This increases the CO_2:O_2 ratio in proximity to Rubisco, preventing RuBP oxygenation. The photorespiration pathway in green algae is significantly different from that of plants, where the processing of glycolate occurs in the peroxisome (Figure 3 of Bauwe, 2023). In algae, glycolate oxidation occurs in the mitochondria, eliminating the peroxisome from the pathway. In addition, the photorespiration rate of *Chlamydomonas reinhardtii* increases significantly in response to decreasing CO_2 concentration, which is thought to protect the plants from increased 2-PG generation. For a more detailed review of the *C. reinhardtii* CCM and its relationship with photorespiration, see (Wang et al., 2015).

Photorespiration also plays a role in the regulation of the algal CCM itself. Previously thought to be induced by low CO_2 concentrations, recent studies (reviewed in (Adler et al., 2022)) suggest that photorespiratory intermediates play a role in regulating the CCM in *C. reinhardtii*. Overall, it appears that photorespiration is still an essential part of the primary metabolism of green algae, protecting metabolism from toxins and acting as a regulator of photosynthesis.

4. Engineering of photorespiratory bypasses as a tool to better understand photorespiraiton

Photorespiration acts as a driving force for the transport of reducing equivalents between organelles during the day and as a pathway that enables the re-routing of carbon (and nitrogen). Bauwe (2023) reminds us that photorespiration is an open pathway that directly taps into core plant metabolism and enables, rather than limits plant photosynthesis and encourages a shift in photorespiration research towards a more positive view of the process.

The study of photorespiration heavily relies on the availability of mutants that are defective in photorespiration-specific enzymes. However, mutations in photorespiration or photorespiration-associated genes are only viable under elevated CO_2 conditions. The strong alterations caused by the accumulation of intermediates in photorespiratory mutants, undeniably cause detrimental effects in several cellular processes (Timm and Bauwe, 2013). Overall, the physiology of photorespiratory mutants complicates the assessment of the impact of gene deletions compared to the impact of altered environmental conditions. While these studies have immensely contributed to a comprehensive understanding of the evolution of the photorespiratory pathway and its interplay with primary metabolism, Bauwe (2023) brings to our attention new research directions for further understanding this complicated process.

In attempts to increase plant yield, numerous approaches are being taken towards so-called CO_2-neutral and CO_2-positive photorespiratory bypasses (Trudeau et al., 2018). The consequences of the implementation of artificial bypasses in relationship to native metabolism and photorespiration itself are not fully understood yet. Taking the complex nature of photorespiration into account, it seems worth considering utilizing novel metabolic routes that bypass photorespiration to gain a more comprehensive view of the additional roles that photorespiration plays in plant metabolism. Photorespiratory bypasses present us with the opportunity to study the function of photorespiratory metabolites while still effectively detoxifying 2-PG, increasing the viability of mutants in ambient conditions.

Declaration of competing interest

The authors declare that they have no known competing financial interests or personal relationships that could have appeared to influence the work reported in this paper.

Data availability

No data was used for the research described in the article.

Acknowledgements

The authors appreciate funding by the ERA-CAPS project "C4BREED" under Project ID WE 2231/20–1, the Cluster of Excellence for Plant Sciences (CEPLAS) under Germany's Excellence Strategy EXC-2048/1 under project ID 390686111, the H2020 EU project "GAIN4-CROPS", and the IRTG 2466 "NextPlant" grant by the German Research Foundation (DFG).

References

Adler, L., Díaz-Ramos, A., Mao, Y., Pukacz, K.R., Fei, C., McCormick, A.J., 2022. New horizons for building pyrenoid-based CO2-concentrating mechanisms in plants to improve yields. Plant Physiol. 190, 1609–1627. https://doi.org/10.1093/plphys/kiac373.

Allen, J.F., Martin, W., 2007. Out of thin air. Nature 445, 610–612. https://doi.org/10.1038/445610a.

Bauwe, H., 2023. Photorespiration – Rubisco's repair crew. J. Plant Physiol. 280, 153899 https://doi.org/10.1016/j.jplph.2022.153899.

Blätke, M.-A., Bräutigam, A., 2019. Evolution of C4 photosynthesis predicted by constraint-based modelling. Elife 8, e49305. https://doi.org/10.7554/elife.49305.

Bloom, A.J., Burger, M., Asensio, J.S.R., Cousins, A.B., 2010. Carbon dioxide enrichment inhibits nitrate assimilation in wheat and arabidopsis. Science 328, 899–903. https://doi.org/10.1126/science.1186440.

Busch, F.A., 2020. Photorespiration in the context of Rubisco biochemistry, CO2 diffusion and metabolism. Plant J. https://doi.org/10.1111/tpj.14674.

Busch, F.A., Sage, R.F., Farquhar, G.D., 2018. Plants increase CO2 uptake by assimilating nitrogen via the photorespiratory pathway. Native Plants 4, 46–54. https://doi.org/10.1038/s41477-017-0065-x.

Friedlingstein, P., O'Sullivan, M., Jones, M.W., Andrew, R.M., Gregor, L., Hauck, J., Quéré, C.L., Luijkx, I.T., Olsen, A., Peters, G.P., Peters, W., Pongratz, J., Schwingshackl, C., Sitch, S., Canadell, J.G., Ciais, P., Jackson, R.B., Alin, S.R., Alkama, R., Arneth, A., Arora, V.K., Bates, N.R., Becker, M., Bellouin, N., Bittig, H.C., Bopp, L., Chevallier, F., Chini, L.P., Cronin, M., Evans, W., Falk, S., Feely, R.A., Gasser, T., Gehlen, M., Gkritzalis, T., Gloege, L., Grassi, G., Gruber, N., Gürses, Ö., Harris, I., Hefner, M., Houghton, R.A., Hurtt, G.C., Iida, Y., Ilyina, T., Jain, A.K., Jersild, A., Kadono, K., Kato, E., Kennedy, D., Goldewijk, K.K., Knauer, J., Korsbakken, J.I., Landschützer, P., Lefèvre, N., Lindsay, K., Liu, J., Liu, Z., Marland, G., Mayot, N., McGrath, M.J., Metzl, N., Monacci, N.M., Munro, D.R., Nakaoka, S.-I., Niwa, Y., O'Brien, K., Ono, T., Palmer, P.I., Pan, N., Pierrot, D., Pocock, K., Poulter, B., Resplandy, L., Robertson, E., Rödenbeck, C., Rodriguez, C., Rosan, T.M., Schwinger, J., Séférian, R., Shutler, J.D., Skjelvan, I., Steinhoff, T., Sun, Q., Sutton, A.J., Sweeney, C., Takao, S., Tanhua, T., Tans, P.P., Tian, X., Tian, H., Tilbrook, B., Tsujino, H., Tubiello, F., van der Werf, G.R., Walker, A.P., Wanninkhof, R., Whitehead, C., Wranne, A.W., Wright, R., Yuan, W., Yue, C., Yue, X., Zaehle, S., Zeng, J., Zheng, B., 2022. Global carbon budget 2022. Earth Syst. Sci. Data 14, 4811–4900. https://doi.org/10.5194/essd-14-4811-2022.

Fu, X., Gregory, L.M., Weise, S.E., Walker, B.J., 2022. Integrated flux and pool size analysis in plant central metabolism reveals unique roles of glycine and serine during photorespiration. Native Plants 1–10. https://doi.org/10.1038/s41477-022-01294-9.

Huma, B., Kundu, S., Poolman, M.G., Kruger, N.J., Fell, D.A., 2018. Stoichiometric analysis of the energetics and metabolic impact of photorespiration in C3 plants. Plant J. 96, 1228–1241. https://doi.org/10.1111/tpj.14105.

Jian, J., Bailey, V., Dorheim, K., Konings, A.G., Hao, D., Shiklomanov, A.N., Snyder, A., Steele, M., Teramoto, M., Vargas, R., Bond-Lamberty, B., 2022. Historically inconsistent productivity and respiration fluxes in the global terrestrial carbon cycle. Nat. Commun. 13, 1733. https://doi.org/10.1038/s41467-022-29391-5.

Levey, M., Timm, S., Mettler-Altmann, T., Borghi, G.L., Koczor, M., Arrivault, S., Weber, A.P., Bauwe, H., Gowik, U., Westhoff, P., 2019. Efficient 2-phosphoglycolate degradation is required to maintain carbon assimilation and allocation in the C4 plant Flaveria bidentis. J. Exp. Bot. 70, 575–587. https://doi.org/10.1093/jxb/ery370.

Mallmann, J., Heckmann, D., Bräutigam, A., Lercher, M.J., Weber, A.P.M., Westhoff, P., Gowik, U., 2014. The role of photorespiration during the evolution of C4 photosynthesis in the genus Flaveria. Elife 3. https://doi.org/10.7554/elife.02478 e02478–e02478.

Omran, A., Menor-Salvan, C., Springsteen, G., Pasek, M., 2020. The messy alkaline formose reaction and its link to metabolism. Life 10, 125. https://doi.org/10.3390/life10080125.

Rachmilevitch, S., Cousins, A.B., Bloom, A.J., 2004. Nitrate assimilation in plant shoots depends on photorespiration. Proc. Natl. Acad. Sci. U.S.A. 101, 11506–11510. https://doi.org/10.1073/pnas.0404388101.

Samuilov, S., Brilhaus, D., Rademacher, N., Flachbart, S., Arab, L., Alfarraj, S., Kuhnert, F., Kopriva, S., Weber, A.P.M., Mettler-Altmann, T., Rennenberg, H., 2018. The photorespiratory BOU gene mutation alters Sulfur assimilation and its crosstalk with carbon and nitrogen metabolism in Arabidopsis thaliana. Front. Plant Sci. 9, 1709. https://doi.org/10.3389/fpls.2018.01709.

Sundermann, E.M., Lercher, M.J., Heckmann, D., 2021. Modeling photosynthetic resource allocation connects physiology with evolutionary environments. Sci. Rep. 11, 15979 https://doi.org/10.1038/s41598-021-94903-0.

Timm, S., Bauwe, H., 2013. The variety of photorespiratory phenotypes - employing the current status for future research directions on photorespiration. Plant Biol. 15, 737–747. https://doi.org/10.1111/j.1438-8677.2012.00691.x.

Trudeau, D.L., Edlich-Muth, C., Zarzycki, J., Scheffen, M., Goldsmith, M., Khersonsky, O., Avizemer, Z., Fleishman, S.J., Cotton, C.A.R., Erb, T.J., Tawfik, D.S., Bar-Even, A., 2018. Design and in vitro realization of carbon-conserving photorespiration. Proc. Natl. Acad. Sci. U.S.A. 115, E11455–E11464. https://doi.org/10.1073/pnas.1812605115.

Wang, Y., Stessman, D.J., Spalding, M.H., 2015. The CO2 concentrating mechanism and photosynthetic carbon assimilation in limiting CO2: how Chlamydomonas works against the gradient. Plant J. 82, 429–448. https://doi.org/10.1111/tpj.12829.

Weiss, M.C., Preiner, M., Xavier, J.C., Zimorski, V., Martin, W.F., 2018. The last universal common ancestor between ancient Earth chemistry and the onset of genetics. PLoS Genet. 14, e1007518 https://doi.org/10.1371/journal.pgen.1007518.

Weiss, M.C., Sousa, F.L., Mrnjavac, N., Neukirchen, S., Roettger, M., Nelson-Sathi, S., Martin, W.F., 2016. The physiology and habitat of the last universal common ancestor. Nat. Microbiol. 1, 16116 https://doi.org/10.1038/nmicrobiol.2016.116.

Zelitch, I., Schultes, N.P., Peterson, R.B., Brown, P., Brutnell, T.P., 2009. High glycolate oxidase activity is required for survival of maize in normal air. Plant Physiol. 149, 195–204. https://doi.org/10.1104/pp.108.128439.

Zimmermann, S.E., Benstein, R.M., Flores-Tornero, M., Blau, S., Anoman, A.D., Rosa-Téllez, S., Gerlich, S.C., Salem, M.A., Alseekh, S., Kopriva, S., Wewer, V., Flügge, U.-I., Jacoby, R.P., Fernie, A.R., Giavalisco, P., Ros, R., Krueger, S., 2021. The phosphorylated pathway of serine biosynthesis links plant growth with nitrogen metabolism. Plant Physiol. 186, 1487–1506. https://doi.org/10.1093/plphys/kiab167.

Acknowledgment

First of all, I would like to thank my supervisor Prof. Dr. Andreas Weber for all his trust and guidance throughout my PhD. Thank you for the opportunities to attend conferences and workshops and invite inspiring guests to Düsseldorf.

I would also like to thank my second supervisor Prof. Dr. Matias Zurbriggen for the opportunity to work in his lab, inspiring discussions and all his help during the last years.
My thanks go to Shizue Matsubara, Robert VanBuren and Björn Usadel for aDending my annual commiDee meetings with fruitful discussions and bringing up creative new projects.
Thanks to all the collaboration partners who turned abstract ideas into experiments.

I am grateful for all the members of the AG Weber, for scientific discussions, new ideas, great lunch breaks, dinners and really good self-made liquors. Especially I want to thank Sebastian Triesch for all his help and patience when I deleted the internet. Work (and the moments when experiments fail) is so much better when you have a great friend. One day, we will open our bar on campus! I would also like to thank Steffi Schulze, Marion Eisenhut, Raja Stracke, Franziska Kuhnert, Vanessa Valencia, Karolina Vogel, Ana PleD, Franziska Fichtner, Philipp Westhoff, Nicole Linka, Mori_ Göbel, Lucas Müller, Patrick Fischbach, Alisandra Denton and Dagmar Lyska for all the discussions about science and life. Thanks to our wonderful technicians for all the help during the experimental work. Moreover, my thanks go to all the people who I shared an office with (and also the whiteboard for creative space). And finally, I would like to thank Kuddel! Thanks to everyone from AG Zurbriggen, to host me, showing me all the techniques and methods and let me be part of your daily work life. I thank the gardeners for taking really good care of the plants. Thanks to Katharina Raba from the UKD for all her initiative and the great hours I spent with her. Moreover, I would like to thank the people from the BMFZ for technical support.

Thanks to my students, especially Marcel Derendorf, Luca Schneider and Dani Aguirre Boyd, for their help and trust. I wish you all the best for the future!

I would also like to thank iGrad plant for funding and a great trip to Michigan. Thanks to Petra Fackendahl for all the organization and to all iGrad plant members. My special thanks go to Natascha Heßler, Gesa Helmsorig, Jonas Schön, Einar Haraldsson and Tianyu Lan for scientific discussions, lunch breaks, escapes from the lab work and becoming wonderful friends.

Thanks to my friends and my swimming team for mental breaks from the PhD. I would like to thank everyone of family for all their support and love. Especially I want to thank Torsten for being the best person in my life.